

Field Test Plan for the Soil Desiccation Pilot Test

Prepared for the U.S. Department of Energy
Assistant Secretary for Environmental Management

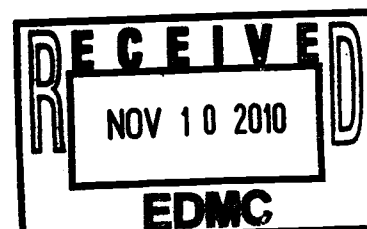


U.S. DEPARTMENT OF
ENERGY

Richland Operations
Office

P.O. Box 550
Richland, Washington 99352

Approved for Public Release;
Further Dissemination Unlimited



2001BC.1
M.015.63

attached to: 00918910 + 00918912

Field Test Plan for the Soil Desiccation Pilot Test

Date Published
September 2010

Prepared for the U.S. Department of Energy
Assistant Secretary for Environmental Management



U.S. DEPARTMENT OF
ENERGY

Richland Operations
Office

P.O. Box 550
Richland, Washington 99352

Lebratton
Release Approval

9/27/2010
Date

Approved for Public Release;
Further Dissemination Unlimited

TRADEMARK DISCLAIMER

Reference herein to any specific commercial product, process, or service by trade name, trademark, manufacturer, or otherwise, does not necessarily constitute or imply its endorsement, recommendation, or favoring by the United States Government or any agency thereof or its contractors or subcontractors.

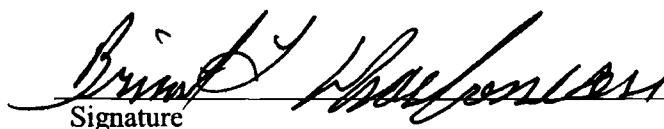
This report has been reproduced from the best available copy.

Printed in the United States of America

Approval Page

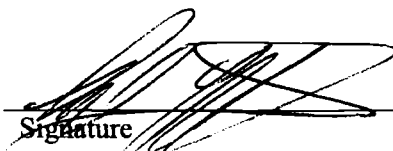
Title Field Test Plan for the Soil Desiccation Pilot Test

Approval Briant L. Charboneau
U.S. Department of Energy, Richland Operations Office


Signature

9-15-10
Date

Approval Rod Lobos
U.S. Environmental Protection Agency


Signature

9-20-2010
Date

Contents

1	Project Description.....	1-1
1.1	Introduction	1-1
1.2	Project Activities	1-2
2	Treatment Technology Description	2-1
3	Test Objectives	3-1
4	Experimental Design and Procedures	4-1
4.1	Test Site Location and Description	4-1
4.2	Experimental Design	4-3
4.2.1	Technical Basis	4-5
4.2.2	Approach.....	4-37
4.3	Procedures	4-44
5	Equipment and Materials.....	5-1
5.1	Desiccation Field Test Instrumentation Plan.....	5-1
5.2	Thermocouple Psychrometers	5-3
5.3	Heat Dissipation Unit.....	5-4
5.4	Thermistor	5-4
5.5	Humidity.....	5-5
5.6	Dual Probe Heat Pulse.....	5-5
5.7	Ground Penetrating Radar	5-6
5.8	Electrical Resistivity Imaging	5-8
5.9	Neutron Probe.....	5-8
6	Sampling and Analysis.....	6-1
7	Data Management.....	7-1
8	Data Analysis and Interpretation	8-1
8.1	Operational Desiccation Performance.....	8-1
8.2	Long-Term Performance	8-2
9	Health and Safety	9-1
10	Waste Management.....	10-1
11	Community Relations	11-1
11.1	Purpose	11-1
11.1.1	Definition of Stakeholders and General Public.....	11-1
11.1.2	Availability of the Treatability Test Plan.....	11-1
11.2	Public Comments	11-1
12	Reports	12-1

13	Schedule	13-1
14	Management and Staffing	14-1
15	Budget	15-1
16	References	16-1

Figures

Figure 1-1.	Layout of the BC Cribs and Trenches Waste Sites	1-2
Figure 4-1.	Location of Soil Desiccation Pilot Test Site	4-1
Figure 4-2.	Distribution of Tc-99 and Moisture in Well 299-E13-62	4-2
Figure 4-3.	Logarithm of Solute Flux Through Deep Vadose Zone of Loamy Sand with Gravity-Driven Steady-State Flow as a Function of Volumetric Water Content	4-6
Figure 4-4.	Examples of Modeled Relationship Between Moisture Content and Matric Potential	4-8
Figure 4-5.	Distribution of Tc-99 in the Vadose Zone in the Year 2012	4-10
Figure 4-6.	Selection of Targeted Desiccation Zones Based on Available Borehole Data	4-11
Figure 4-7.	Case 10t-15d Simulated Moisture Content Distribution.....	4-13
Figure 4-8.	Case 10t-35d Simulated Moisture Content Distribution.....	4-14
Figure 4-9.	Case 10t-45d Simulated Moisture Content Distribution.....	4-15
Figure 4-10.	Case 30t-35d Simulated Moisture Content Distribution.....	4-16
Figure 4-11.	Moisture Content Within the Desiccated Zone.....	4-17
Figure 4-12.	Moisture Content Within the Desiccated Zone for Multiple Desiccation Applications	4-18
Figure 4-13.	Temporal Profile of Average Water Flux in the Domain Across the Water Table from the Vadose Zone to the Groundwater.....	4-20
Figure 4-14.	Temporal Profile of Average Water Flux in the Domain Across the Water Table from the Vadose Zone to the Groundwater.....	4-21
Figure 4-15.	Cumulative Technetium Mass Moved Across the Water Table from the Vadose Zone to the Groundwater	4-22
Figure 4-16.	Cumulative Technetium Mass Moved Across the Water Table from the Vadose Zone to the Groundwater	4-23
Figure 4-17.	Temporal Profile of Average Mass Flux in the Domain Across the Water Table from the Vadose Zone to the Groundwater.....	4-24
Figure 4-18.	Temporal Profile of Average Mass Flux in the Domain Across the Water Table from the Vadose Zone to the Groundwater.....	4-25
Figure 4-19.	Conceptual Model of Well Configuration Used to Simulate Air Flow Between Two Wells.....	4-28
Figure 4-20.	Simulated Desiccation (Change in Water Content) Along the Centerline Between the Injection and Extraction Wells.....	4-29
Figure 4-21.	Simulated Desiccation (Change in Water Content) Along the Centerline Between the Injection and Extraction Wells.....	4-30
Figure 4-22.	Simulated Desiccation (Change in Water Content) Along the Centerline Between the Injection and Extraction Wells.....	4-31

Figure 4-23. Simulated Temperature Profile During Desiccation Along the Centerline Between the Injection and Extraction Wells.....	4-31
Figure 4-24. Simulated Temperature Profile During Desiccation Along the Centerline Between the Injection and Extraction Wells.....	4-32
Figure 4-25. Simulated Temperature Profile During Desiccation Along the Centerline Between the Injection and Extraction Wells.....	4-32
Figure 4-26. Plan (Mid-Screen Depth) and Cross-Sectional Views of the Pressure Gradients.....	4-33
Figure 4-27. Plan (Mid-Screen Depth) and Cross-Sectional Views of the Pressure Gradients.....	4-34
Figure 4-28. Plan (Mid-Screen Depth) and Cross-Sectional Views of the Pressure Gradients.....	4-35
Figure 4-29. Test Site Layout.....	4-38
Figure 7-1. Vadose Zone Monitoring Components, Instrumentation, and Data-Collection Management Flow Diagram for the Soil Desiccation Pilot Test	7-1
Figure 8-1. Conceptualization of Anticipated Data Response from In Situ Probes	8-1
Figure 8-2. Conceptualization of Anticipated Data Response from Periodic Neutron Logging	8-2
Figure 13-1. Soil Desiccation Pilot Test Schedule	13-2
Figure 14-1. Project Organization Chart	14-1

Tables

Table 4-1. Overview of In Situ Monitoring Techniques.....	4-4
Table 4-2. Mid-Depths and Thicknesses for the Imposed Desiccated Zones and Shorthand Notation for the Different Scenarios	4-11
Table 4-3. Water Removed from Desiccation Zone When Desiccation Condition is Imposed	4-19
Table 4-4. Desiccation Rate Versus Injected Nitrogen Flow Rate	4-27
Table 4-5. Data Collection at Extraction Well.....	4-37
Table 4-6. Summary of In Situ Monitoring Instrumentation.....	4-39
Table 4-7. Measured Parameters for Baseline Data Collection	4-40
Table 4-8. Injection Nitrogen Flow Operational Targets.....	4-41
Table 4-9. Summary of Data Collection Approach During Active Desiccation.....	4-42
Table 4-10. Summary of Data Collection Approach During Post-Desiccation Period.....	4-43
Table 5-1. In Situ Sensors and Measurements, Field Conditions, and Sensor Filter Pack	5-2
Table 13-1. Project Schedule	13-1

Terms

bgs	below ground surface
CERCLA	<i>Comprehensive Environmental Response, Compensation, and Liability Act of 1980</i>
CHPRC	CH2M HILL Plateau Remediation Company
Cs-137	cesium-137
DOE	U.S. Department of Energy
DPHP	dual probe heat pulse
DQA	data quality assessment
DQO	data quality objective
DVZTT	Deep Vadose Zone Treatability Test
Ecology	Washington State Department of Ecology
EM	electromagnetic
EPA	U.S. Environmental Protection Agency
ERT	electrical resistance tomography
FS	feasibility study
FTP	field test plan
FY	fiscal year
GPR	ground penetrating radar
HDU	heat dissipation unit
MOG	multiple-offset gather
N/A	not applicable
NTC	negative temperature coefficient
OU	operable unit
PNNL	Pacific Northwest National Laboratory
RL	DOE Richland Operations Office
SAP	sampling and analysis plan
SDPT	soil desiccation pilot test
SF ₆	sulfur hexafluoride
STOMP	Subsurface Transport Over Multiple Phases
SVE	soil vapor extraction

Tc-99	technetium-99
TCP	thermocouple psychrometer
TPA	Tri-Party Agreement
ZOP	zero-offset profile

1 Project Description

In response to the Tri-Party Agreement (TPA) milestone M-015-50, the *Deep Vadose Treatability Test Plan for the Hanford Central Plateau* (DOE/RL-2007-56) was issued in March 2008. That plan defines tests focused on mitigating the potential of technetium-99 (Tc-99) and uranium to contaminate groundwater. This field test plan (FTP) and its associated sampling and analysis plan (SAP) are not only an extension of the Deep Vadose Zone Treatability Test (DVZTT) Plan, but are necessary parts of the remedial investigation (RI)/feasibility study (FS) being conducted to support a cleanup decision for the 200-BC-1 operable unit (OU). The 200-BC-1 OU includes the BC Cribs and Trenches waste sites which are located in the southeastern portion of the 200 Area National Priorities List Site.

The overarching RI/FS document for the 200-BC-1 OU is the *200-TW-1 Scavenged Waste Group Operable Unit and 200-TW-2 Tank Waste Group Operable Unit RI/FS Work Plan* (DOE/RL-2000-38). The BC Cribs and Trenches waste sites have since been moved into the 200-BC-1 OU in order to focus on their characterization and eventual remediation. This FTP specifically defines the parameters for evaluating soil desiccation as a potential remedy, with focus on Tc-99. The SAP associated with this FTP is the *Sampling and Analysis Plan for the Soil Desiccation Pilot Test* (DOE/RL-2010-83).

1.1 Introduction

Soil desiccation is described in DOE/RL-2007-56 as the most promising of various technologies evaluated to protect groundwater from Tc-99 residing in the deep vadose zone of the Hanford Site Central Plateau. Deep is a vague term, but is regarded as beyond the depth which can practicably and economically be excavated, or somewhere in the vicinity of 15 m (50 ft) and deeper below ground surface (bgs) at the Hanford Site. Groundwater risk mitigation is derived from reduction of vadose zone sediment pore water associated with the contamination, which is the primary driving force for mobile contaminant transport. Soil desiccation will be evaluated in a pilot test conducted in the 200-BC-1 OU that is located on the southern edge of the 200 East Area of the Hanford Site. Specific focus is within the grouping of cribs in this OU. Figure 1-1 illustrates the layout of the BC Cribs and Trenches waste sites and their location within the Hanford Site.

Previous characterization of the cribs region indicates a plume of mobile contamination beneath the cribs (PNNL-17821). Nature and extent of the plume is defined by waste stream composition, the quantity of waste discharged, and the heterogeneity of the vadose zone sediments. At the site of the 299-E13-62 borehole, located between the 216-B-17 and 216-B-19 Cribs, significant concentrations of Tc-99 and nitrate contamination were observed from near 12.2 m (40 ft) bgs to approximately 76.2 m (250 ft) bgs. Contaminant maxima were observed at 15.2 m (50 ft), 27.4-29.0 m (90-95 ft), 38.1-39.6 m (125-130 ft), and 67.1-70.1 m (220-230 ft) bgs. During a period of high applied suction during the characterization phase performed in fiscal year (FY) 2009 (DOE/RL-2009-119, *Characterization of the Soil Desiccation Pilot Test Site*), a significant concentration of Tc-99 was observed in collected condensate. Evaluation of this unexpected phenomenon is the subject of a separate treatability test being planned.

Near-surface contamination within the footprint of the 216-B-14 Crib has been characterized by geophysical logging of shallow boreholes (DOE/RL-2009-36, *BC Cribs and Trenches Excavation-Based Treatability Test Report*). High concentrations of cesium-137 (Cs-137) were observed, with peak concentrations located near the bottom of the as-built crib excavation and extending several feet deeper. Strontium-90 is expected to coexist with the Cs-137, based on characterization of the 216-B-26 Trench, which included sampling for that radionuclide (PNNL-14907). It should be noted that, in contrast to the excavation-based treatability test (DOE/RL-2009-36) which included partial excavation of the 216-B-26 trench, this treatability test will avoid high-activity contamination associated with the footprint of the cribs and, instead, will focus on mobile contamination that has migrated laterally from the cribs.

Although the overall objective of the DVZTT Plan is to address groundwater threat from mobile contaminants deep in the vadose zone, the pilot test will focus on the shallowest component of significant Tc-99 and nitrate contamination that is centered near 13.7 to 15.2 m (45 to 50 ft) bgs. Installation of injection/extraction wells and monitoring instrumentation is less costly at this depth while allowing critical elements of soil desiccation to be evaluated. The deep vadose zone will be mimicked by covering the ground surface with an impermeable barrier to prevent surface interaction with the test.

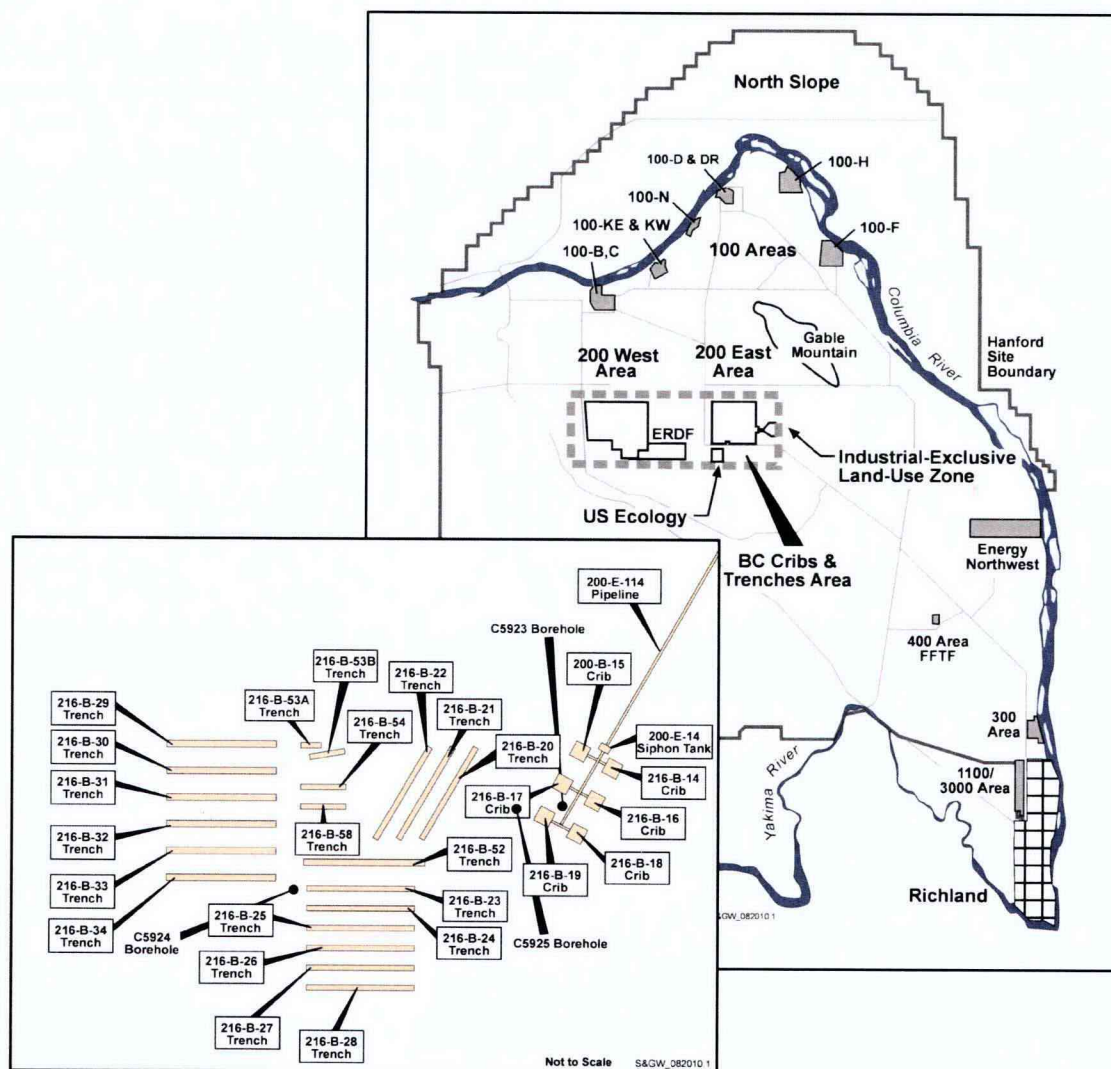


Figure 1-1. Layout of the BC Cribs and Trenches Waste Sites

1.2 Project Activities

This FTP describes the methodologies that will be used to evaluate soil desiccation as a potential remedy for protecting groundwater from deep vadose zone contamination. Test focus is to support feasibility study (FS) evaluation of soil desiccation, with particular attention to short-term evaluation, long-term evaluation, and cost.

Short-term effectiveness considers potential effects on human health and the environment during the implementation phase of the remedy, and the time required to achieve the remedial action objectives.

Extracted gas could expose workers and/or the public if it is contaminated. Another attribute of this criterion where data will be collected is the rate that desiccation can be effected.

Long-term effectiveness and permanence considers the magnitude of residual risk to human and ecological receptors, and the adequacy and reliability of controls. Soil desiccation is not expected to remove contamination, but leave it relatively immobilized in the vadose zone; hence, it will be necessary to rely on numerical simulations to predict to what extent contaminant transport is slowed and its eventual impact on groundwater. Because "rewetting" of the desiccation zone following treatment has potential to undo the treatment, that process and the associated controlling parameters will be considered in the evaluation of soil desiccation effectiveness. Rewetting could result from surface recharge, vapor phase water, and/or lateral migration of moisture from the edges of the desiccation region back into the region that was treated. Surface recharge can be controlled using a surface barrier, which would be expected to accompany soil desiccation, if deployed. Thus, evaluations need to consider how desiccation can work in conjunction with a surface barrier. Rewetting mechanisms are expected to be slow compared to the field test timeframe, resulting in dependence on numerical simulations and complementary laboratory studies. Institutional controls, being administrative in nature, are not considered germane to this investigation.

Finally, cost will be considered. Data relating to cost will be collected to enable inclusion of this *Comprehensive Environmental Response, Compensation, and Liability Act of 1980* (CERCLA) criterion.

Already, initial characterization of the pilot test site has been performed (DOE/RL-2009-119) to augment data previously obtained from characterization of the 299-E13-62 borehole, which is located in the cribs region, that displayed significant relatively shallow Tc-99 contamination (PNNL-17821, *Electrical Resistivity Correlation to Vadose Zone Sediment and Pore-Water Composition for the BC Cribs and Trenches Area*). Although relatively shallow, mobile contaminants such as Tc-99 have potential to contaminate groundwater (see DOE/RL-2007-35, *200-UW-1 Operable Unit Remedial Action Goals for Removal/Treatment/Disposal Waste Sites*, which describes a methodology for calculating the contaminant concentration [as a function of depth] having potential to contaminate groundwater). Furthermore, initial evaluation of extracted soil gas and condensate has been performed. This test will use a pair of screened boreholes to inject dry nitrogen and extract moisture-saturated soil gas. Soil desiccation is expected in the injection borehole vicinity, with the region of desiccation moving outward with time toward the extraction borehole. Desiccation progress will be monitored via a set of instrumented boreholes that monitor soil temperature, humidity, moisture content, and changes in soil electrical properties and collect soil gas containing tracers. Other boreholes will provide for periodic ground penetrating radar (GPR), or cross-hole radar, assessment and neutron logging to monitor desiccation progress. Data evaluation will lead to recommendations for development of a model to treat the entire cribs region of the 200-BC-1 OU.

2 Treatment Technology Description

The treatment technology being tested is soil desiccation. In July 2004, Pacific Northwest National Laboratory (PNNL) completed a preliminary evaluation of remediation technologies focused on immobilization of Tc-99 (Truex, 2004) that recommended pursuing soil desiccation, because it had the least uncertainty. Subsequently, an independent vadose zone technical panel from the DOE Richland Operations Office (RL) and Fluor Hanford convened to review alternative remedial actions for deep vadose zone contamination and came to the same conclusion (WMP-27397).

In concept, soil desiccation is much like soil vapor extraction (SVE), the well-known technology used to remove volatile contaminants from the vadose zone. Because soil gas is generally saturated with moisture due to its intimate long-term contact with soil moisture, the SVE technology removes substantial quantities of water as a by-product of removing the target contaminant, i.e., vapor. In this case, the target is the soil moisture itself. To focus the desiccation region and increase desiccation efficiency, dry nitrogen will be forced into a borehole screened at an interval containing significant soil moisture and contamination. The moisture-saturated soil gas will be pulled out of a nearby borehole that is also screened at the target depth, and is close enough such that the distance between is within the influence of the exhaust blower.

By removing water from the vadose zone, the overall driving force for water and associated contamination toward the water table will be reduced. Where gravity-driven steady-state flow is the dominant transport mechanism, sediment moisture content is directly related to contaminant flux toward the groundwater. Also, as soil moisture content decreases, the unsaturated hydraulic conductivity also decreases to reduce further overall contaminant flux to the water table. Because of the heterogeneous vadose zone, desiccation should increase the effectiveness of capillary breaks by reducing the water contents of adjacent coarse and fine-textured sediment layers.

If deployed as a remedial action, soil desiccation would be expected to be combined with a recharge-limiting cap. Otherwise, recharge from the surface would, over time, replenish the water removed by desiccation and undo its benefit. Not all rewetting of the desiccated zone would originate at the surface, though, because eventually, the overall system would tend toward equilibrium via diffusion processes. Sources of water arriving via diffusion would likely be from points beyond the effect of the recharge-limiting cap. Monitoring will follow the active desiccation portion of the test, and associated modeling will be performed to describe observed phenomena and predict future behavior. Both vapor and liquid diffusion contributions into the desiccation region will be modeled.

3 Test Objectives

Overall objectives of the soil desiccation treatability test, as defined by the DVZTT Plan (DOE, 2008), are as follows:

- Determine the design parameters for applying soil desiccation, including operational parameters such as injected nitrogen flow rate and injected temperature, and identifying soil moisture reduction targets to achieve acceptable reduction of contaminant transport in the vadose zone.
- Demonstrate field-scale desiccation for targeted areas within the vadose zone.
 - Quantify the nitrogen flow, water extraction rate, and other operational parameters to evaluate implementability of the process on a large scale.
 - Determine the extent of soil moisture reduction in the targeted treatment zone to evaluate the short-term effectiveness of the process.
 - After desiccation is completed, determine the rate of change in soil moisture for the desiccated zone.
 - Determine the best types of instrumentation, for monitoring key subsurface and operational parameters, to provide feedback to operations and to evaluate long-term effectiveness.
- Determine the number of injection and extraction wells, screened intervals, type of equipment and instrumentation, and operational strategy such that costs for full-scale application can be effectively estimated.

The first two bullets apply directly to the design and conduct of the soil desiccation pilot test (SDPT). Test operational parameters and moisture reduction targets have been established separately using numerical simulation, independent calculations, and bench testing. During test conduct, operational parameters and desiccation progress will be monitored. It is expected that operational parameters will be refined, to some extent, based on desiccation performance. Following the active portion of the test, vadose zone monitoring will continue so that rewetting progress can be assessed. However, because rewetting is anticipated to occur slowly relative to desiccation and the time frame of the overall test, it is anticipated that numerical simulation will be necessary to evaluate this phenomenon. The last bullet requires test results to be scaled to a specific site. In this case, the cribs portion of the BC Cribs and Trenches Area has been selected. Data from the SDPT will be combined with numerical simulation studies to evaluate operational strategies.

Overall design of the SDPT has been defined using the data quality objective (DQO) process that considered recommendations of an independent technical panel (SGW-41327, *Data Quality Objectives Summary Report for the Soil Desiccation Pilot Test*; SGW-43938, *Independent Technical Review of the Deep Vadose Zone Treatability Test: Second Review*). Initial design considered a central injection well surrounded by three extraction wells to yield a roughly cylindrical desiccation zone. Following the expert review panel, a simple dipole arrangement was adopted, consisting of one injection well and one extraction well. Monitoring locations will be located throughout the region anticipated to be affected.

4 Experimental Design and Procedures

The treatability test design is intended to evaluate soil desiccation as a potential remedy for groundwater protection. Basically, the test consists of a pair of wells screened within an interval of the vadose zone where significant sediment moisture and contamination exist. Dry nitrogen will be injected into one of the wells, and moisture-saturated soil gas will be withdrawn from the other. The intervening and surrounding area will include a number of instruments and sampling ports to monitor the desiccation progress. The fundamental objective is to evaluate the process of drying out a targeted section of the vadose zone, so that contaminant transport is interrupted, and to predict how long that benefit will prevail.

4.1 Test Site Location and Description

The SDPT will be conducted at the BC Cribs and Trenches (Figure 4-1) which is part of the 200-BC-1 OU. This site was selected because it is known to have Tc-99 contamination in the vadose zone, and characterization data for the vadose zone is available. Relatively high concentrations of mobile contamination (Tc-99) and moisture are present at relatively shallow depth, which is accessible by inexpensive direct push technology.

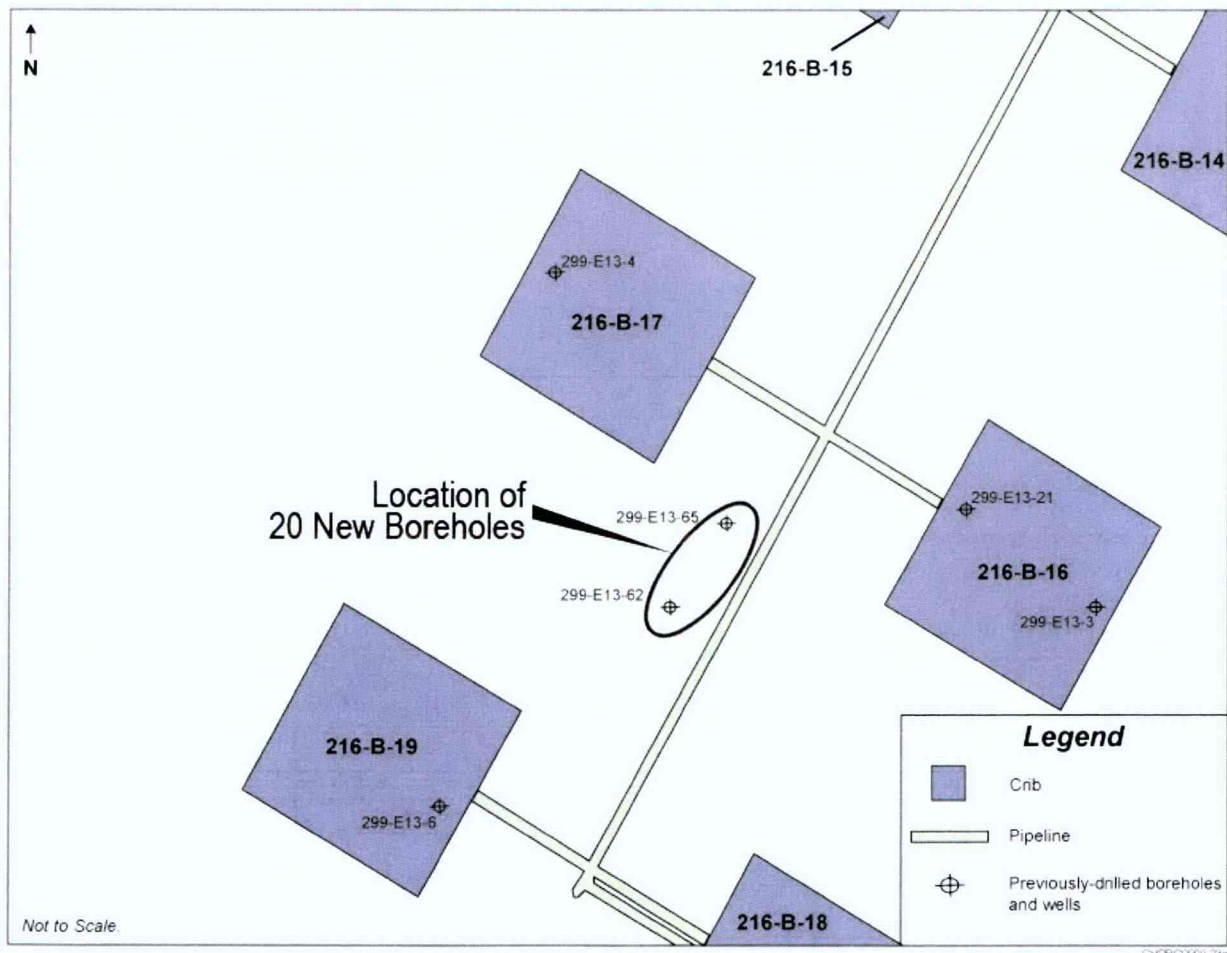


Figure 4-1. Location of Soil Desiccation Pilot Test Site

The pilot test is planned to focus on the 9.1 m to 15.2 m (30 ft to 50 ft) bgs vicinity of the 299-E13-62 Well (Figure 4-1). Detailed characterization data are available at this well. Figure 4-2 shows an example of the technetium and moisture distribution in relation to the well screen interval. The well is located between cribs, such that the subsurface was impacted by discharges from the cribs, but drilling and other test operations can take place outside the footprint of the cribs to avoid high concentrations of Cs-137.

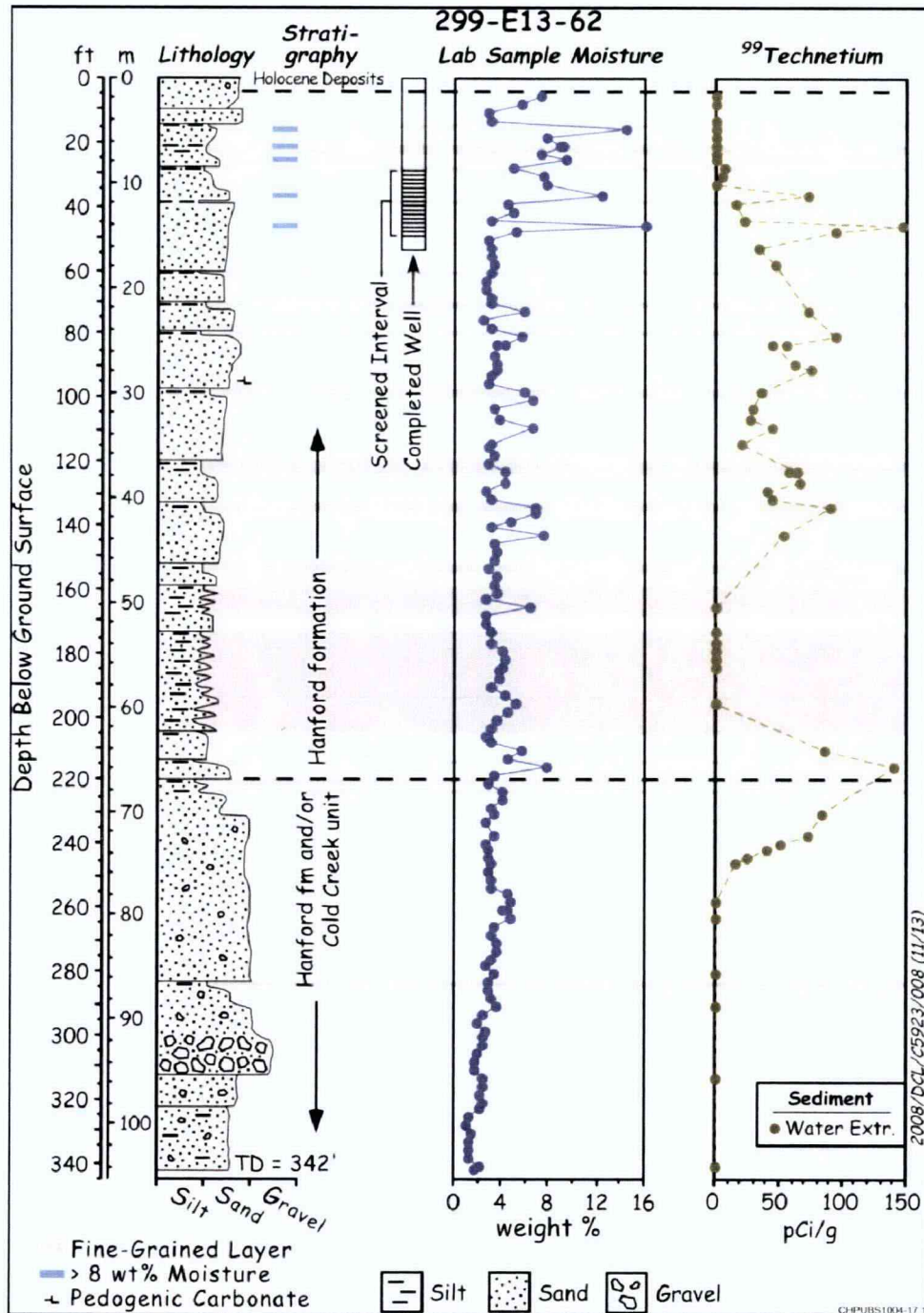


Figure 4-2. Distribution of Tc-99 and Moisture in Well 299-E13-62

Previous characterization efforts have included electrical resistivity measurements to characterize the subsurface distribution of contaminants in three dimensions, borehole sampling, borehole logging, cone penetrometer tip pressure and resistivity logging, air permeameter testing, and air permeability testing. The following relevant test site information has been collected and compiled:

- Sediment air permeability of the targeted desiccation depth interval (PNNL-17821)
- Sediment air permeability contrast as a function of depth at five locations using the air permeameter technique (DOE/RL-2009-119)
- Extracted soil gas humidity, temperature, and pressure at selected volumetric flow rates (DOE/RL-2009-119)
- Quantification of contaminants in the extracted soil gas and extracted water (DOE/RL-2009-119)
- Logging and laboratory sediment data that characterizes the heterogeneity, especially in terms of the distribution of sandy and silty layers within the targeted desiccation depth interval (PNNL-17821)
- Intrinsic properties of key sediment types from borehole samples (PNNL-17821; DOE/RL-2009-119)
- Moisture content distribution at borehole locations (PNNL-17821; DOE/RL-2009-119)
- Permeability-moisture content relationships from borehole samples (PNNL-17821)
- Contaminant distribution from borehole samples and inferred from an electrical resistivity survey (PNNL-17821; PNNL-18800, *Characterization of Sediments from the Soil Desiccation Pilot Test (SDPT) Site in the BC Cribs and Trenches Area*)
- Surface features that may constrain field testing (including configuration of existing wells)

4.2 Experimental Design

The experimental design for the field test is guided by the objectives outlined in Chapter 3. These objectives are targeted at collecting information to support inclusion of soil desiccation as a technology in future CERCLA FSs.

The desiccation technology relies on removal of water from a portion of the subsurface such that the resultant low moisture conditions inhibit downward movement of water and dissolved contaminants. Implementation requires establishing sufficiently dry conditions within the targeted portion of the vadose zone to inhibit downward water transport effectively. Nominally, the targeted zone would need to extend laterally across the portion of the vadose zone where contaminants have the potential to move downward at a flux that will impact groundwater above the remediation objective groundwater concentration. Thus, the experimental design was developed to evaluate the process of establishing a desiccated zone that extends laterally away from a dry air injection well within a specific depth interval of the vadose zone. To obtain this type of desiccation zone, the field test design uses a nitrogen injection/extraction approach with wells screened in the target depth interval to control soil gas flow within this interval. The intent of this approach is to establish a distinct zone of desiccation that can be monitored to evaluate the rate and extent of desiccation based on the operational parameters and field site characteristics.

During active desiccation, above-ground equipment for nitrogen injection and soil gas extraction will be monitored to document operational conditions. Operational monitoring will include the temperature, pressure, humidity, and flow rate of the injected nitrogen and extracted soil gas. Periodic sampling of extracted gas, including condensate, is anticipated.

The experimental design includes in situ monitoring of desiccation progress during the active desiccation process with multiple types of measurements. At selected monitoring locations between the injection and extraction locations, data will be collected to monitor breakthrough of injected nitrogen (i.e., via tracers) and the desiccation front. Data collected at these selected monitoring locations will include gas phase samples (primarily tracer concentrations); in situ temperature, humidity, and soil moisture/pressure monitoring; and vertical profiling of soil moisture with neutron logging. Because the subsurface access and configuration for some of these monitoring techniques are not compatible, clustered subsurface access will be used at each monitoring location. Sweep volume of the injected nitrogen and the volume of the desiccated zone are needed to evaluate desiccation performance. Gas phase tracers, natural (e.g., radon, carbon dioxide) and introduced, will be used to assist in monitoring air flow within the subsurface and to help interpret the soil moisture conditions periodically in the targeted area by use of introduced partitioning tracers. Electrical resistance tomography (ERT) and GPR techniques will be used to provide volumetric information about changes in the subsurface conditions during desiccation and to augment the tracer information. Confirmation borehole sampling will be conducted to evaluate the soil moisture content and contaminant concentrations in the test zone at the end of active desiccation operations. Table 4-1 provides a general description of the in situ monitoring devices. Selected instruments/sensors and monitoring techniques will provide redundancy. An objective of the overall treatability test is to evaluate monitoring instrumentation.

Table 4-1. Overview of In Situ Monitoring Techniques

Instrument	Function
Thermistor	In situ probe that measures temperature. Temperature can be a measure of when the desiccation front passes a location (due to evaporative cooling effect).
Gas Sampler	Samples of soil gas can be used to monitor movement of tracers. Humidity and tracers measure humidity as indicators of desiccation progress. Coupled with an above-ground pressure transducer, soil gas pressure at the monitoring screen location can be measured. Pressure drop between locations is proportional to sediment air permeability. Air permeability will increase as soil dries.
Humidity Sensor	In situ probe to measure humidity in soil gas, with suitability for RH between 0--90%. Humidity will stay near 100% relative humidity until the desiccation front passes.
Thermocouple Psychrometer	In situ probe that collects data to measure soil gas humidity, with suitability for RH>90%.
Heat Dissipation Unit	In situ probe that collects data to calculate sediment water content or pressure. Also measures sediment temperature.
Dual Probe Heat Pulse Sensor	In situ probe that collects data to calculate soil moisture content.
Neutron Probe	Logging to determine vertical soil moisture profile.
Ground Penetrating Radar Probe (Cross-hole Radar)	Two-dimensional or three-dimensional depiction of radar response. Potential to track changes in moisture content by observing differences in radar signal. Used to infer lithology.
Resistivity Electrodes	Allows use of electrical resistance tomography (two-dimensional or three-dimensional depiction of sediment resistance to electrical current). Potential to track changes in moisture content and solute concentration. Response to desiccation will be a combination of drying and increases in solute concentration. Drying increases resistance. Increased solute concentrations decrease resistance.

The duration over which desiccation can inhibit downward movement through the desiccated zone is related to the rate at which the soil moisture in this zone increases to a point where downward transport can continue at a flux that will impact groundwater above the remediation objective. The rate of rewetting is dependent on the properties of the desiccated zone and the conditions in the surrounding vadose zone. As such, the experimental design includes monitoring of the re-wetting rate through monitoring of the desiccated zone and surrounding area after active desiccation is completed.

Once the desiccation process is completed, test operations will switch to long-term monitoring for changes in soil moisture and contaminant concentrations within the targeted treatment zone. Similar to performance monitoring of surface barrier performance, the performance monitoring of desiccation is expected to continue for a long duration. Methods of monitoring include gas-phase samples (relative humidity, and tracer concentration); in situ temperature, humidity, and soil moisture/pressure monitoring; and vertical profiling of soil moisture with neutron logging. Confirmation borehole sampling and, if warranted, in situ sensor deployment will be conducted periodically to evaluate the soil moisture content and contaminant concentrations in the test zone.

4.2.1 Technical Basis

Technical bases are provided below for the moisture reduction target, the rate of moisture reduction, and the zone of pressure influence.

4.2.1.1 Moisture Reduction Target

The moisture reduction target is defined using a combination of scoping calculations and numerical simulation.

4.2.1.2 Scoping Calculations

The moisture content in borehole 299-E13-62 is nominally 10 wt percent within the 9.1 m to 15.2 m (30 ft to 50 ft) bgs region (peak moisture content is near 16 wt percent) selected for the field test. The 2005 Vadose Zone Technical Panel provided a means to examine reduction in flux as a function of reduction in water content. Text from the Vadose Zone Technical Panel report Appendix D (WMP-27397) is presented as follows:

In deep vadose zones, gravity forces dominate water flow and as a result an (almost) steady downward flux develops below the root zone (Eq. [1]). This long-term flux q (L/T) determines the water content $\theta(L/L_3)$ in the vadose zone and in the absence of capillary forces

$$q = K(\theta) \quad [1]$$

where:

$K(\theta)$ is the unsaturated hydraulic conductivity (L/T) at water content θ .

The convective flux of solutes J (M/T) is

$$J = q C = K(\theta) * C(\theta) \quad [2]$$

where:

C is the concentration of the solutes (m/L³)

As shown in Eq. [2], both the downward flux q and concentration C depend on the volumetric water content θ . If the water content decreases due to desiccation, the flux will

decrease and the solute concentration will increase. The increase of the solute concentration is a linear function of the decrease in water content, while the decrease of the unsaturated hydraulic conductivity and downward flux is a strongly non-linear function of the decrease in water content. Therefore, it is expected that the convective solute flux will decrease after desiccation in a deep homogeneous vadose zone where gravity-driven steady-state flow dominates. For example, the solute flux in loamy sand is calculated using Eq. [2] assuming a solute concentration at saturation of 1,000 ppm.

The logarithm of the solute flux is plotted against volumetric water content (Figure 4-3). If the media becomes drier, the solute flux dramatically decreases, because the decrease of the water flux is much larger than the increase in solute concentration. These theoretical results, based on steady-state flow in the deep vadose zone, make desiccation an attractive remediation strategy.

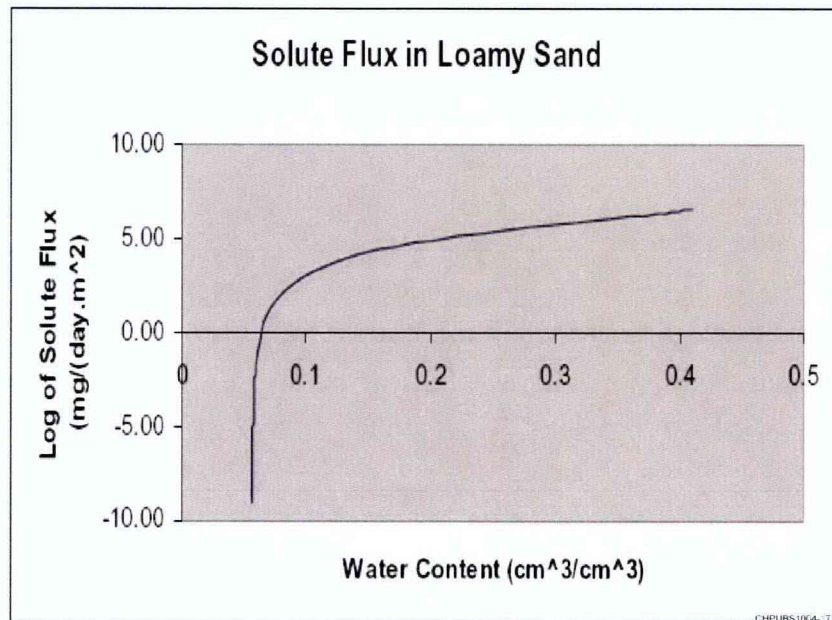


Figure 4-3. Logarithm of Solute Flux Through Deep Vadose Zone of Loamy Sand with Gravity-Driven Steady-State Flow as a Function of Volumetric Water Content

The 10 wt percent average water content is approximately 0.18 volumetric water content. Cutting this initial value in half to 5 wt percent would result in a volumetric water content of about 0.09, which is at the beginning of the steep part of the flux curve shown in Figure 4-3. Thus, as a first approximation, cutting the water content in half is a relevant target to create a significant reduction in flux.

The above analysis is for steady-state flow conditions. Note that the water content flux relationship for each type of layer present in the subsurface is different, and this analysis does not account for a layered system or the impact of capillary breaks. An overall reduction of moisture content by 5 wt percent would be expected to result in some layers having a much lower endpoint moisture content and some layers having a higher endpoint moisture content.

The 2005 Vadose Zone Technical Panel also indicated that under transient flow conditions, the effect of increased solute concentrations caused by desiccation may create conditions leading to a higher flux at the water table, although this flux is substantially delayed in time compared to base case conditions

(Appendix D of WMP-27397). The transient analysis was for a homogeneous subsurface using a one-dimensional model. The following section describes additional modeling that has been conducted to evaluate transient flow conditions.

4.2.1.3 Numerical Simulation

Simulations were conducted to provide initial estimates for the impact of desiccation at a larger scale as input to setting desiccation performance targets for the field test. Simulations examined different desiccation scenarios, including variations in the desiccation target endpoint, location, and configuration for the desiccation zone, and the surface infiltration conditions. The simulations were conducted using the same model configuration as described in PNNL-14907. The model is for the trench portion of the BC Cribs and Trenches Site, centered on the B-26 trench where borehole C4191 was installed. In PNNL-14907, simulations examined the impact of different surface infiltration conditions on contaminant transport. The work reported below extends these simulations to include selected desiccation scenarios.

These simulations need to be interpreted with respect to the impact of desiccation on contaminant flux with the two significant considerations. First, the simulations did not include water vapor transport. In addition, all imposed desiccation zones and surface infiltration conditions extended laterally across the entire model domain; thus, no lateral water movement into the desiccated zone was considered. These two configuration constraints limit interpretation of the results to desiccation performance under conditions of advective downward water movement.

The irreducible water saturation from the PNNL-14907 model equates to a lower bound of the moisture content of about 1 to 2 wt percent depending on the particle size distribution in the grid cell. The model configuration is highly heterogeneous where each model node may have different properties. As an example, the relationship between matric potential and moisture content is shown in Figure 4-4 for three different sediments within the domain. With this configuration, the model truncates desiccation at this lower bound of moisture content, and effects of lower moisture conditions on water migration are, therefore, not included in the simulations. As such, the simulation results would tend to underestimate the impact of desiccation on moisture movement if desiccation could result in lower endpoint moisture content as has been observed in laboratory experiments. However, the simulations may also underestimate the impact of solute concentration in the desiccated zone.

Technical Approach

To determine the potential impact of soil desiccation on aqueous and contaminant fluxes in the vadose zone and groundwater, simulations were executed with an imposed desiccated zone beneath the 216-B-26 trench area. This site was selected for investigation due to its proximity to the crib field site, and because a detailed fate and transport analysis had already been performed and could be used for comparison (PNNL-14907). Although the process of desiccation is best represented using governing equations for water, air, and energy transport, the simulations conducted in this investigation assumed that desiccation had already taken place. Hence, only water flow and contaminant transport were simulated using the water mode in the Subsurface Transport Over Multiple Phases (STOMP) simulator. Vapor transport was also not included in these simulations, although later simulations will incorporate vapor transport based on the results of planned laboratory testing. All simulations were executed on Linux workstations.

Physical Domain

Because the simulation was set up in the same manner as reported in PNNL-14907, the simulation domain is only briefly described here. The physical domain represented a two-dimensional north-south cross-section through trenches 216-B-52 at the north to 216-B-28 to the south. The domain consisted of 70 nodes in the x-direction and 1,322 in the vertical, yielding a total of 92,540 nodes. A unit meter thickness was used for the two-dimensional cross-section.

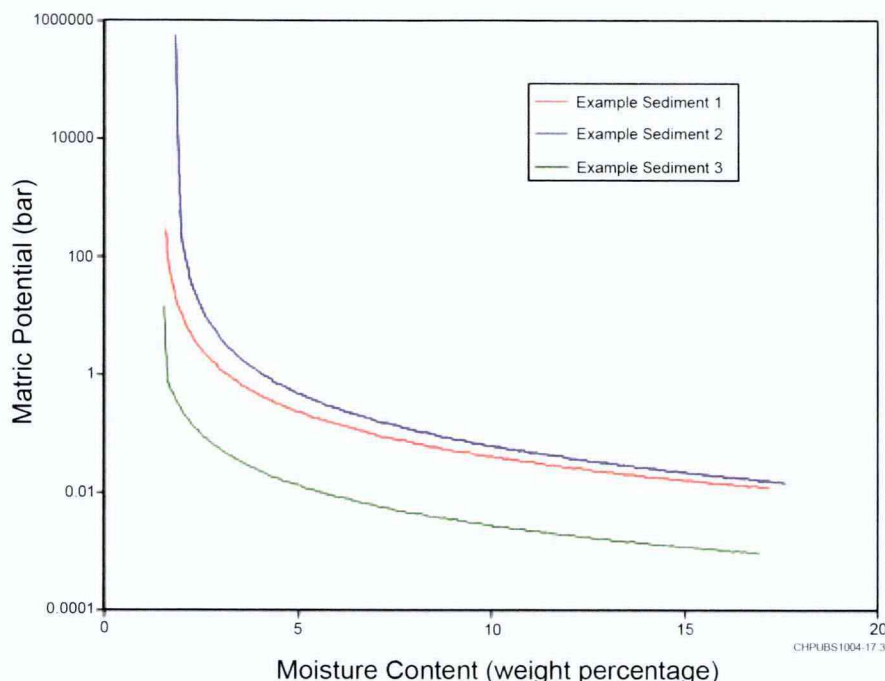


Figure 4-4. Examples of Modeled Relationship Between Moisture Content and Matric Potential

The physical domain was discretized using a Cartesian grid, with variable horizontal spacing, and a fixed spacing in the vertical. Because water has been observed to leave the monitored domain at the 299-E24-111 test site via fine-textured layers, the horizontal scale of the modeling domain was increased by 400 m (1,312.3 ft) on each of the horizontal boundaries. In the horizontal, the computational domain extended over a distance of 1,036.5 m (3,400.6 ft) in the north-south direction, including the 400 m (1,312.3 ft) extensions on both sides of the domain. The vertical spacing in the vadose zone was 0.075 m (0.25 ft). The water table was located at 103.17 m (338.5 ft) below the surface, and a 5-m (16.4-ft) thick unconfined aquifer was assumed beneath the water table. Thus, in the vertical, the domain extended 108.17 m (354.9 ft).

The stratigraphy at this site shows extensive layering resulting from an alluvial depositional environment. The two-dimensional cross-section is equivalent to section Q'-Q'' in RHO-LD-45, and provided the gross stratigraphy for the site. Small-scale heterogeneities were derived from grain-size distributions used in conjunction with high-resolution neutron logs from surrounding boreholes. Every cell in the domain was assigned unique hydraulic and transport properties derived from the small-scale heterogeneity analysis. The Brooks and Corey (1964) relationship was used to describe the pressure saturation curve.

Boundary Conditions and Source Terms

A no-flow boundary was assigned at the bottom of the domain to represent the base of the 5-m (16.4-ft) thick confined aquifer at 108.17 m (354.9 ft). Vertical boundaries were designated as zero-flux boundaries for water flow and solute transport. Groundwater was assumed to flow in a southerly direction under a gradient of 1.486×10^{-3} m/m (1.783 in./ft). Thus, the south boundary of the aquifer was assigned a hydrostatic pressure distribution that allowed water and solutes to flow out. The north boundary of the aquifer was treated as a flux boundary with a steady influx of water at a Darcy velocity of 0.24 m/day (0.8 ft/day). Recharge conditions at the top boundary were varied for the different simulation periods and are described in the following subsection (*Simulation Execution*).

Source terms consisted of fluid and contaminant discharges to the series of trenches during the period of trench operations. Fluid volumes and inventory were determined by the median values predicted by the soil inventory model run for August 18, 2004, and then adjusted to account for the two-dimensional slice used to represent the three-dimensional domain. The complete time history of fluid and contaminant discharges is summarized in PNNL-14907. Fluid discharges are reported to have started in late 1956 and ended in early 1957 for most trenches, except for the 216-B-52 Trench, which was operational until 1958. During the operational period, 37,044 m³ (37 million L or 9,774,365.4 gal) of fluids were applied. On average, Trenches 216-B-23 through 216-B-28 received around 4,752 m³ (4,752,000 L or 1,255,345.5 gal) of discharge, while Trench 216-B-52 received 8,529 m³ (8,529,000 L or 2,253,123.3 gal).

Simulation Execution

The simulations were first initiated with a steady flow field to simulate the period before construction and operation of the trenches. In this stage, nodes representing the trenches were inactive, and the recharge boundary condition was applied over the trench bottom at a rate of 77 mm/yr (3 in./yr). The steady flow condition was then obtained by simulating flow from time zero to the year 1956 with a constant recharge rate representative of the pre-Hanford operation phase. Establishment of the initial condition focused only on the subsurface distribution of water as it was assumed that all contaminant inventories were zero.

In the second phase, the simulations were re-executed from the PNNL-14907 analysis. The steady flow solution was used as an initial condition for the period 1956-2012, which includes the years in which the contaminant discharges occurred (1956-1958) until the year in which a surface barrier is presumed to be installed (2012). The second stage represented the period after trench operations following backfilling of the trenches. During this stage, the inactive trench nodes were converted to active nodes with a material type identical to the material surrounding the trenches. From 1956-1982, recharge was applied at the top boundary at a rate of 77 mm/yr (3 in./yr), the estimated rate during trench operations (PNNL-14907). In 1982, the recharge was reduced to 25 mm/yr (1 in./yr), to represent post-operational conditions.

Both flow and contaminant transport was simulated for Tc-99, which is one of the contaminants of concern reported in PNNL-14907. The simulated Tc-99 distribution in the year 2012 is shown in Figure 4-5, which contains ~0.812 Ci per unit width in the two-dimensional domain. The focus of this investigation was on the transport behavior of Tc-99.

In the third phase of the simulation, a surface barrier was imposed. Three different recharge rates were assumed: 0.5 mm/yr (0.02 in./yr), 3.5 mm/yr (0.14 in./yr), and 25 mm/yr (1 in./yr) to represent a surface barrier, a degraded barrier, and a sparsely vegetated surface, respectively. In this stage, the simulations departed from those executed in PNNL-14907 by imposing a desiccated zone on the final condition simulated in the second stage for the year 2012. This was accomplished by overwriting the pressure distribution for a selected zone. Six different zones were selected based on the distribution of Tc-99 measured in the subsurface (Figure 4-6) and are listed in Table 4-2 along with the shorthand notation used to describe each set of scenarios. A range of initial pressures was also assumed for the desiccated zone to determine flow and transport behavior associated with the extent of desiccation (-0.5, -1.0, -2.5 and -5.0 bars).

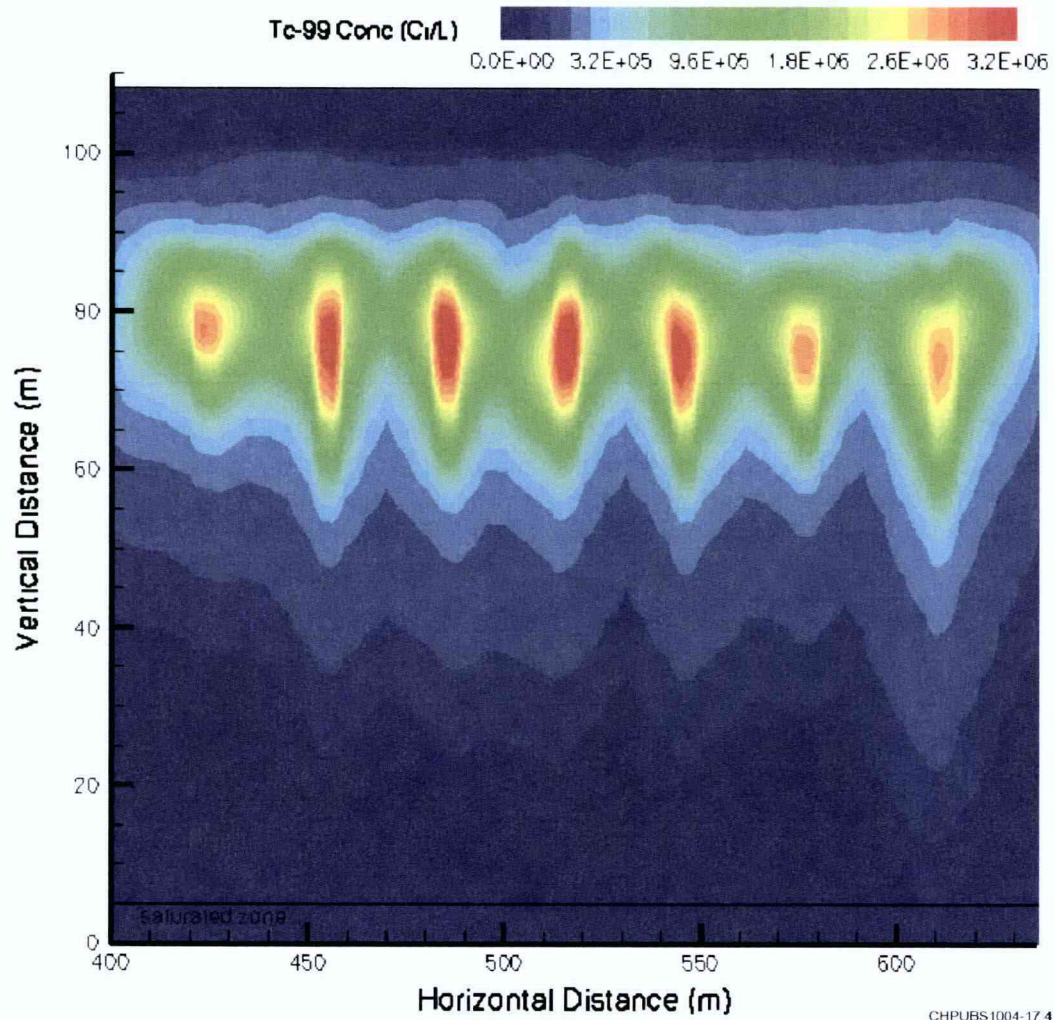
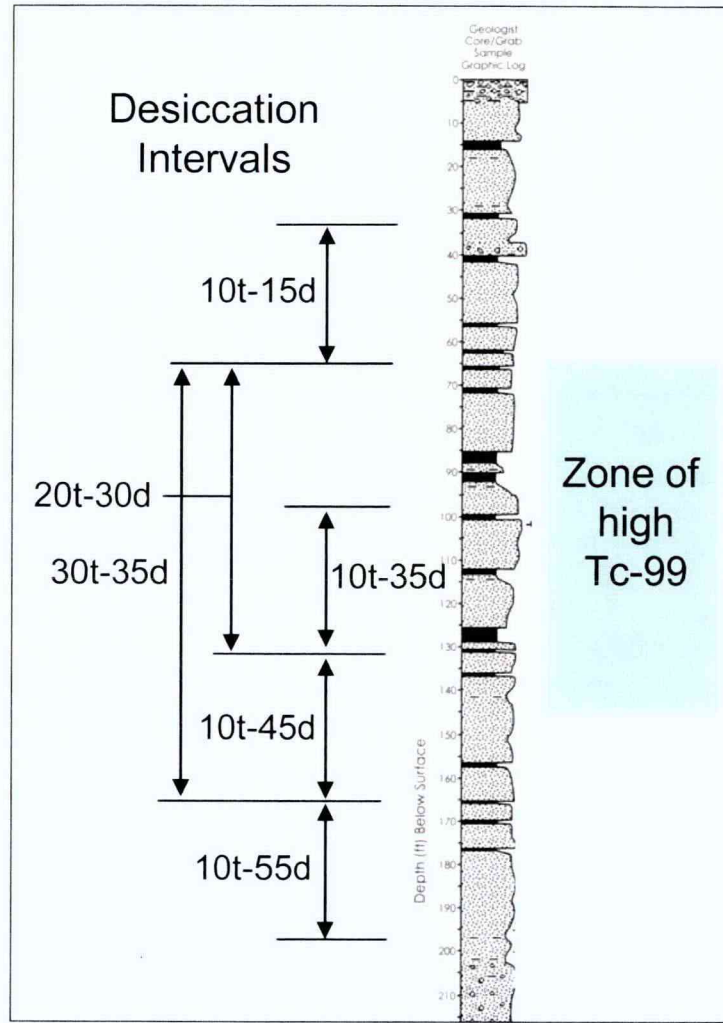


Figure 4-5. Distribution of Tc-99 in the Vadose Zone in the Year 2012



Notes:

Data are available as presented in PNNL-14907. Desiccation intervals are designated as Xt-Yd, where X is the thickness of the zone (meters) and Y is the mid-depth of the zone (in m bgs).

Figure 4-6. Selection of Targeted Desiccation Zones Based on Available Borehole Data

Table 4-2. Mid-Depths and Thicknesses for the Imposed Desiccated Zones and Shorthand Notation for the Different Scenarios

Thickness (m [ft])	Mid-Depth (m [ft] bgs)	Scenario Abbreviation
10 (32.8)	15 (49.2)	10t-15d
10 (32.8)	35 (114.8)	10t-35d
10 (32.8)	45 (147.6)	10t-45d
10 (32.8)	55 (180.5)	10t-55d
20 (65.6)	30 (98.4)	20t-30d
30 (98.4)	35 (114.8)	30t-35d

Given the 6 different zones, and 4 different initial pressures for the zones of desiccation, 24 simulations were executed for a given recharge rate. All of the simulations were executed from the year 2012-12005 (i.e., the simulation period assumed in the PNNL-14907). In addition to the imposed desiccation scenarios, scenarios without an imposed desiccation zone were simulated using both a barrier and no barrier recharge rate. These simulations were used for comparison to the transient flow and transport behavior of the desiccation scenarios. Aqueous fluxes and moisture content distributions were examined to determine impacts from the imposed desiccated zones. Mass fluxes and cumulative mass for Tc-99 entering the water table were also generated. Simulation results were written to three types of output files: (1) files echoing the input and reference node file, (2) a series of plot files that report a spatial distribution of selected variables over time, and (3) a series of surface flux files to track the flux of water and contaminants across selected surfaces in the domain. The output file contains the input file echo, as well as data for selected nodes, and the OutputTo.pl program was used to convert the data to a time series suitable for plotting with Gnuplot. Plot files contain variable data for all grid points at selected simulation times. These files were used to generate color scaled plots and animations through Tecplot. A utility program, PlotTo.pl, was used to translate STOMP plot files into Tecplot-formatted input files. A utility program, mcCalc.x, was used to calculate the integrated water content from the STOMP plot files for a user-defined zone. Surface-flux files contain rate and integral information on fluxes crossing user-defined internal or external boundaries. A utility program, surfcalc.x was used to translate STOMP surface-flux files into formatted input files suitable for plotting with Gnuplot.

Results

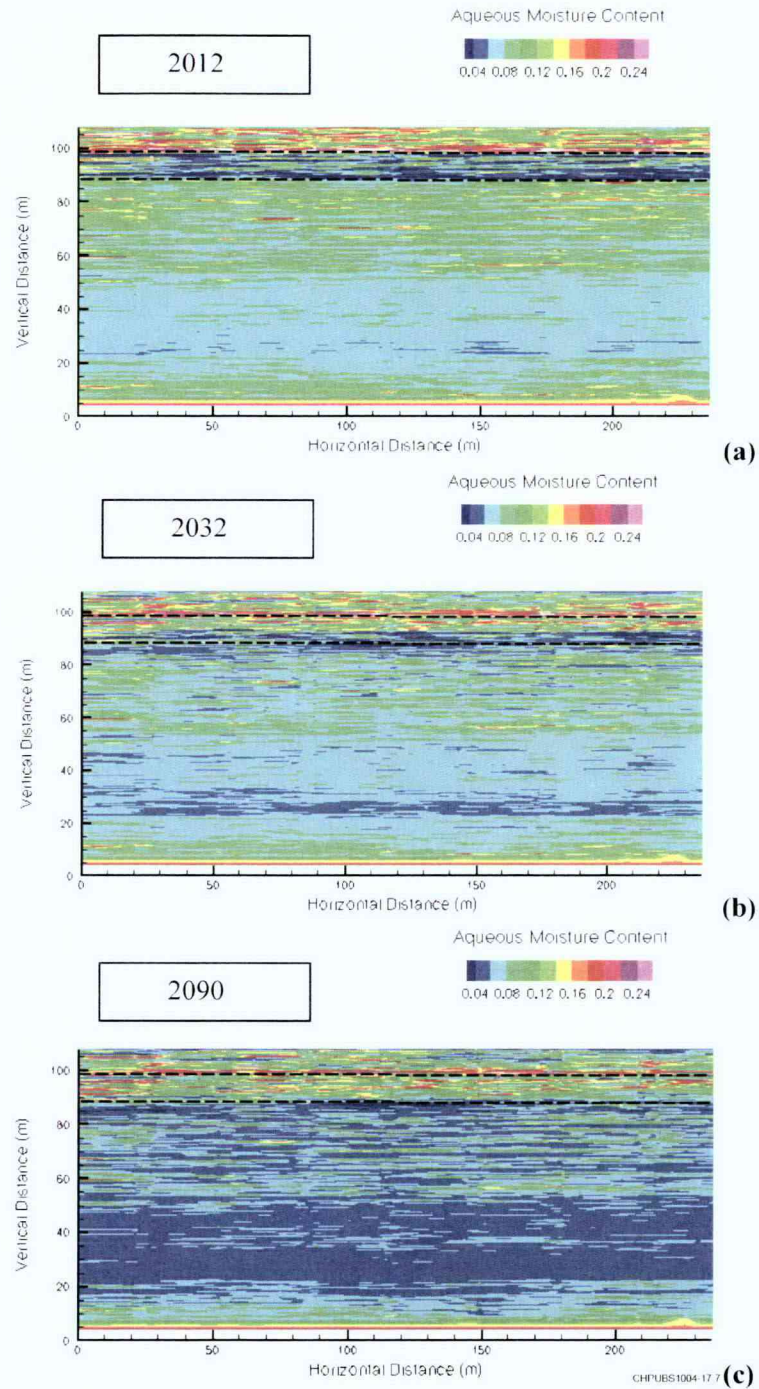
Simulation results were examined to provide insight into temporal moisture conditions that lead to wetting of the desiccated zone, and to evaluate the impact of desiccation on contaminant migration. Because the simulations did not include water vapor transport, or lateral water movement into the desiccated zone, the simulations can only provide insight into desiccation performance under conditions of downward water movement through the vadose zone.

Temporal Changes Predicted Within the Desiccated Zone

An understanding of how moisture is redistributed in the vadose zone following a period of desiccation is useful to interpret the performance of a desiccated zone. The results examining the temporal changes within the desiccation zone are focused on the 0.5 mm/yr (0.02 in./yr) surface infiltration condition. The basic trends for the 3.5 mm/yr (0.14 in./yr) case are similar to those presented for the 0.5 mm/yr (0.02 in./yr) case.

The temporal dynamics of moisture content for the entire domain were depicted via animations of the moisture content. Figure 4-7 through Figure 4-10 are selected slides from these animations showing a progression of the moisture content for -5 bar imposed desiccation in the 10t-15d case, 10t-35d case, 10t-45d case, and the 30t-35d case, respectively. These figures depict how the benefit of desiccation propagates in time and is related to desiccation zone configuration (location and thickness). The figures also suggest that multiple application of desiccation may be beneficial to mitigate moisture transport.

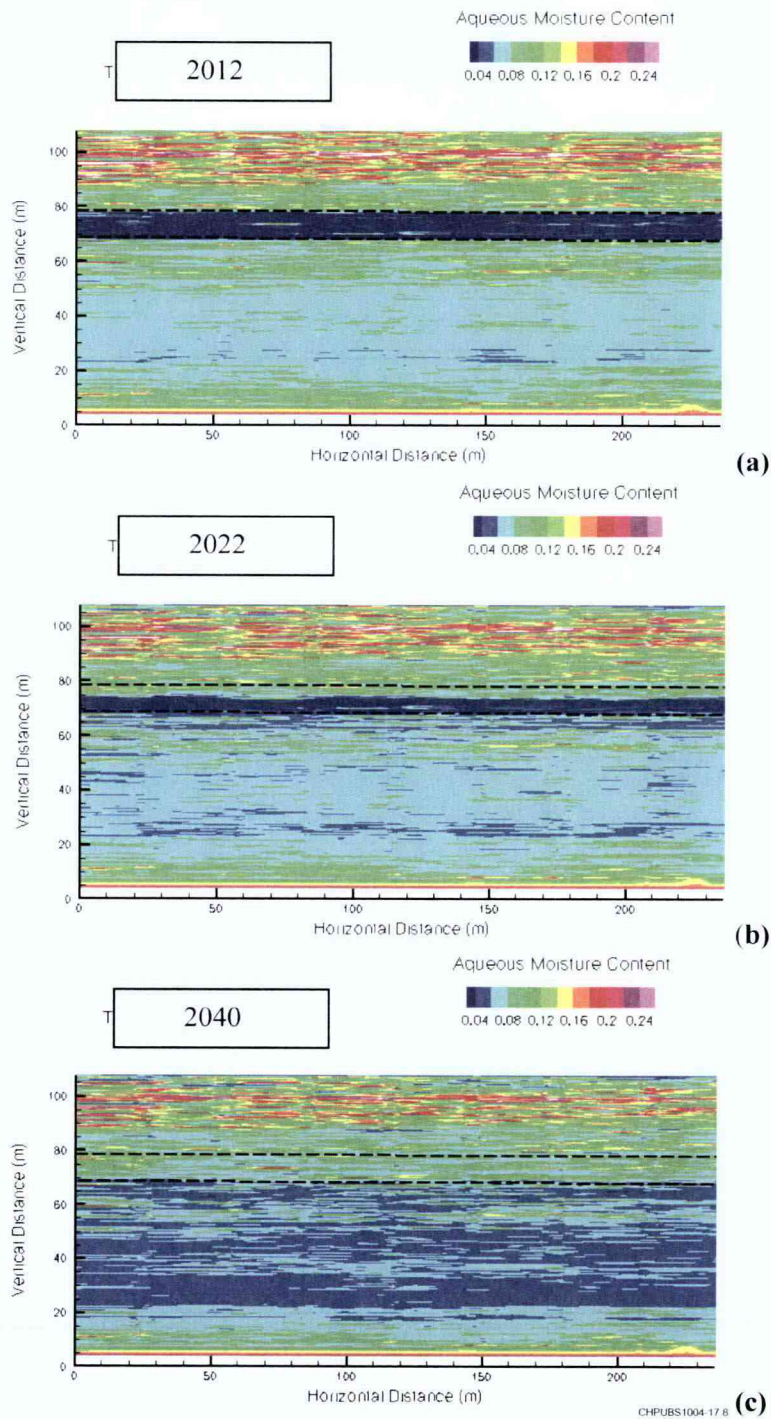
The figures provide a visual depiction of the imposed desiccation zone and post-desiccation water movement. For further evaluation of the temporal aspects of water migration through a desiccated zone, the total integrated water content in the desiccation zone was also tracked as a function of time to evaluate how the desiccated zone rewets.



Notes:

- a. Just after imposed desiccation (year 2012)
- b. When the desiccated zone is half rewetted (year 2032)
- c. When the desiccated zone is fully rewetted (year 2090)

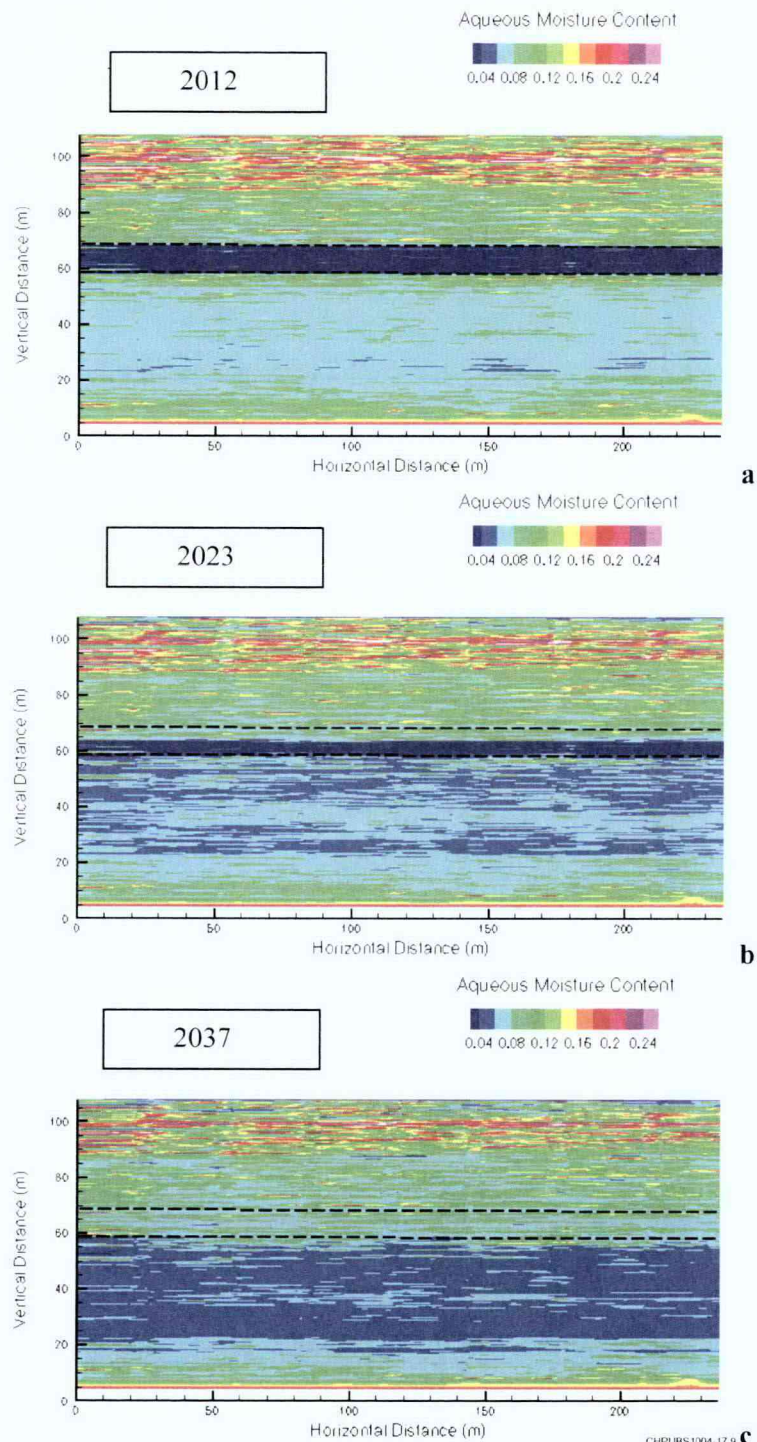
Figure 4-7. Case 10t-15d Simulated Moisture Content Distribution



Notes:

- a. Just after imposed desiccation (year 2012)
- b. When the desiccated zone is half rewetted (year 2022)
- c. When the desiccated zone is fully rewetted (year 2040)

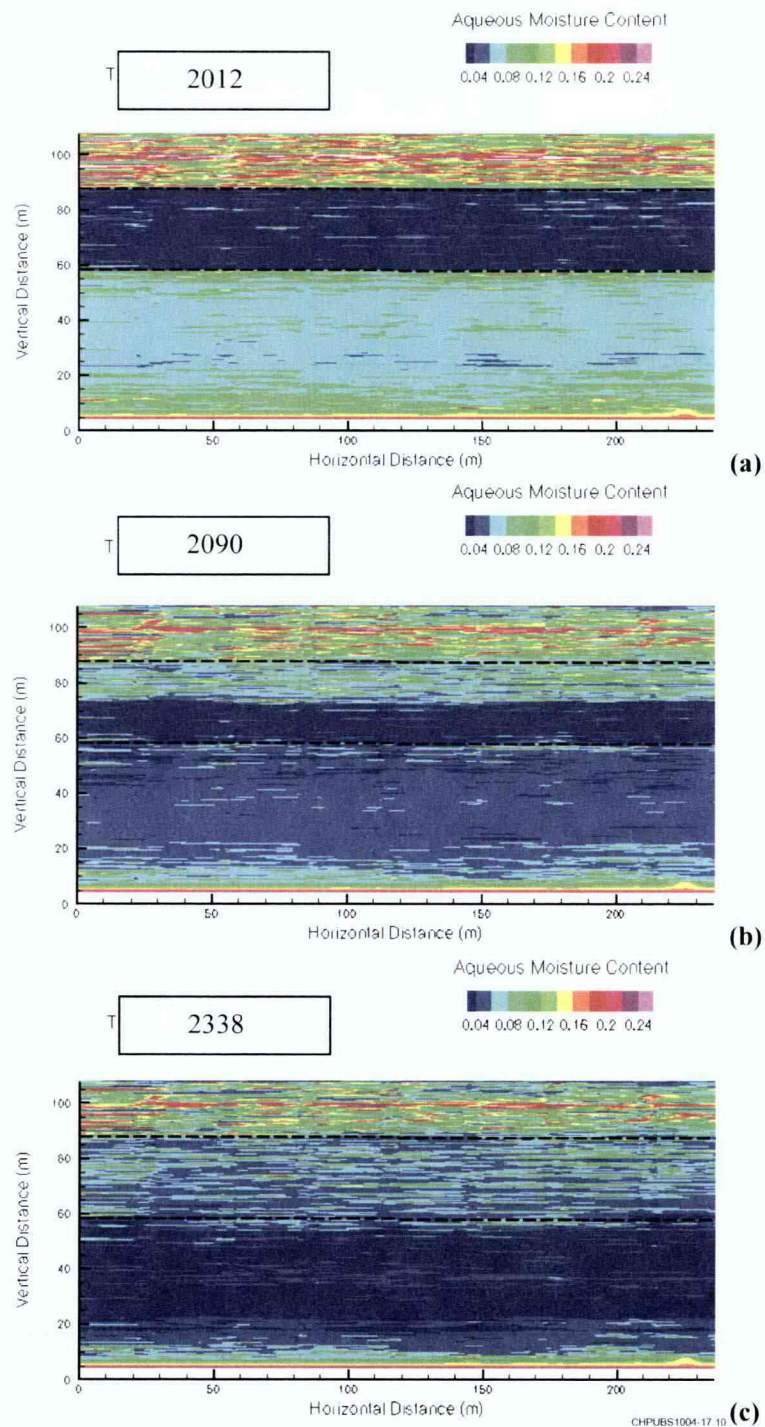
Figure 4-8. Case 10t-35d Simulated Moisture Content Distribution



Notes:

- a. Just after imposed desiccation (year 2023)
- b. When the desiccated zone is half rewetted (year 2032)
- c. When the desiccated zone is fully rewetted (year 2037)

Figure 4-9. Case 10t-45d Simulated Moisture Content Distribution

**Notes:**

- a. Just after imposed desiccation (year 2012)
- b. When the desiccated zone is half rewetted (year 2090)
- c. When the desiccated zone is fully rewetted (year 2338)

Figure 4-10. Case 30t-35d Simulated Moisture Content Distribution

The total integrated water content (per meter thickness) in the desiccation zone is shown with time in Figure 4-11. These plots illustrate the timeframe for the aqueous flux to return the desiccation zone to moisture conditions associated with water movement controlled by the surface barrier. As expected, Figure 4-11 illustrates that the thickness of the desiccated zone has a large impact on the time period required to rewet the desiccated zone completely. The magnitude of flux into the top of the desiccated zone is also important; for instance, where the time scale for rewetting of the 10t-15d case is longer because it is close to the surface and the aqueous flux into this zone is relatively lower than for the other desiccation zones. The total integrated water content in the desiccated zone is shown with time for the multiple desiccation applications (Figure 4-12). Applying desiccation multiple times in the near term can continue to interrupt water drainage and limit the flux of water and contaminants in the subsurface. Impacts of these near term applications of desiccation help the flux stay low over long time periods.

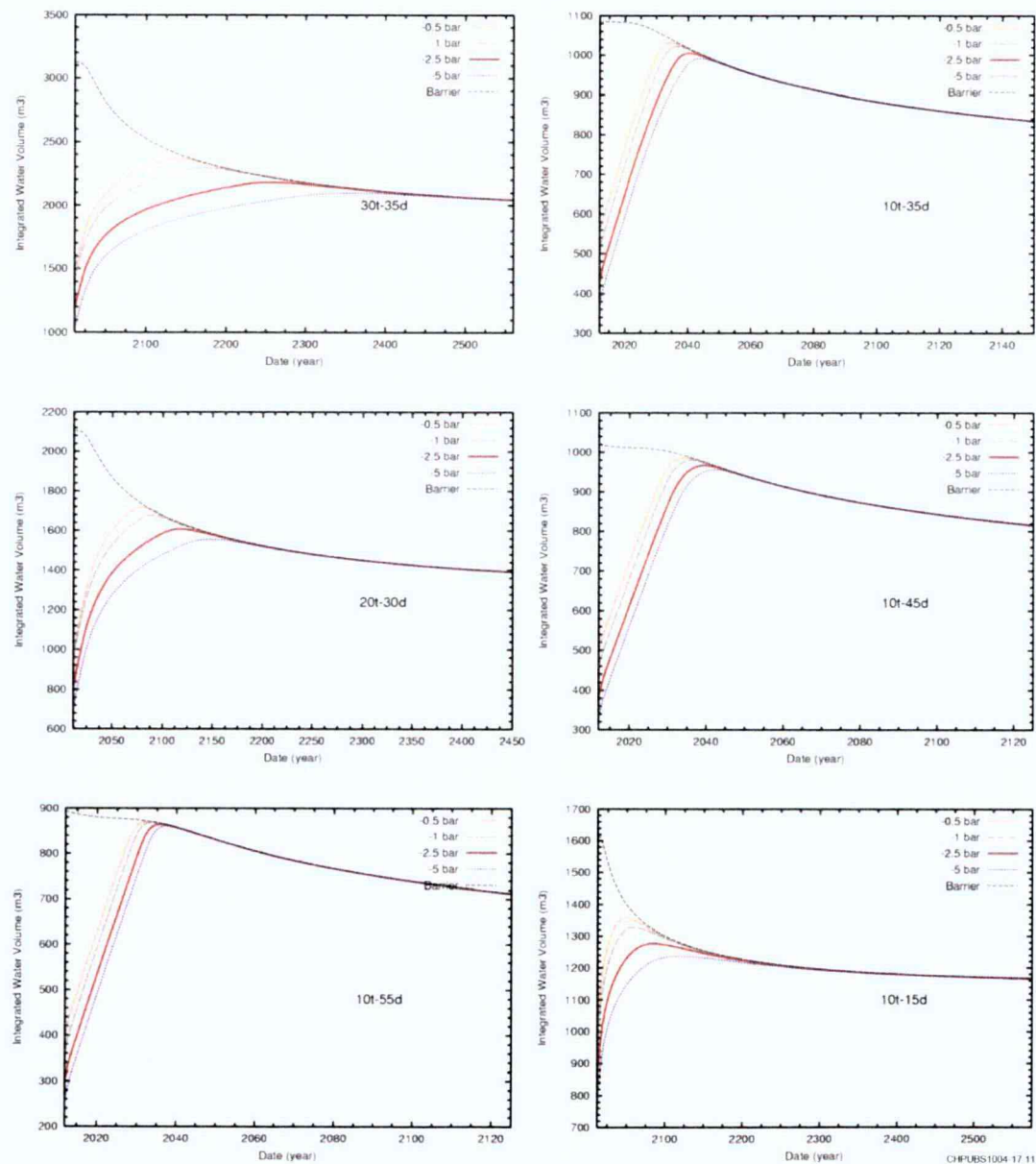


Figure 4-11. Moisture Content Within the Desiccated Zone

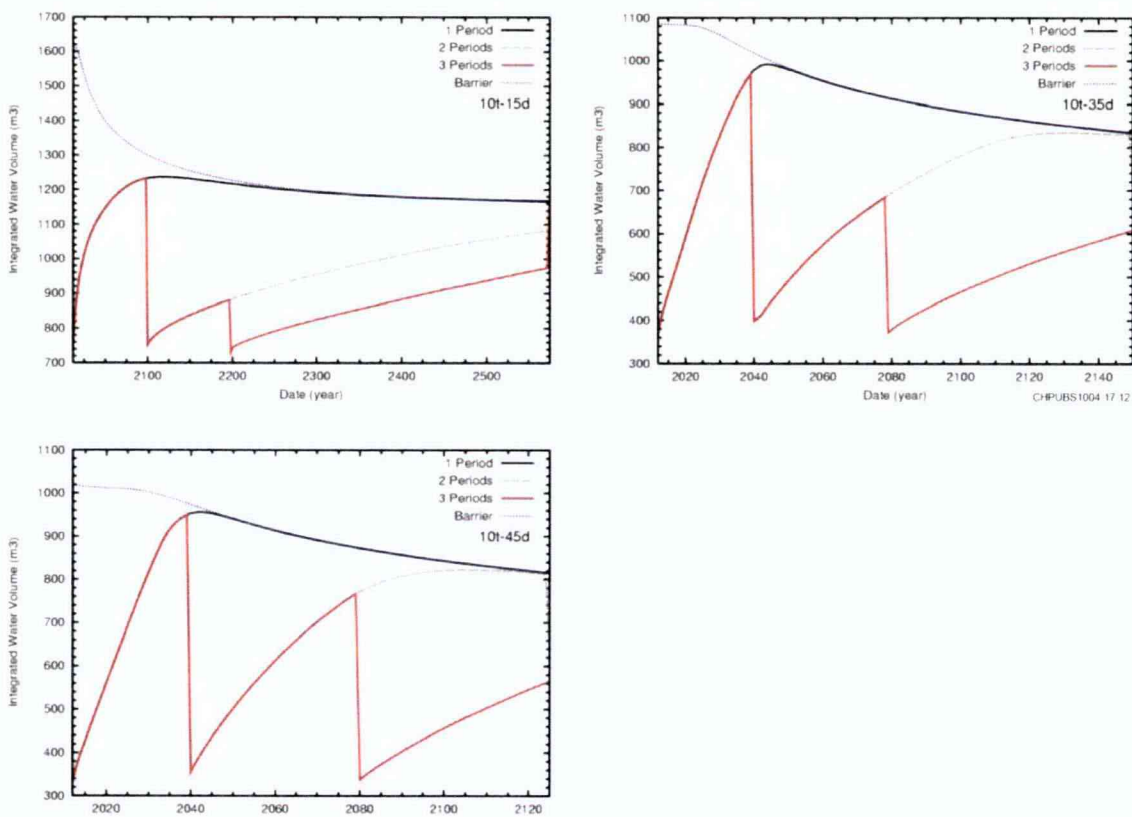


Figure 4-12. Moisture Content Within the Desiccated Zone for Multiple Desiccation Applications

Desiccation Impact on Contaminant Migration

Several metrics were applied to evaluate how the configuration (depth, thickness, and whether or not the zone is within the contaminated interval) and moisture content/matric potential within a desiccation zone impact contaminant migration to the groundwater. As indicated in discussion earlier, each combination of configuration and desiccation zone moisture content/matric potential was evaluated for three different surface infiltration conditions: 0.5 mm/yr (0.02 in./yr), 3.5 mm/yr (0.14 in./yr), and 25 mm/yr (1 in./yr). For each metric, results were plotted showing the metric for each imposed desiccation zone matric potential, the barrier case (e.g., the imposed surface infiltration condition of 0.5 mm/yr [0.02 in./yr]), the degraded barrier case (e.g., the imposed surface infiltration condition of 3.5 mm/yr [0.14 in./yr]), and the no barrier case (e.g., the 25 mm/yr [1 in./yr] infiltration condition with no imposed desiccation) with a separate plot for each configuration.

Presentation of results focuses on the 0.5 mm/yr (0.02 in./yr) and 3.5 mm/yr (0.14 in./yr) surface conditions because desiccation had negligible impact on contaminant migration for the 25 mm/yr (1 in./yr) surface condition. Additionally, results focus on the -0.5 through -5 bar imposed matric potential because there were only incremental differences at the -10 and -20 matric potential conditions. There may be a significant effect of imposing dryer conditions in the field, but configuration of the simulations imposed an irreducible water content corresponding to between 1 and 2 wt percent water and were, therefore, not configured to provide an accurate evaluation of dryer conditions. Laboratory tests are underway to provide the technical basis for evaluating the impact of dryer conditions on rewetting and advection post desiccation.

To help interpret the starting conditions for each case, the total quantity of water removed (per unit thickness) by the imposed desiccation condition was compiled (Table 4-3). The total quantity of water removed is, as expected, a function of the desiccation zone thickness. However, it also varies with the depth of the desiccation zone because the initial moisture conditions also vary with depth. For instance, the 10t-15d case removes significantly more water than any of the other 10-m (32.8-ft) thick cases due to the elevated initial moisture content in this zone.

Table 4-3. Water Removed from Desiccation Zone When Desiccation Condition is Imposed

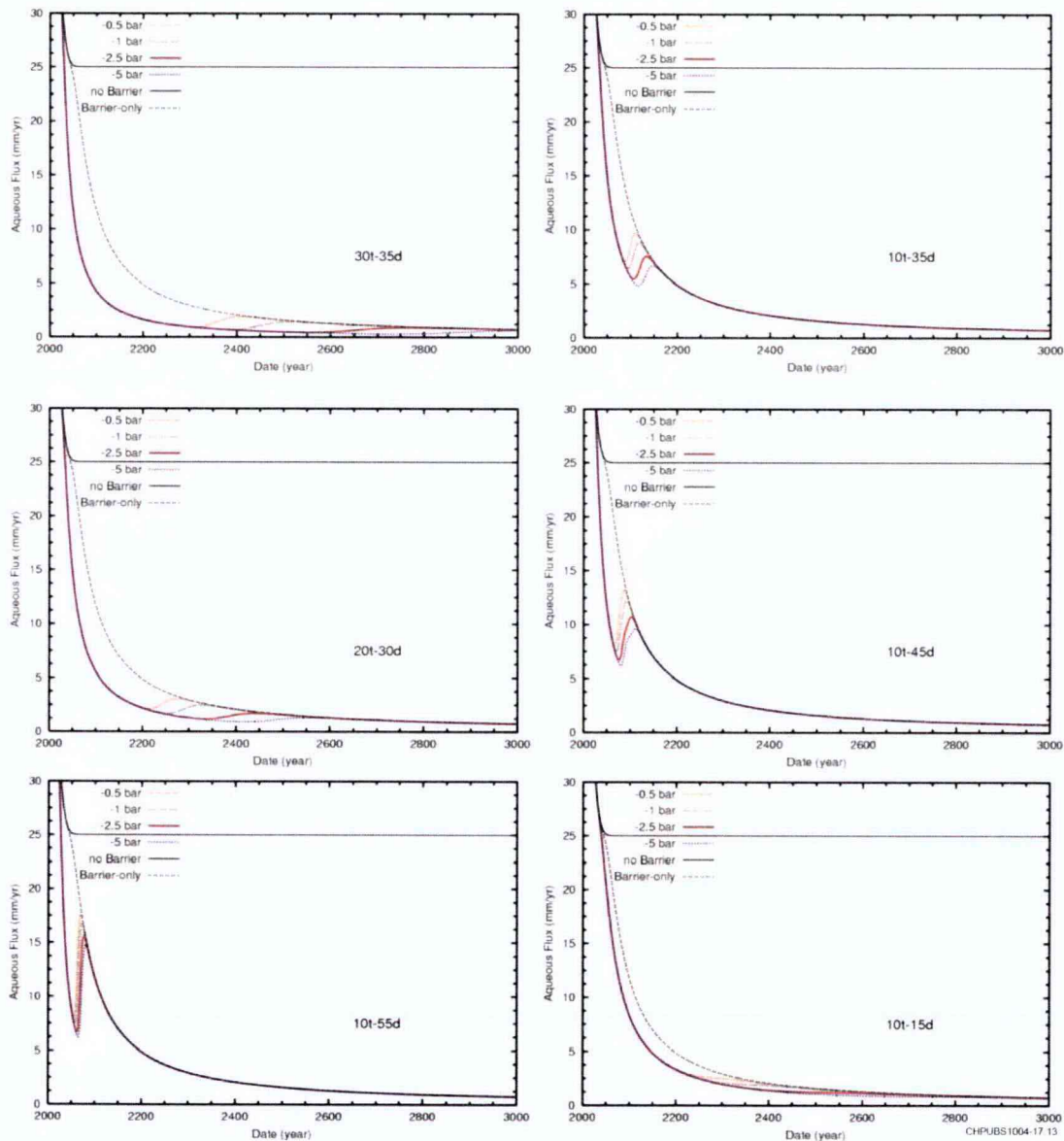
Imposed Pressure (bar)	10t-15d (m³/m [ft³/ft])	10t-35d (m³/m [ft³/ft])	10t-45d (m³/m [ft³/ft])	10t-55d (m³/m [ft³/ft])	20t-30d (m³/m [ft³/ft])	30t-35d (m³/m [ft³/ft])
-0.5	543 (5,844)	467 (5,026)	447 (4,811)	437 (4,703)	942 (10,139)	1,392 (14,982)
-1	601 (6,467)	505 (5,435)	483 (5,199)	471 (5,069)	1,023 (11,011)	1,508 (16,231)
-2.5	700 (7,534)	568 (6,113)	539 (5,801)	524 (5,640)	1,151 (12,388)	1,693 (18,221)
-5	778 (8,374)	615 (6,619)	581 (6,253)	563 (6,060)	1,248 (13,432)	1,833 (19,729)
-10	849 (9,138)	656 (7,061)	618 (6,652)	597 (6,426)	1,332 (14,336)	1,953 (21,020)
-20	911 (9,805)	689 (7,415)	647 (6,964)	623 (6,705)	1,400 (15,068)	2,051 (22,075)

The first metric was the temporal profile of average water flux in the domain across the water table from the vadose zone to the groundwater. Comparisons between different cases for this metric show the duration and extent of changes to the water flux caused by the desiccation condition. Results for the desiccation configurations in combination with 0.5 mm/yr (0.02 in./yr) and 3.5 mm/yr (0.14 in./yr) surface infiltration conditions are shown in Figure 4-13 and Figure 4-14, respectively. In all cases, desiccation causes a temporary reduction in water flux across the water table. The water flux then returns to match the flux profile of the barrier-only surface infiltration condition. The characteristics of the change in water flux are most strongly impacted by the quantity of water removed (thickness of desiccation zone and initial water content) and the amount of water above the desiccated zone (i.e., depth of desiccation zone). The imposed matric potential, within the range of -0.5 bar to -5 bar, has a minor effect on the water flux.

Another metric was the cumulative mass of Tc-99 transferred from the vadose zone to the groundwater. Comparisons between different cases for this metric show how the desiccation condition delayed migration of technetium into the groundwater compared to the barrier-only case (e.g., the case with the same surface infiltration condition). In all cases, the cumulative mass approaches the same maximum demonstrating conservation of mass in the model. This result also illustrates that the primary impact of surface barriers and desiccation is to reduce the flux of contaminant to the groundwater, but not to immobilize technetium permanently. Results for the desiccation configurations in combination with 0.5 mm/yr (0.02 in./yr) and 3.5 mm/yr (0.14 in./yr) surface infiltration conditions are shown in Figure 4-15 and Figure 4-16, respectively. In all cases, desiccation causes a delay in migration to the water table, although the delay is small for some of the desiccation configurations. The characteristics of the delay are most strongly impacted by the quantity of water removed (thickness of desiccation zone and initial water content), the amount of water above the desiccated zone (i.e., depth of desiccation zone), and whether or not the desiccation zone was within the contaminated interval. For instance, the 10t-35d, 10t-45d, 20t-30d, and 30t-35d cases desiccate contaminated intervals. In these cases, the onset of contaminant mass into the groundwater is delayed compared to the barrier-only case. However, the slope of the cumulative mass curve is steeper than the barrier-only case. For the 10t-15d and 10t-55d cases that

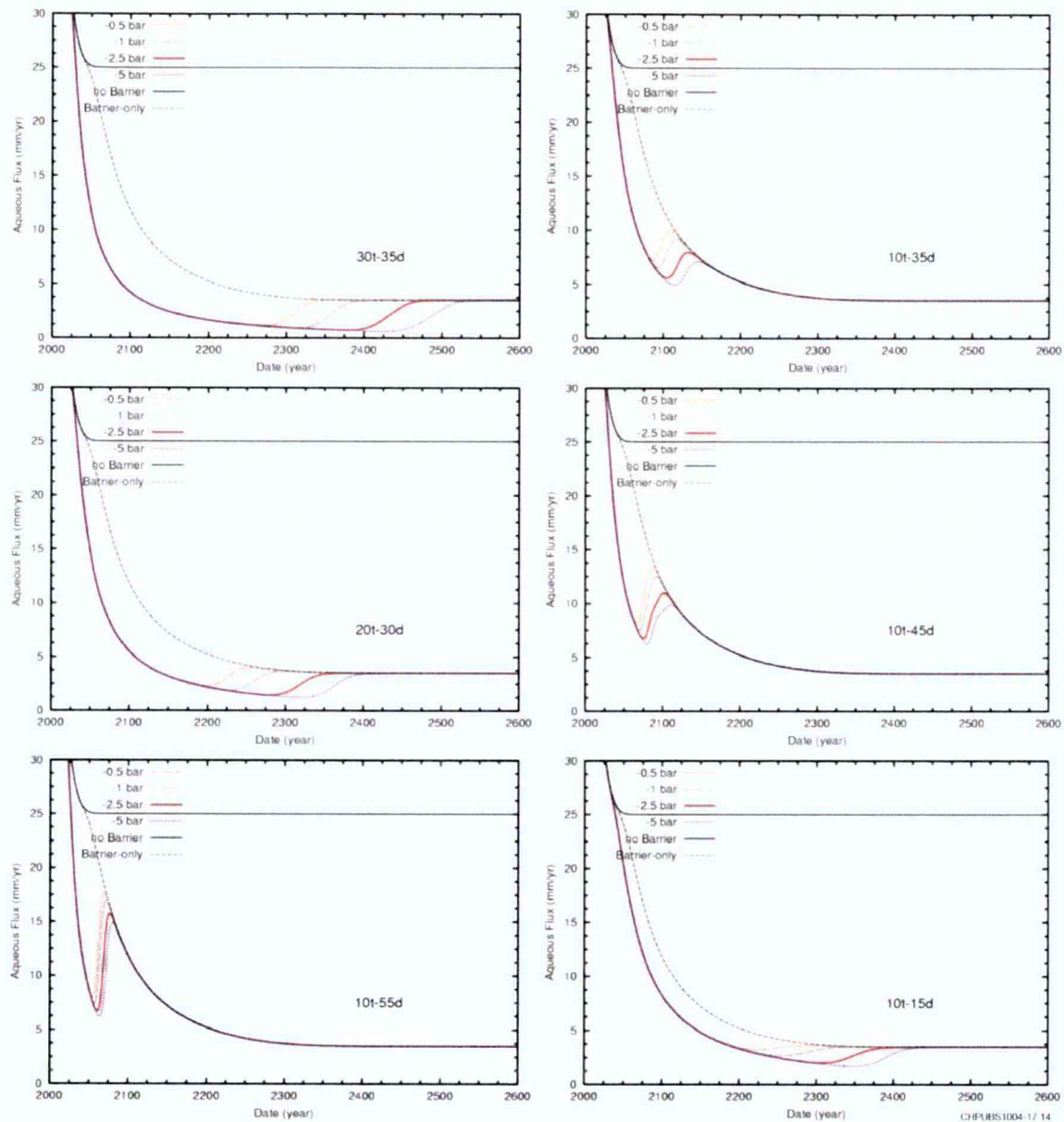
desiccate in “clean” zones, the slope of the cumulative mass curve is essentially the same as for the barrier-only case. The endpoint matric potential, within the range of -0.5 bar to -20 bar, has a minor effect on the delay in migration.

Another metric applied for the comparison was the average mass flux of Tc-99 in the domain across the water table from the vadose zone to the groundwater. Comparisons between different cases for this metric show the duration and extent of changes to the Tc-99 mass flux caused by the desiccation condition. Results for the desiccation configurations in combination with 0.5 mm/yr (0.02 in./yr) and 3.5 mm/yr



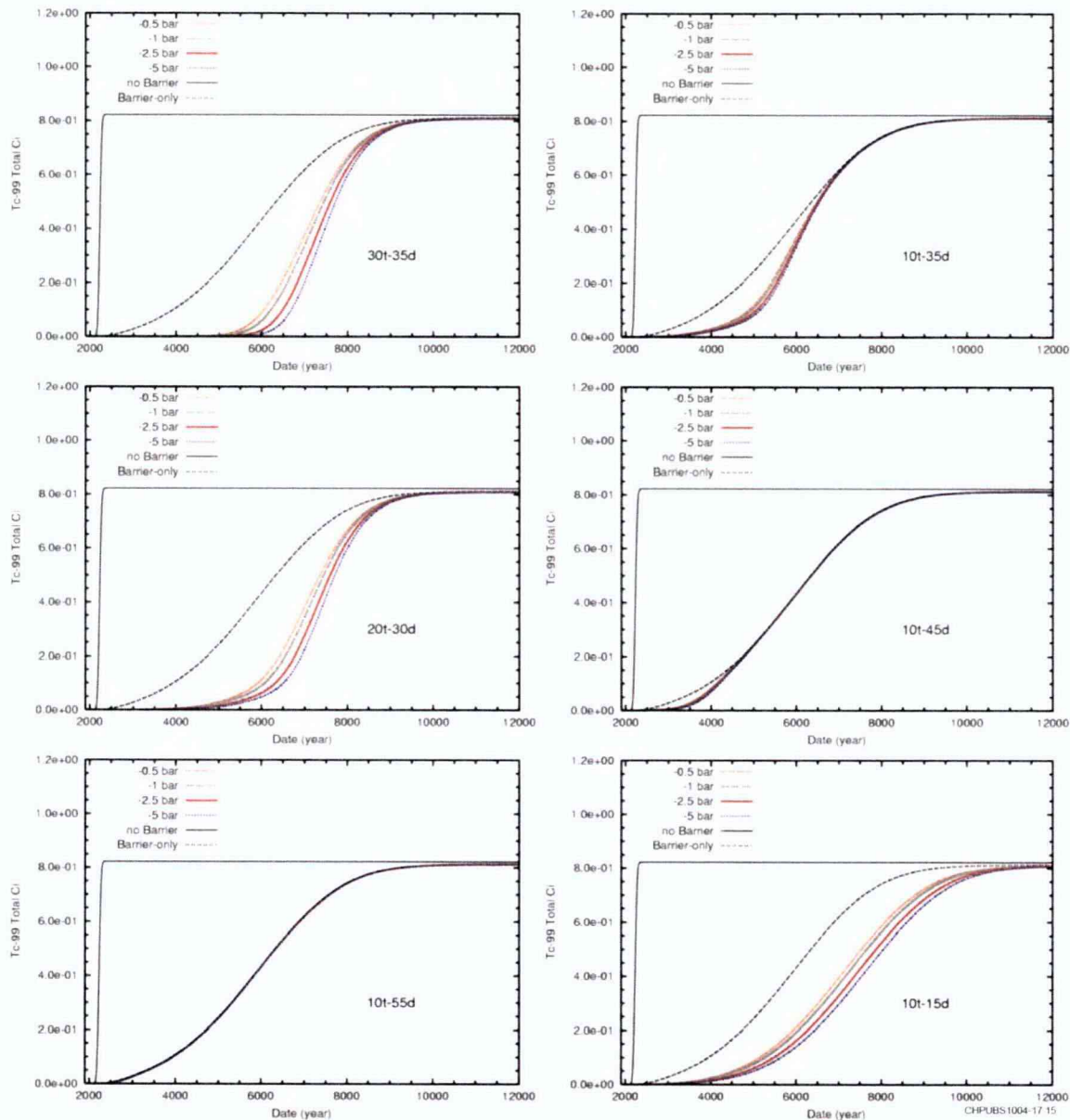
Note: Individual plots denote the mid depth of the imposed desiccation zone and its thickness. The no barrier response is for a surface infiltration condition of 25 mm/yr. The barrier-only response is for a surface infiltration condition of 0.5 mm/yr. All of the imposed desiccation conditions, denoted by the imposed water pressure, are for a surface infiltration condition equivalent to the barrier-only condition.

Figure 4-13. Temporal Profile of Average Water Flux in the Domain Across the Water Table from the Vadose Zone to the Groundwater



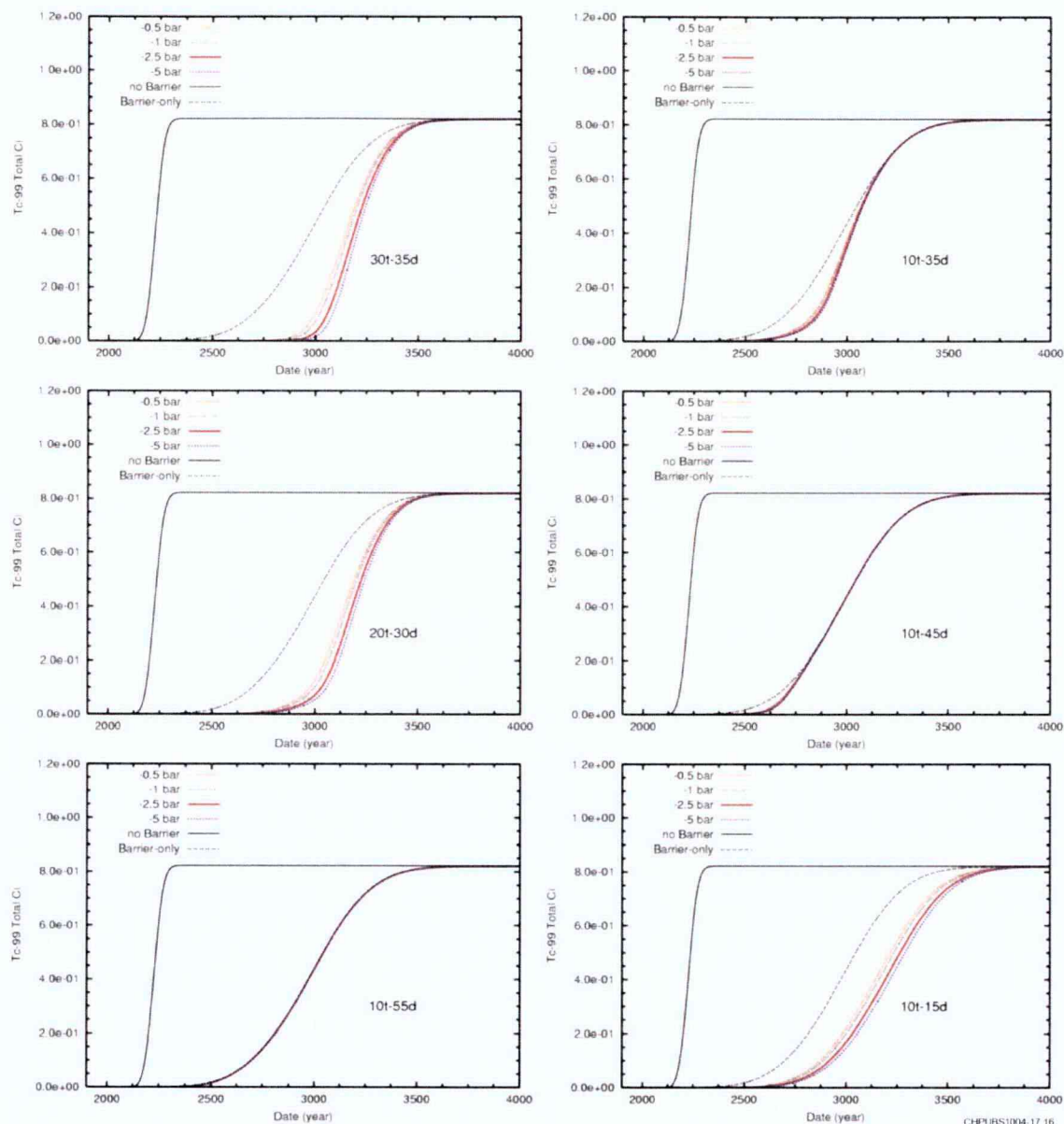
Note: Individual plots denote the mid depth of the imposed desiccation zone and its thickness. The no barrier response is for a surface infiltration condition of 25 mm/yr. The barrier-only response is for a surface infiltration condition of 3.5 mm/yr. All of the imposed desiccation conditions, denoted by the imposed water pressure, are for a surface infiltration condition equivalent to the barrier-only condition.

Figure 4-14. Temporal Profile of Average Water Flux in the Domain Across the Water Table from the Vadose Zone to the Groundwater



Note: Individual plots denote the mid depth of the imposed desiccation zone and its thickness. The no barrier response is for a surface infiltration condition of 25 mm/yr. The barrier-only response is for a surface infiltration condition of 0.5 mm/yr. All of the imposed desiccation conditions, denoted by the imposed water pressure, are for a surface infiltration condition equivalent to the barrier-only condition.

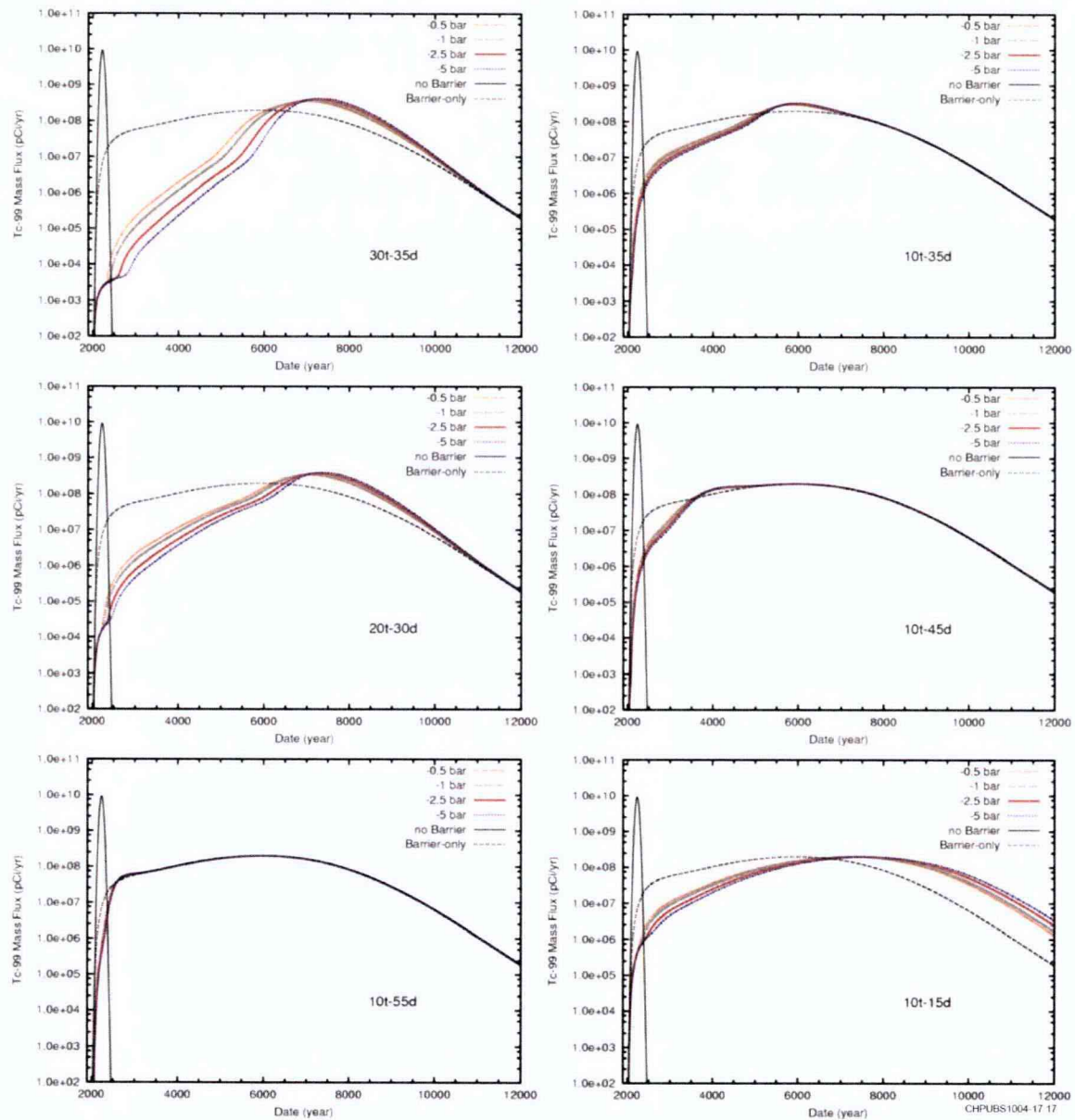
Figure 4-15. Cumulative Technetium Mass Moved Across the Water Table from the Vadose Zone to the Groundwater



Note: Individual plots denote the mid depth of the imposed desiccation zone and its thickness. The no barrier response is for a surface infiltration condition of 25 mm/yr. The barrier-only response is for a surface infiltration condition of 3.5 mm/yr. All of the imposed desiccation conditions, denoted by the imposed water pressure, are for a surface infiltration condition equivalent to the barrier-only condition.

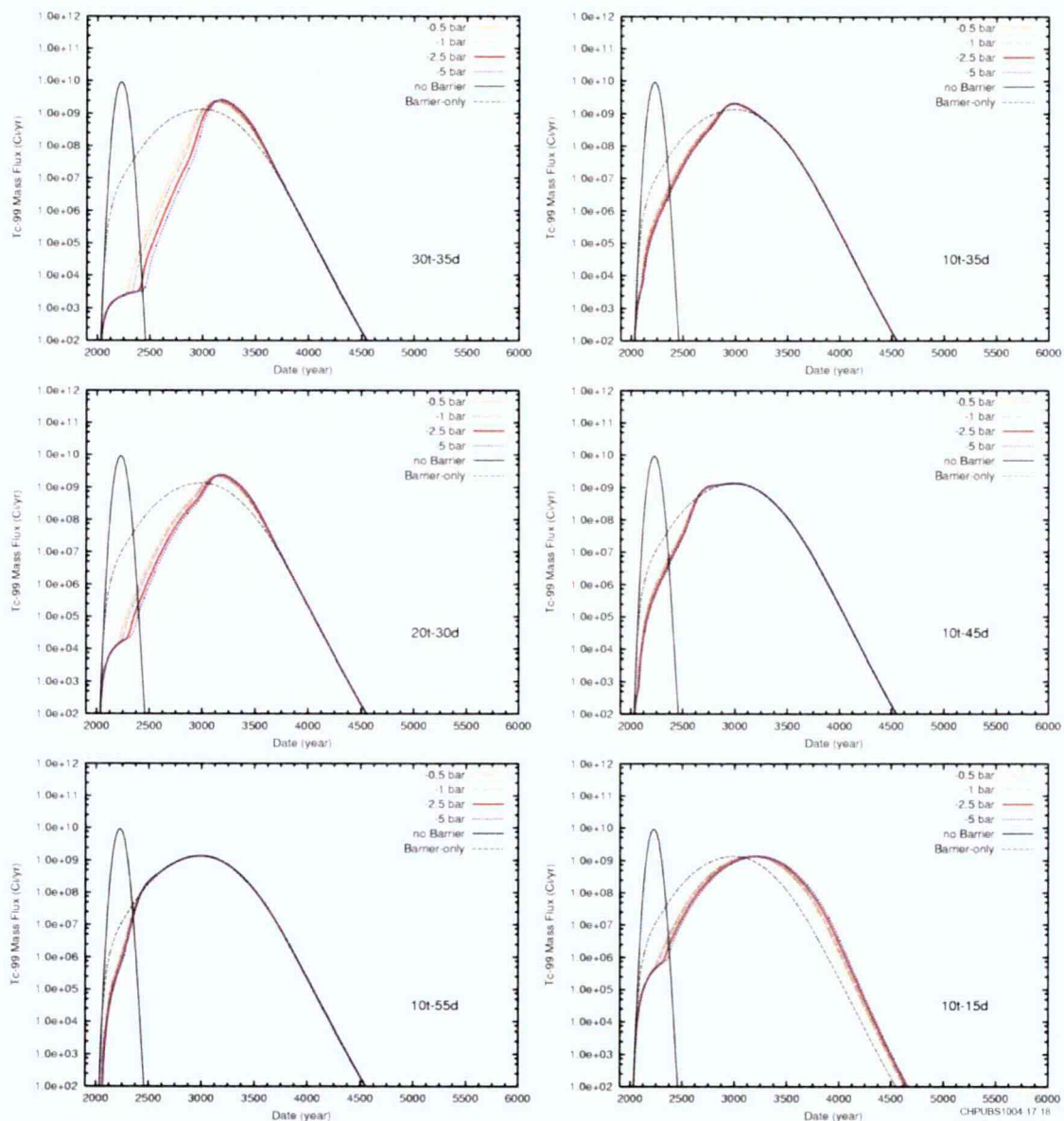
Figure 4-16. Cumulative Technetium Mass Moved Across the Water Table from the Vadose Zone to the Groundwater

(0.14 in./yr) surface infiltration conditions are shown in Figure 4-17 and Figure 4-18, respectively. In all cases, desiccation causes a temporary reduction in mass flux across the water table, in some cases for a very long time period. The water flux then generally returns to match the flux profile of the barrier-only surface infiltration condition. However, when desiccation was imposed within the contaminated zone, there is an increase in the mass flux compared to the barrier-only case as the mass flux returns toward the barrier-only flux. For instance, in the 30t-35d figure, note that the mass flux at year 8000 is higher for the desiccation conditions than for the barrier-only case. This result is interpreted as the impact of desiccation



Note: Individual plots denote the mid depth of the imposed desiccation zone and its thickness. The no barrier response is for a surface infiltration condition of 25 mm/yr. The barrier-only response is for a surface infiltration condition of 0.5 mm/yr. All of the imposed desiccation conditions, denoted by the imposed water pressure, are for a surface infiltration condition equivalent to the barrier-only condition.

Figure 4-17. Temporal Profile of Average Mass Flux in the Domain Across the Water Table from the Vadose Zone to the Groundwater



Note: Individual plots denote the mid depth of the imposed desiccation zone and its thickness. The no barrier response is for a surface infiltration condition of 25 mm/yr. The barrier-only response is for a surface infiltration condition of 3.5 mm/yr. All of the imposed desiccation conditions, denoted by the imposed water pressure, are for a surface infiltration condition equivalent to the barrier-only condition.

Figure 4-18. Temporal Profile of Average Mass Flux in the Domain Across the Water Table from the Vadose Zone to the Groundwater

concentrating the solute within the desiccated zone, and then this solute is carried downward as a “slug” of high concentration contamination once water breaks through the desiccation zone. This effect was also observed for cases with desiccation in a contaminated interval in the cumulative mass curves where the slope of the cumulative mass curve was greater than for the barrier-only case.

This effect was hypothesized by the vadose zone technical panel (WMP-27397), but the extent of the effect was not known. The results presented herein provide an estimate for the extent of this effect for the conditions of the study and the configuration of the model. In all cases, the temporary change in mass flux

from the “slug” of contaminant is small in context of the difference between the mass flux for the barrier-only or barrier plus desiccation compared to the no-barrier case. As for the cumulative mass results, the characteristics of the change in mass flux are most strongly impacted by the quantity of water removed (thickness of desiccation zone and initial water content), whether or not the desiccation zone was within the contaminated interval, and the amount of water above the desiccated zone (i.e., depth of zone). The endpoint matric potential, within the range of -0.5 bar to -5 bar, has a minor effect on the change in mass flux.

Conclusions

Simulations were conducted to provide initial estimates for the impact of desiccation at a larger scale as input to setting desiccation performance targets for the field test. Simulations examined different desiccation scenarios, including variations in the desiccation target endpoint, location, and configuration for the desiccation zone, and the surface infiltration conditions.

These simulations need to be interpreted with respect to the impact of desiccation on contaminant flux with the following considerations. First, the simulations did not include vapor transport of water. In addition, all imposed desiccation zones and surface infiltration conditions extended laterally across the entire model domain; thus, no lateral water movement into the desiccated zone was considered. These two configuration constraints limit interpretation of the results to desiccation performance under conditions of advective downward water movement. Future modeling will include vapor transport and lateral liquid transport contributions.

The irreducible water saturation from the PNNL-14907 model equates to a lower bound of the moisture content of about 1 to 2 wt percent depending on the particle size distribution in the grid cell. The model configuration is highly heterogeneous where each model node may have different properties. With this configuration, the model truncates desiccation at this lower bound of moisture content, and effects of lower moisture conditions on water migration are, therefore, not included in the simulations. As such, the simulation results would tend to underestimate the impact of desiccation on moisture movement if desiccation could result in lower endpoint moisture content as has been observed in laboratory experiments. However, the simulations may also underestimate the impact of solute concentration in the desiccated zone.

In all cases, desiccation causes a delay in contaminant migration to the water table, although the delay is small for some of the desiccation configurations. The characteristics of the delay are most strongly impacted by the quantity of water removed (thickness of desiccation zone and initial water content), the amount of water above the desiccated zone (i.e., depth of desiccation zone), and whether or not the desiccation zone was within the contaminated interval.

When the desiccation is imposed within a contaminated portion of the subsurface, desiccation appears to concentrate the solute, and then this solute is carried downward as a “slug” of higher concentration once water breaks through the desiccation zone, a potential impact first identified by the vadose zone technical panel (WMP-27397). The results presented herein provide an estimate for the extent of this effect for the conditions of the study and the configuration of the model. In all cases, the temporary change in mass flux from the “slug” of contaminant is small relative to the no-barrier case.

Overall, desiccation in conjunction with a surface barrier reduces contaminant migration through the vadose zone more than a barrier alone. Desiccation also can be applied multiple times in the near term to enhance its overall effectiveness in the long term.

4.2.1.4 Rate of Moisture Reduction

Assuming that injected nitrogen has no moisture and the extracted soil gas will be saturated with moisture, the rate of moisture reduction is dependent on the permeability of the sediment and the dry nitrogen injection rate. At 15°C (59°F), air should contain $>13 \text{ g H}_2\text{O/m}^3$ ($8.1 \times 10^{-3} \text{ lb/ft}^3$) (the same value is assumed for nitrogen). Table 4-4 shows the water removed per month, and estimated desiccation volume over a six-month operational period as a function of injected nitrogen flow rate. The desiccation volume was estimated assuming a 5 wt percent reduction in sediment moisture content and a sediment bulk density of $1,800 \text{ kg/m}^3$ (112 lb/ft^3). This calculation provides input to selecting the layout of the desiccation test, the associated monitoring locations, and the expected duration of the test.

Table 4-4. Desiccation Rate Versus Injected Nitrogen Flow Rate

Injected Nitrogen Flow Rate (scfm [m³/min])*	Water Removed per Month (kg [lb])	Desiccation Volume in 6 Months (m³ [ft³])
100 (2.83)	1,590 (3,504)	106 (3,743)
200 (5.66)	3,180 (7,009)	212 (7,487)
300 (8.49)	4,770 (10,513)	318 (11,230)
400 (11.32)	6,360 (14,017)	424 (14,973)

* Assumes a relative humidity of zero.

4.2.1.5 Zone of Pressure Influence

Zone of pressure influence is the limit of measurable pressure influence resulting from an extraction well. Given the heterogeneity of the mostly sandy sediment, the zone of pressure influence could extend to $>15 \text{ m}$ (49.2 ft) (EM 1110-1-4001) which is confirmed by initial sediment air permeability characterization of the test site. The field air permeability testing confirms that (1) extraction flow rates up to 400 cfm ($11.32 \text{ m}^3/\text{min}$) are feasible, and (2) the bulk air permeability in response to induced air extraction is relatively uniform around the injection well with a value of approximately $5 \times 10^{-11} \text{ m}^2$ ($5.4 \times 10^{-10} \text{ ft}^2$). Pressure response from extraction of soil gas was observed at a radial distance of 12 m (39.4 ft), which was the furthest radial monitoring location during the test.

4.2.1.6 Simulations Supporting Test Design

Subsurface soil gas flow patterns and related desiccation rates in a homogeneous domain were used to provide information useful for evaluating field test operational conditions. A series of three-dimensional simulations was conducted using the STOMP simulator (PNNL-15782) examining different injection and extraction flow rates. Injection and extraction flow rates were varied in the range of 100 to 400 cfm (2.83 to $11.32 \text{ m}^3/\text{min}$) for both balanced (e.g., 300/300 cfm [$8.49/8.49 \text{ m}^3/\text{min}$] injection/extraction) and unbalanced (e.g., 300/100 cfm [$8.49/2.83 \text{ m}^3/\text{min}$] injection/extraction) conditions.

Unlike the single injection/extraction well or the single injection with multiple extraction wells configurations which, owing to symmetry, can be simulated two-dimensionally with cylindrical coordinates, a dipole system requires a three-dimensional simulation. Figure 4-19 shows a cross-sectional view of the conceptual model for simulating the dipole test. Two vertical wells of radius r_w , with a screen from a depth d to a depth l , are installed in an effective homogeneous soil above a water table at depth b . For these simulations, $r_w = 0.152$ m (0.5 ft), $d = 9.1$ m (30 ft), $l = 15.24$ m (50 ft), and $b = 103$ m (338 ft). The injection and extraction wells are spaced 12 m (39 ft) apart.

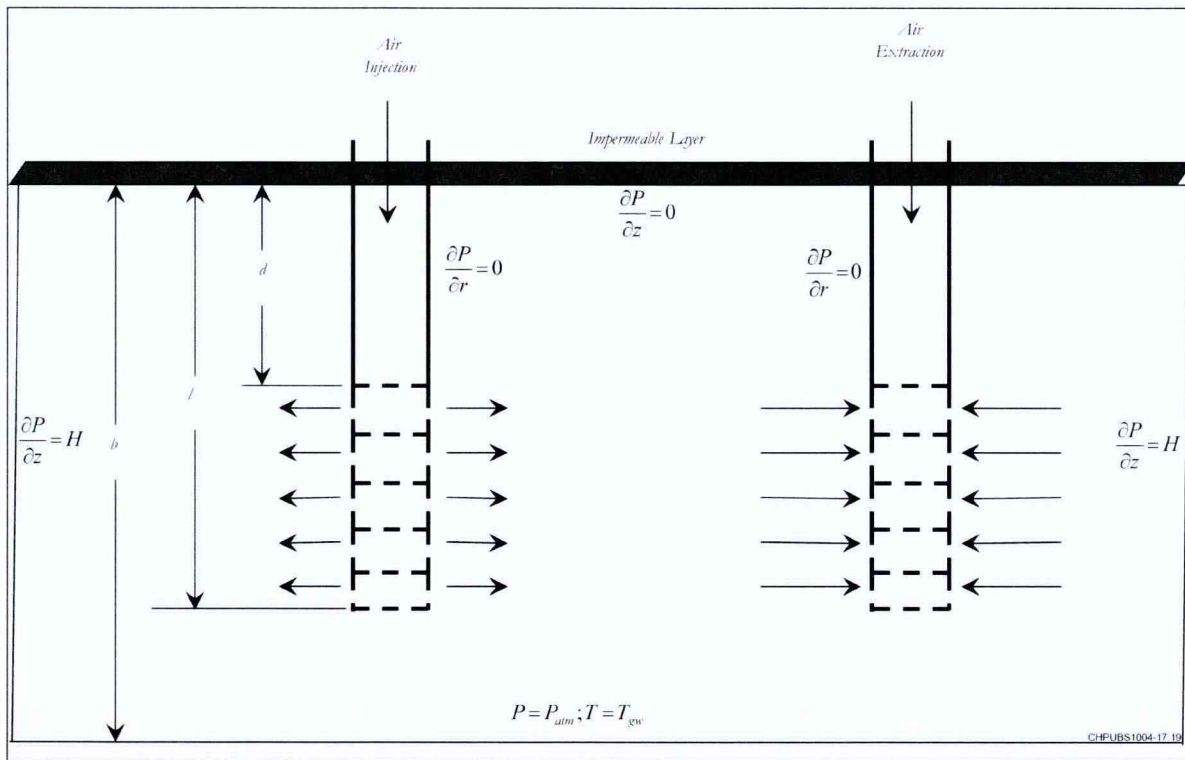


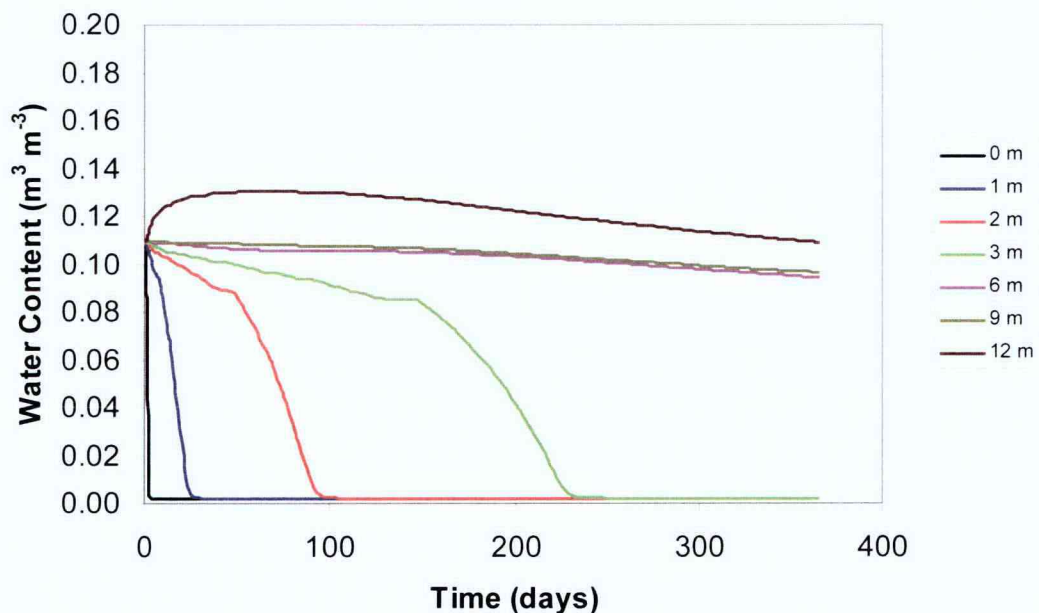
Figure 4-19. Conceptual Model of Well Configuration Used to Simulate Air Flow Between Two Wells

Boundary conditions are needed for the aqueous mass gaseous mass and energy conservation equations. At the surface (100 m by 100 m [328 ft by 328 ft]), a no-flow (zero flux) boundary was specified for the aqueous phase across the entire surface. For the gas phase, a no-flow (zero flux) boundary was specified across the areal extent of the surface impermeable layer (45 m by 45 m [148 ft by 148 ft]), whereas the remainder of the surface was held constant at atmospheric pressure, P_{atm} . For the energy conservation equation, the upper surface is kept at a constant temperature of 23°C, whereas the initial temperature in the domain is assumed to be 17°C. Owing to the presence of the water table at the bottom boundary, both the aqueous and gas pressures were held constant at P_{atm} , corrected for the difference in elevation. Temperature was held constant at a groundwater temperature, T_{gw} , of 17°C. The four vertical boundaries of the three-dimensional domain were specified as hydraulic gradient boundaries for the aqueous and gaseous phases ($\delta P/\delta z = H$) and as outflow boundaries for energy.

Simulations used an air inlet temperature of 20°C with a 10 percent relative humidity, a subsurface initial temperature of 17°C, and an initial moisture content of $0.11 \text{ m}^3 \text{ m}^{-3}$ (11 volume %). Thermal properties are also important in modeling the evaporation and condensation processes. Thermal properties of the porous media were estimated from PNL-4015. The porous media pneumatic properties were homogeneous with

an anisotropy ratio of 10:1 ($K_v:K_z$) and set to match the results from the constant rate permeability test. These simulations would tend to be somewhat conservative (slow desiccation front movement) with respect to the most permeable portions of the test site because flow is more uniform than is expected in the field. In the field, lower permeability lenses are expected to focus flow in the higher permeability layers such that these would dry more quickly. However, the simulations likely over predict the reduction in moisture content within the dry zone because it does not account for drying of the less permeable lenses.

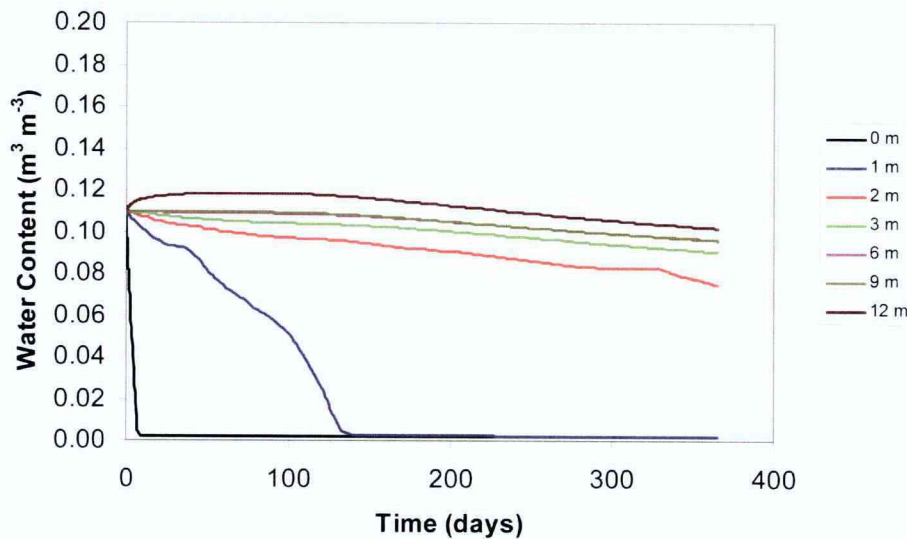
Under the simplified conditions of the simulations, desiccation volumes with time are similar to the calculations shown in Section 4.2.1.2 for comparable injected air rates. For instance, the volume of desiccation over 100 days was approximately 50 m³ (1766 ft³) of soil observed in simulations with a 300 cfm (8.49 m³/min) injection flow rate. A desiccation volume can also be hand calculated assuming a 13 g/m³ water capacity of air (at ~15°C), a 300 cfm (8.49 m³/min) injection flow rate of air with 10 percent relative humidity, and a change in moisture content of 0.11 m³/m³ (11 volume %). This hand calculated value is ~ 48 m³-soil. Maintaining relatively higher injection rates (e.g., 300 cfm [8.49 m³/min]) provides for a larger desiccation volume within the targeted six-month operational period. The larger desiccated volume would likely be more favorable for monitoring of the process because monitoring intervals can be on the order of the planned layout, and the desiccation front will intersect multiple monitoring locations. Lower injection flow rates (e.g., 100 cfm [2.83 m³/min]) would require a well spacing likely infeasible for installation in the field, or a longer operational time. As an example, the time course of desiccation was simulated with a 100 cfm (2.83 m³/min) extraction rate and a 300 cfm (8.49 m³/min) injection rate (Figure 4-20) and a 100 cfm (2.83 m³/min) injection rate (Figure 4-21).



CHPUBS1004-17.20

Note: Mid-screen depth for 300/100 cfm injection/extraction Flow Rates.

Figure 4-20. Simulated Desiccation (Change in Water Content) Along the Centerline Between the Injection and Extraction Wells



Note: Mid-screen depth for 100/100 cfm injection/extraction flow rates.

Figure 4-21. Simulated Desiccation (Change in Water Content) Along the Centerline Between the Injection and Extraction Wells

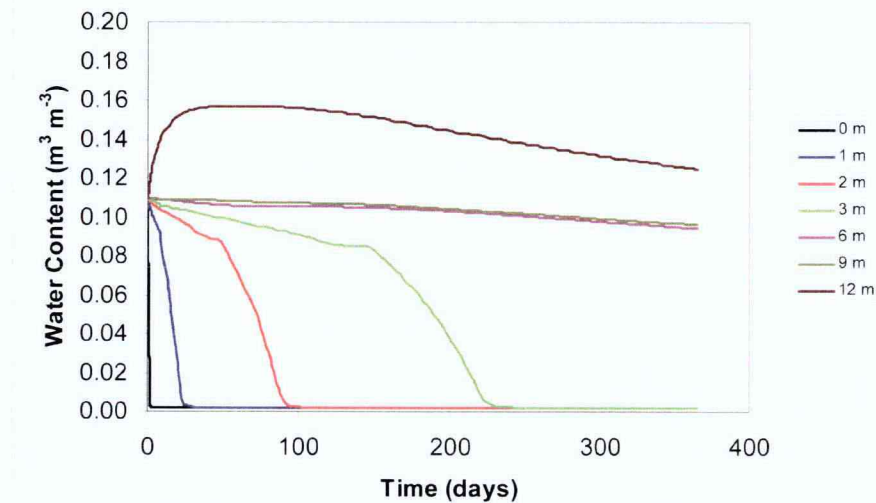
Desiccation near the injection well (i.e., within 3 m [10 ft]) is primarily controlled by the injection flow rate. Note that the rate of desiccation is essentially the same for both a 300 cfm (8.49 m³/min)/100 cfm (2.83 m³/min) injection/extraction condition (Figure 4-20) compared to a 300 cfm (8.49 m³/min)/300 cfm (8.49 m³/min) injection/extraction condition (Figure 4-21) within the first 3 m (10 ft) of the injection well. Differences are observed over longer time periods at monitoring locations closer to the extraction well. Use of a dipole arrangement helps focus the soil gas flow to within a targeted monitoring zone and depth interval defined generally by the screened intervals of the wells. The extraction rate can be lower than the injection rate and still direct flow to the monitored test zone. This situation may be preferred for the test for the following reasons:

- It maintains extraction flow rates lower than the critical velocity that may entrain droplets in the extracted soil gas.
- It helps minimize short circuiting between the injection and extraction wells due to the lower induced pressure gradients than would occur with matched high injection/extraction rates.
- It tends to result in more lateral flow (off the injection extraction well axis) of the dry air for a more three-dimensional drying pattern.

Simulations also show a moderate increase in moisture content near the extraction well (see Figure 4-19 through Figure 4-22). While lower pressure tends to decrease relative humidity, the lower temperature induced at the extraction well (see Figure 4-23 through Figure 4-25) apparently causes some condensation to occur. This condensation is focused around the extraction well because of the higher air flow rate through this region.

These results suggest that field operations could be appropriately adjusted by selecting a desired influent air flow rate (e.g., nominally 300 cfm [8.49 m³/min]) and then increasing the extraction flow rate until a desired flow pattern (e.g., as measured by pressure and tracer response) is obtained. Pressure gradients, and therefore the flow field, vary with the selected injection and extraction flow rates. For example,

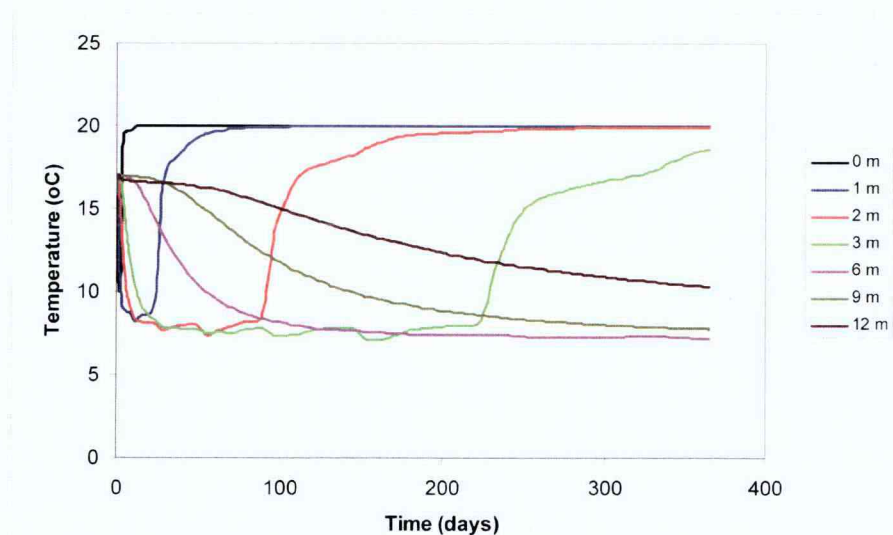
Figure 4-26 through Figure 4-28 show the pressure gradients for the 300 cfm (8.49 m³/min)/100 cfm (2.83 m³/min) injection/extraction, the 100 cfm (2.83 m³/min)/100 cfm (2.83 m³/min) injection/extraction, and the 300 cfm (8.49 m³/min)/300 cfm (8.49 m³/min) injection/extraction conditions, respectively. These results, in conjunction with previous scoping simulations (PNNL-17274), also suggest that increased injection gas temperature may be an important control for desiccation rate where higher temperatures favor quicker desiccation. Because monitoring instrumentation would be impacted by the injected gas temperature, only moderate increases in injection gas temperature should be considered for the field test.



CHPUBS1004-17.22

Note: Mid-screen depth for 300/300 cfm injection/extraction Flow Rates.

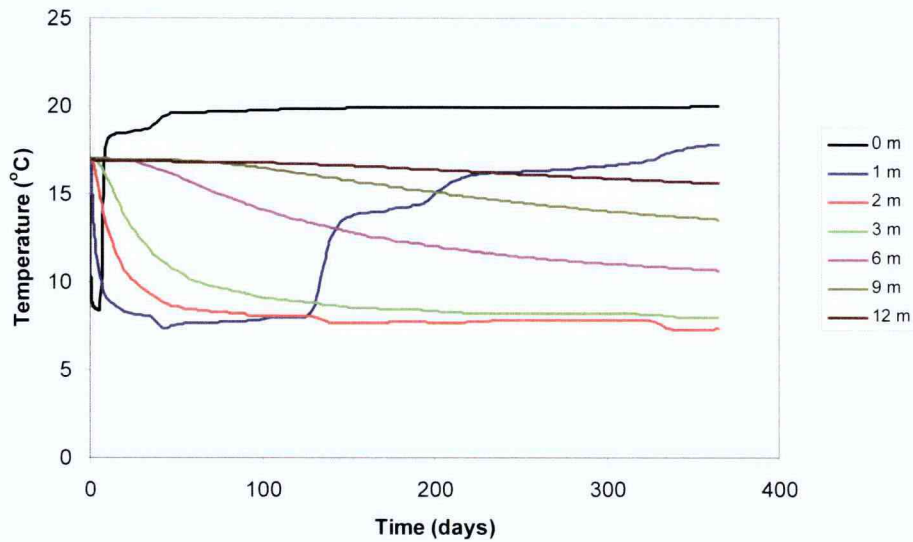
Figure 4-22. Simulated Desiccation (Change in Water Content) Along the Centerline Between the Injection and Extraction Wells



CHPUBS1004-17.23

Note: Mid-screen depth for 300/100 cfm Injection/Extraction Flow Rates.
The Injected Air Temperature is 20°C.

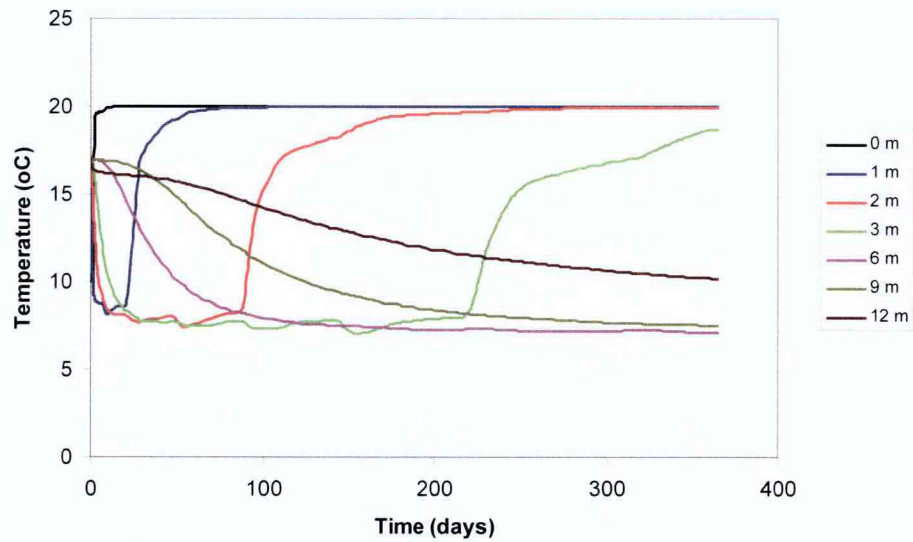
Figure 4-23. Simulated Temperature Profile During Desiccation Along the Centerline Between the Injection and Extraction Wells



CHPUBS1004-17 24

Note: (mid-screen depth) for 100/100 cfm injection/extraction flow rates. The injected air temperature is 20°C.

Figure 4-24. Simulated Temperature Profile During Desiccation Along the Centerline Between the Injection and Extraction Wells



CHPUBS1004-17 25

Note: (mid-screen depth) for 300/300 cfm injection/extraction flow rates. The injected air temperature is 20°C.

Figure 4-25. Simulated Temperature Profile During Desiccation Along the Centerline Between the Injection and Extraction Wells

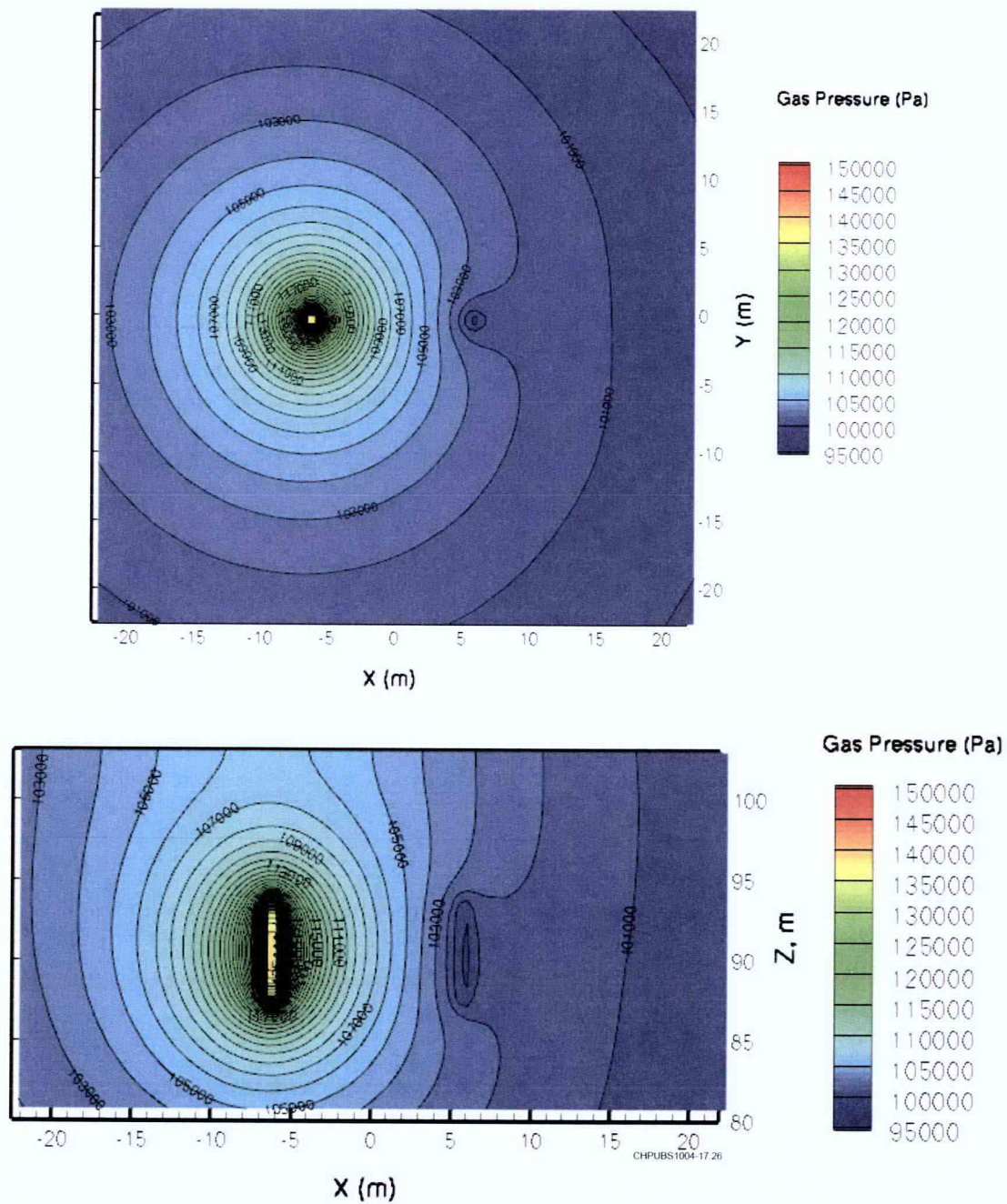
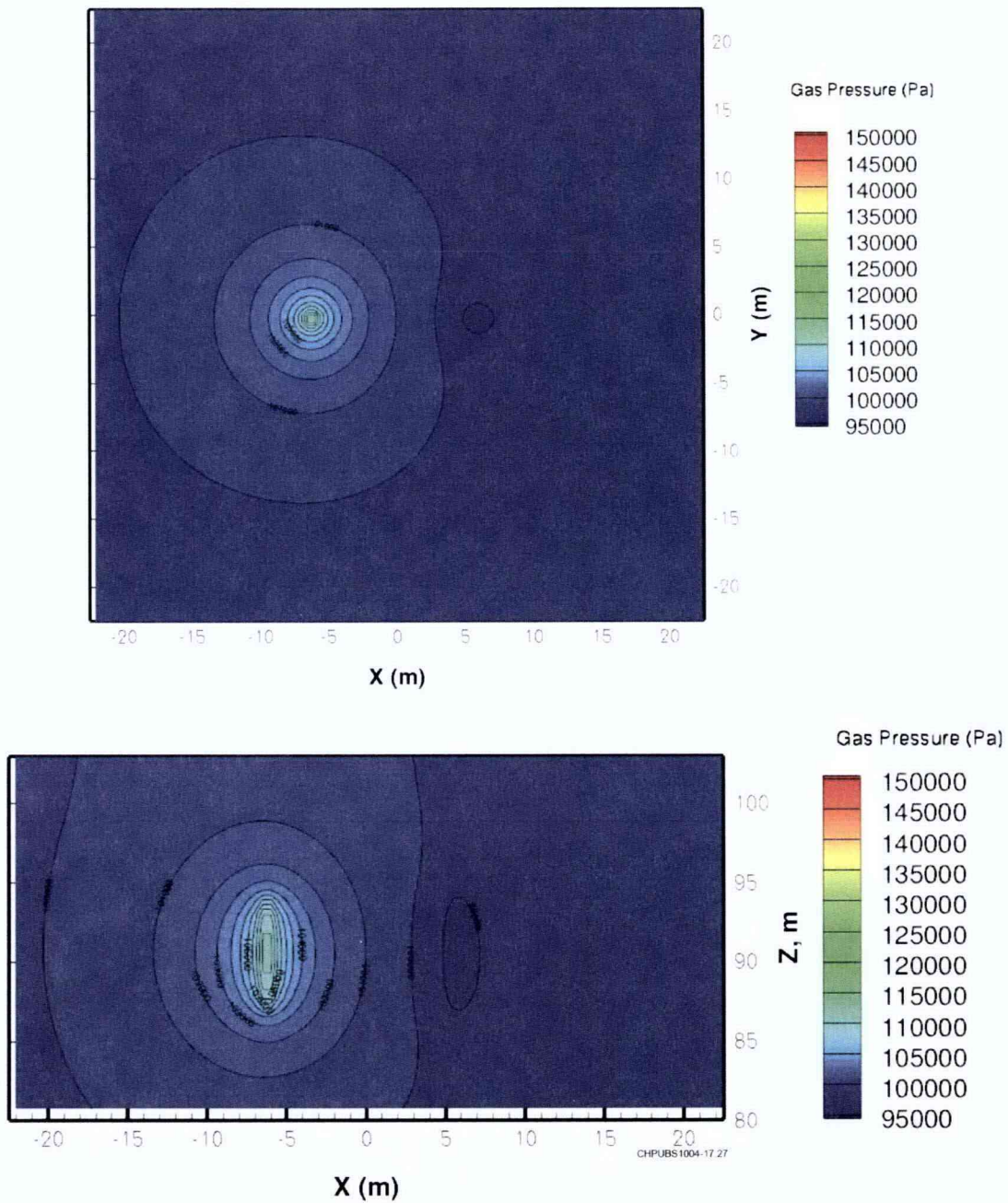
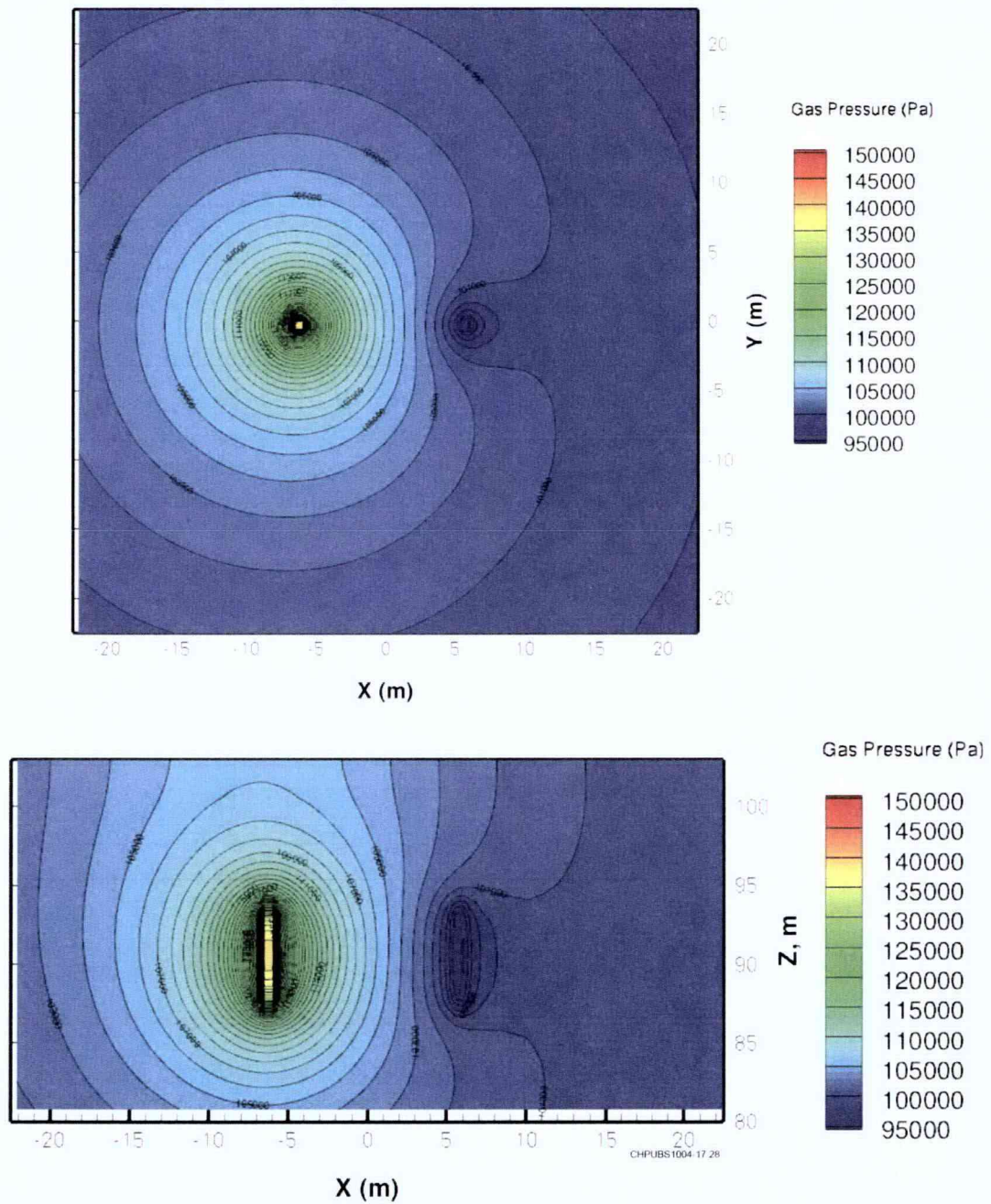


Figure 4-26. Plan (Mid-Screen Depth) and Cross-Sectional Views of the Pressure Gradients



Note: 300/100 cfm injection/extraction flow rates. Injection well is at -6 m, and the extraction well is at 6 m.

Figure 4-27. Plan (Mid-Screen Depth) and Cross-Sectional Views of the Pressure Gradients



Note: 300/300 cfm injection/extraction flow rates. Injection well is at -6 m and the extraction well is at 6 m.

Figure 4-28. Plan (Mid-Screen Depth) and Cross-Sectional Views of the Pressure Gradients

4.2.1.7 Laboratory Investigation of Design Factors for Desiccation

The evaporative cooling solute effects during desiccation and the use of gas phase tracers were examined in the laboratory and results are summarized below. A full description of laboratory testing to provide technical support for the desiccation field test is compiled in a pending PNNL document, *Laboratory and Modeling Evaluations in Support of Field Testing for Desiccation at the Hanford Site*.

Effect of Evaporative Cooling and Simple Heterogeneities on Desiccation

Soil desiccation (drying), involving water evaporation induced by dry gas injection and extraction, is a potentially robust vadose zone remediation process to limit migration of inorganic or radionuclide contaminants through the vadose zone. Desiccation also has the potential to improve gas-phase-based treatments by reducing water saturation and, therefore, increasing sediment gas-phase permeability. Before this technology can be deployed in the field, concerns related to energy limitations, osmotic effects, and potential contaminant remobilization after rewetting must be addressed. A series of detailed, intermediate-scale laboratory experiments, using unsaturated homogeneous and heterogeneous systems, was conducted to improve understanding of energy balance issues related to soil desiccation. The experiments were subsequently simulated with the multifluid flow simulator STOMP, using independently obtained hydraulic and thermal porous medium properties. In all experiments, the injection of dry air proved to be an effective means for removing essentially all moisture from the test media. Observed evaporative cooling generally decreased with increasing distance from the gas inlet chamber. The fine-grained sand embedded in the medium-grained sand of the heterogeneous system showed two local temperature minima associated with the cooling. The first one occurred because of evaporation in the adjacent medium-grained sand, whereas the second minimum was attributed to evaporative cooling in the fine-grained sand itself. Results of the laboratory tests were simulated accurately only if the thermal properties of the flow cell walls and insulation material were taken into account, indicating that the appropriate physics were incorporated into the simulator.

Solute Transport

Experiments were conducted to examine the impact of solute concentration on the desiccation process. Results suggest that desiccation rate is not a function of solute concentration. Thus, inclusion of solute concentrations in estimates of desiccation rate is not necessary. The experimental results also suggest that for slowly moving desiccation fronts and high solute concentrations (>100 g/L [0.83 lb/gal]), some redistribution of solute may occur in the soil moisture and in the direction of the solute concentration gradient. Because the sediment is relatively dry behind the desiccation front, solute migration will occur in the direction of the desiccation front movement or laterally at the edges of the desiccated area. Maximum concentration factors of about 120 percent of the initial concentration were observed in the one-dimensional column experiments.

Additional experiments examining the impact of solute concentration on rewetting processes are planned to determine how solute concentration impacts the effectiveness of desiccation in mitigating water and contaminant migration in the vadose zone.

Laboratory Examination of Tracers as a Means to Evaluate Desiccation in the Field Test

The application of gas-phase partitioning tracer tests has been proposed as a means to estimate initial water volumes and to monitor the progress of the desiccation process at pilot-test and field sites. Laboratory tracer tests were conducted in porous medium columns with various water saturations using sulfur hexafluoride as the conservative tracer and trichlorofluoromethane and difluoromethane as the water-partitioning tracers. For porous media with minimal silt and/or organic matter fractions, tracer tests provided reasonable saturation estimates for saturations close to zero. However, for sediments with significant silt and/or organic matter fractions, tracer tests only provided satisfactory results when the

water saturation was at least 0.1 - 0.2. For dryer conditions, the apparent tracer retardation increases due to air – soil sorption, which is not included in traditional retardation coefficients derived from advection-dispersion equations accounting only for air – water partitioning and water – soil sorption. Based on these results, gas-phase partitioning tracer tests may be used to determine initial water volumes in sediments, provided the initial water saturations are sufficiently large. However, tracer tests are not suitable for quantifying moisture content in desiccated sediments.

Details of these laboratory tracer experiments are reported by Oostrom et al. (2010b) and summarized below.

4.2.2 Approach

The desiccation field test will include characterization of baseline conditions within the test site and evaluation of subsurface air flow, installation of a test system layout appropriate to meet the operational and data needs for the test, and test operations. These test elements are described in the subsections below.

4.2.2.1 Field Test Site Characterization

During installation of the test system, additional subsurface characterization data necessary to interpret the test data and finalize the system design will be collected. Permeability testing will be conducted at the extraction well (299-E13-65), similar to what was done at the injection well (299-E123-62) during the characterization phase of this test (Table 4-5).

Table 4-5. Data Collection at Extraction Well

Data	Use
Air permeability testing per EM-1110-1-4001	Provides data to infer in situ bulk sediment air permeability
Borehole anemometry (Pneulog® testing)	Provides an estimate of the vertical distribution of air permeability

4.2.2.2 Subsurface Monitoring Locations

The field test layout is based on the following overall elements:

- Data are needed to monitor the progression of the desiccation front between the injection and extraction well axis (primary soil gas flow zone) and off of this axis (secondary soil gas flow zone).
- The selected monitoring and sampling techniques require different types of subsurface access, some of which are not compatible.
- Monitoring at selected locations should collect multiple types of data so that these data can be interpreted together. Thus, clustered monitoring installations are needed. It should be noted, though, that heterogeneity will likely result in varied conditions, even for closely spaced instrument probes.
- Some of the selected monitoring techniques are targeted at interrogating the subsurface between access points. For those techniques, the layout needs to provide for appropriate line-of-site and sensor-to-sensor distances.
- The vertical layout should enable data collection from above, within, and beneath the targeted desiccation zone.

- A monitoring location outside the zone of pressure influence will be used for collecting background instrument response data over the duration of the field test.

A lateral layout for the monitoring locations is shown in Figure 4-29. Instrumentation is clustered at locations to interpret the desiccation progress. Drying front movement past the selected monitoring locations will be inferred from continuous logging of sediment temperature, humidity, and sediment moisture, and periodic monitoring of sediment moisture (neutron probe logging). The passage of the drying front will likely not be uniform with depth. Thus, thermistors, humidity sensors, and sediment moisture sensor data and gas samples will be collected at multiple depths. Neutron logging will also provide detailed information about the vertical distribution of sediment moisture. Two-dimensional and three-dimensional interpretation of desiccation progress will be supported by periodically collecting GPR data, and conducting cross-hole resistivity tomography. Table 4-6 summarizes the test site instrumentation layout.

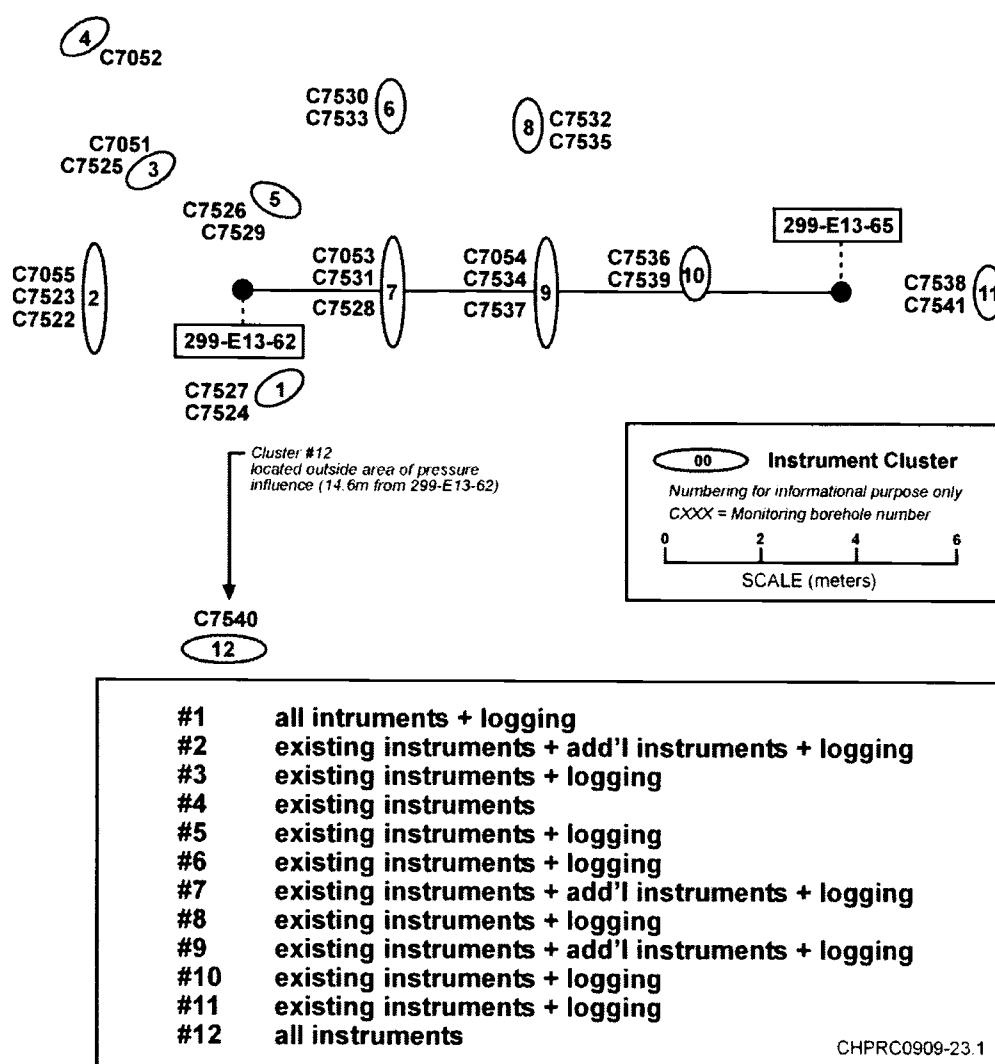


Figure 4-29. Test Site Layout

Table 4-6. Summary of In Situ Monitoring Instrumentation

Location	Instrument	Depth*	Basis
Separate hole in each instrument cluster	Thermistor	Every 0.6 m (2 ft) from 3.35 m (11 ft) to 21 m (69 ft)	Monitor passage of desiccation front by measuring sediment temperature
	Resistivity electrode	Every 1.5 m (5 ft) from 3 m (10 ft) to 21.3 m (70 ft)	Perform electrical resistivity characterization to assess far-field moisture/solute content
	Gas sampler	9.9 m (32.5 ft), 11.4 m (37.5 ft), 12.9 m (42.5 ft), and 14.5 m (47.5 ft)	Monitor desiccation front passage by measuring sediment gas tracer gas concentrations; measure in situ gas pressure
	Humidity sensor/thermocouple psychrometer/heat dissipation unit/dual probe heat pulse sensor	9.9 m (32.5 ft), 11.4 m (37.5 ft), 12.9 m (42.5 ft), and 14.5 m (47.5 ft)	Monitor in situ humidity and matric potential changes associated with passage of desiccation front
Separate hole in each instrument cluster	Neutron logging	Continuous	Monitor near-field moisture change associated with passage of desiccation front
	GPR	Continuous	Monitor far-field moisture change associated with passage of desiccation front
Isolated hole outside of anticipated desiccation zone	Gas sampler	9.9 m (32.5 ft), 11.4 m (37.5 ft), 12.9 m (42.5 ft), and 14.5 m (47.5 ft)	Monitor sediment gas tracer gas concentrations; measure in situ gas pressure

* If possible, some of the monitoring locations will be selected to target coarse and fine layers.

GPR = ground penetrating radar (cross-hole radar)

TBD = to be determined

4.2.2.3 Field Test Operations

The elements of field test operations are described in the subsections below. Subsurface conditions will be measured prior to desiccation to establish the baseline initial conditions for comparison to the conditions induced by the desiccation process. Operational elements include setting appropriate flow and conditioning of the injected nitrogen, setting similar conditions for the extracted soil gas, operating the system for active desiccation, sampling and monitoring during desiccation operations, and post-desiccation sampling and monitoring.

Baseline Data Collection

The amount and distribution of soil moisture is the primary subsurface condition that will be affected by the desiccation process. Solute (contaminant) concentration will change as a result of decrease in soil moisture and will also be a key measured subsurface condition. Multiple measurement parameters will be used to determine changes in the soil moisture and solute concentration during the test. A baseline value for each of these parameters will be established prior to desiccation operations. Prior to collection of baseline data, there will be an equilibration period where sensors will be monitored to ensure that they come to equilibrium with the subsurface after installation. Sensors emplaced in locations isolated by

bentonite seals may initially be affected by different moisture content of the seal material relative to the native soil. Likewise, sensors emplaced in “native soil” may require a significant period to achieve equilibration. Table 4-7 shows the measured parameters and sampling/monitoring techniques that will be applied during the baseline data collection to establish the starting conditions for the test.

Table 4-7. Measured Parameters for Baseline Data Collection

Attribute	Instrument	Data Collection
Sediment temperature	Thermistor	Monitor from installation up to start of active desiccation (anticipated to be 3-6 months) or longer depending on whether data indicate instrument equilibration
Sediment moisture content	Heat dissipation unit	Monitor from installation up to start of active desiccation (anticipated to be 3-6 months) or longer depending on whether data indicate instrument equilibration
Sediment moisture content	Dual probe heat pulse	Monitor from installation up to start of active desiccation (anticipated to be 3-6 months) or longer depending on whether data indicate instrument equilibration
Sediment gas humidity	Gas sampling tube	Two samples over a 2-week timeframe at the end of the equilibration period
Sediment gas humidity	Humidity probe	Monitor from installation up to start of active desiccation (anticipated to be 3-6 months) or longer depending on whether data indicate instrument equilibration
Sediment gas humidity	Thermocouple psychrometer	Monitor from installation up to start of active desiccation (anticipated to be 3-6 months) or longer depending on whether data indicate instrument equilibration
Sediment moisture content	Neutron probe (logging)	Once at access installation within temporary steel casing, once at access installation within the polyvinyl chloride casing, and once at the end of the equilibration period
Sediment moisture content	Cross-hole radar between pairs of logging holes	Once during baseline period
Sediment moisture content and solute concentration	Cross-hole electrical resistance tomography	Once during baseline period

Injection Nitrogen Flow Equipment Operational Conditions

The desiccation process design is based on maintaining influent nitrogen conditions within a specified range of temperature and humidity and directing soil gas flow toward the extraction well. Target injection nitrogen flow equipment operational conditions are listed in Table 4-8. These targets may be adjusted based on final design calculations and equipment specifications. Prior to desiccation operations, air flow equipment will be tested to verify that these or acceptable alternative target ranges can be achieved and effectively modulated during the test to maintain the desired operational set points over the range of ambient conditions expected during the field test period.

Table 4-8. Injection Nitrogen Flow Operational Targets

Parameter	Target
Influent Nitrogen Temperature	19°C minimum, nominally 20°C
Influent Nitrogen Relative Humidity	Near zero, dependant on LN ₂ properties
Influent Nitrogen Pressure	As determined by flow balance operations
Influent Nitrogen Flow Rate	To be determined based on initial tracer tests

Desiccation Operations

Active desiccation is intended to operate nominally continuously (24 hours a day/7 days a week) for approximately six months. Nitrogen flow will be shut down, as required, for maintenance of equipment or for specified sampling and monitoring events, as necessary.

Field operations will be conducted in phases and will include periodic evaluation of operational conditions and set points as desiccation progresses. Because desiccation will change some subsurface properties, adjustments will be needed to maintain the targeted operational conditions. Key phases of operation are listed below. Detailed procedure for use by field personnel will be developed for these operational phases based on the final field equipment configuration.

Injection/Extraction Flow Adjustment Operations

Blower systems for injection and extraction will be operated and adjusted to regulate flow into and out of the subsurface and meet operational targets. Pressure and tracer testing will be used to adjust the flow rate between the well pair based on the following two goals and using input from simulations of the field test: observation of tracers at internal monitoring locations and at the extraction well, and ability to maintain stable soil gas flow and injection nitrogen conditions.

The soil gas flow pattern as a function of operational conditions needs to be established under the starting soil moisture conditions for the selected desiccation configuration. Thus, gas tracer testing will also include assessment of soil gas flow patterns (e.g., capture effectiveness and travel times). As necessary, these data will be used to adjust operational conditions to obtain targeted soil gas flow conditions most appropriate for reaching desiccation goals. Permeability is a function of water saturation and will, therefore, change during desiccation operations. Baseline pressure responses will also be measured to establish baseline flow conditions.

During initial soil gas flow testing, a range of operational flow rates, and their impact on water extraction from the extraction well, will be evaluated. In the characterization tests conducted in FY 2009, nitrate measured in the water condensate from soil gas extraction suggests the potential for water (e.g., mist) entrainment during soil gas extraction. However, this phenomenon may be limited to high extraction flow rates and/or of limited duration only occurring initially to remove water near the extraction well within the high gas velocity region near the well. Thus, testing during the initial soil gas flow operations and monitoring of condensate during initial desiccation operations will be used to ensure that this phenomenon does not occur. The primary metric for entrainment of moisture in addition to removal of soil gas humidity will be monitoring of nitrate concentration in condensate samples. Samples with nitrate present indicate entrainment, whereas clean water indicates water only from soil gas humidity.

Start Up and Desiccation Operations

Primary operations for desiccation include injection of conditioned dry nitrogen, extraction of soil gas, and monitoring of surface and subsurface parameters, per the sampling and analysis plan (DOE/RL-2010-83, to evaluate the progress of desiccation. Ongoing review of sampling/monitoring data will be conducted to determine the adjustments necessary to refine operations and collect desired information.

Terminating the active desiccation phase will be considered based on the following three criteria:

- Evidence that the desiccation front has passed the 6 m (19.7 ft) monitoring location along the axis of the injection/extraction well pair.
- Sufficient dry nitrogen has been injected to decrease the moisture content by 5 wt percent in 300 m³ (79,251.6 gal) of the subsurface.
- Neutron log data of moisture content at monitoring locations within or near the anticipated desiccation region indicate a significant decrease compared to baseline conditions and is corroborated by data from thermistors, moisture probes, humidity probes, thermocouple psychrometers (TCPs), tracer data, and GPR tomography.

Final decision will include Regulator and DOE concurrence. Testing may be extended until dry air breakthrough occurs at the extraction well pending review of the desiccation performance results during the test.

Sampling and Monitoring During Desiccation Operations

Sampling and monitoring during active desiccation operations is targeted at quantifying the rate and extent of the desiccation process and impacts to the distribution of moisture and solutes. Sampling and monitoring includes both subsurface conditions and the influent and effluent air properties. Table 4-9 summarizes the data collection approach. Full details are provided in the SAP (DOE/RL-2010-83).

Table 4-9. Summary of Data Collection Approach During Active Desiccation

Attribute	Instrument	Data Collection Frequency
Sediment temperature	Thermistor	Continuous at logging frequency determined by field hydrologist
Sediment moisture content	Heat dissipation unit and dual probe heat pulse sensor	Continuous at logging frequency determined by field hydrologist
Soil gas humidity	Humidity sensor/ thermocouple psychrometer	Continuous at logging frequency determined by field hydrologist
Sediment gas pressure	Gas sampling tube	Continuous at logging frequency determined by field hydrologist
Sediment gas composition	Gas sampling tube	Periodically as needed to assess breakthrough of tracer gases Monthly to monitoring humidity or at a higher frequency at selected locations if other instruments indicate more rapid changes (e.g., near the injection well)
Sediment moisture content	Neutron probe (logging)	Monthly at a minimum and additionally at selected locations based on information about the drying front obtained through other

Table 4-9. Summary of Data Collection Approach During Active Desiccation

Attribute	Instrument	Data Collection Frequency
		instruments
Sediment moisture content	Cross-hole radar between pairs of logging holes	Monthly with locations selected based on information about the drying front obtained through other instruments
Sediment moisture distribution and air flow patterns	Conservative and partitioning tracer tests	Monthly and augmented as necessary based on indication of desiccation progress or flow field changes from other monitoring data
Injected gas temperature, humidity, pressure, flow rate	Pressure sensor, thermocouple, humidity sensor, pitot tube	Continuous at logging frequency determined by field hydrologist
Extracted gas temperature, humidity, pressure, flow rate	Pressure sensor, thermocouple, humidity sensor, pitot tube	Continuous at logging frequency determined by field hydrologist
Condensate chemistry, radiological activity	Analysis of collected sample	Data will be collected as needed for waste disposition of any condensate that accumulates

Post-Desiccation Sampling and Monitoring

The post-desiccation portion of the test will involve sampling and monitoring over a relatively long time period (at least five years) to examine the rate and extent to which re-wetting occurs in the desiccated zone. Post-desiccation monitoring could be performed as part of the final remedy for the 200-BC-1 OU. No soil gas flow will be induced during this phase of the test other than small volume soil gas samples. Table 4-10 summarizes the data collection approach. This approach may be modified depending on the results from the active desiccation phase of the test. Full details are provided in the SAP (DOE/RL-2010-83).

Table 4-10. Summary of Data Collection Approach During Post-Desiccation Period

Attribute	Instrument	Data Collection Frequency
Sediment temperature	Thermistor	Continuous at logging frequency determined by field hydrologist
Sediment moisture content	Heat dissipation unit and dual probe heat pulse sensor	Continuous at logging frequency determined by field hydrologist
Soil gas humidity	Humidity sensor/thermocouple psychrometer	Continuous at logging frequency determined by field hydrologist
Sediment gas composition	Gas sampling tube selected locations	Weekly for first month then monthly and then reduced if warranted based on the initial response and the response observed in other instruments
Sediment moisture content	Neutron probe (logging) of selected holes	Monthly and then reduced if warranted based on the initial response and the response observed in other instruments
Sediment moisture	Cross-hole radar between selected pairs	Monthly and then reduced if warranted based on the initial

Table 4-10. Summary of Data Collection Approach During Post-Desiccation Period

Attribute	Instrument	Data Collection Frequency
content	of logging holes	response and the response observed in other instruments
Sediment moisture content and solute concentration	Analysis of collected sediment sample	<p>Within 4 months after termination of active desiccation</p> <p>Additional boreholes may be collected pending the response observed in other instruments</p> <p>Locations (near selected* instrument clusters):</p> <p>a) within desiccated region, including fringe area where solutes may have concentrated</p> <p>b) where disparate geophysical data exist</p>
* Selection is based on position relative to desiccation front at time blower was shut down.		

4.3 Procedures

Procedures for field operations will be prepared as field test instructions. The following examples of operational instructions topics are listed:

- Modified SVE operations
- Nitrogen injection
- Neutron probe
- GPR
- Conservative tracer for soil gas flow
- Data management procedure
- Sampling and manual measurements
- Instrument equilibration and operational testing/verification

5 Equipment and Materials

Equipment planned for the SDPT is basically simple. Blowers with capability to regulate flow rate will be used for both injected nitrogen and extracted soil gas. It is planned to use the same fixed speed blower at the extraction well that was used during the characterization phase of this treatability test. With this blower, extracted soil gas flow is adjusted via a bypass valve that allows air to be introduced downstream of the well. Extracted soil gas will pass through a condenser to remove water containing contaminants. If it is determined that the extracted soil gas is essentially uncontaminated, the condenser will be bypassed. Injected nitrogen will be provided from a liquid nitrogen source and conditioned to achieve a near-constant temperature using a heater.

The real focus of the treatability test is on data. As described previously, a variety of in situ instruments and sensors will be employed to monitor sediment temperature, moisture content and water content, and soil gas humidity. Also, a combination of geophysical logging and tracer gas analyses will be used to supplement data from the in situ instruments and sensors. Below, is described the plan to define instrument response and assure collection of needed data.

5.1 Desiccation Field Test Instrumentation Plan

A number of instruments will be emplaced in situ for monitoring of the desiccation test. Table 5-1 shows the instruments and the parameters that are being monitored.

The heat dissipation units (HDUs), TCPs, humidity probes, and the dual probe heat pulses (DHPs) will be installed within four discrete sand packs in the borehole. The signals from these instruments will be related to the properties of the sand pack, most particularly for the HDU, TCP, and DPHP instruments. Thus, selection of the sand pack material needs to consider instrument operational capabilities. For this reason, a laboratory flow cell was used to evaluate the instrument response during desiccation for use as a baseline to compare the responses observed in the field. The flow cell was packed with porous media approximating the dominant particle size distribution observed at the field test site. The flow cell included a section constructed like the borehole with a bentonite plug above and below the sand pack.

Instrumentation will be installed in the sand pack sections and in the surrogate field material. The flow cell was desiccated to observe the instrument response. Desiccation was stopped at several points during the test for a period of time to evaluate water vapor redistribution and the associated instrument response.

The GPR and ERT will require field and laboratory data as part of assessing the baseline response and change during desiccation. Prior to the field test, the GPR and ERT techniques will be tested using the existing infrastructure at the test site. For ERT, this field information will be coupled with laboratory data that evaluates the change in conductance versus moisture content as sediment is dried.

The following sections provide background on the measurement basis for the instruments.

Table 5-1. In Situ Sensors and Measurements, Field Conditions, and Sensor Filter Pack

Parameter	Relative Humidity	Temperature	Water Content	Water Potential	Electrical Conductivity
Heat dissipation unit	N/A	N/A	N/A	Range: 0.1-5MPa Accuracy: 1kPa	N/A
Thermocouple psychrometer	N/A	N/A	N/A	Range: 0.2-8MPa Accuracy: 30kPa	N/A
Dual probe heat pulse	N/A	N/A	Range: 0 m ³ m ⁻³ to Saturation Accuracy: Θ 0.03-0.05 m ³ m ⁻³ ΔΘ 0.01-0.02 m ³ m ⁻³	N/A	N/A
Humidity	Range: 0-100%, Accuracy: 2% (0-90% RH) 4%(0-100% RH)	N/A	N/A	N/A	N/A
Thermistor	N/A	Range: 0-50°C Accuracy: 0.05°C	N/A	N/A	N/A
Cross-hole radar (or ground penetrating radar)	N/A	N/A	Range: 0 m ³ m ⁻³ to Saturation Accuracy: Soil dependant 0.01-0.05 m ³ m ⁻³	N/A	N/A
Electrical resistance tomography	N/A	N/A	N/A	N/A	Range: Depends on ground conditions and survey types Accuracy: <1% of reading for ideal conditions
Field starting condition	100%	17°C	0.10 m ³ m ⁻³	Variable	0.01-5 mS/cm
Estimated field change	0-100%	10-20°C	May approach zero	Transition to very high suction	May increase then decrease
Filter pack initial condition	100%	17°C	TBD in laboratory	TBD in laboratory	TBD in laboratory
Estimated filter pack change	0-100%	10-20°C	May approach zero	Transition to very high suction	None
N/A = Not applicable					

5.2 Thermocouple Psychrometers

Thermocouple psychrometry is a method for determining water potential from very precise measurements of relative humidity. The water potential of a system that possesses water with liquid and vapor phases in equilibrium can be described by the Kelvin equation:

$$\psi = \frac{RT}{V_w} \ln\left(\frac{p}{p_0}\right) \quad [1]$$

Where:

Ψ = water potential

R = the gas constant

T = temperature

V_w = the molar volume for water

p/p_0 = the relative humidity

The sensor consists of two adjacent thermocouples. The primary thermocouple is surrounded by a porous membrane or stainless steel screen in contact with the sample to be measured. The second thermocouple is sealed in the sensor housing preventing any vapor contact. The temperature depression of the wet sensing junction relative to the dry depends upon the relative humidity of the surrounding air.

Theoretically, water potential can be calculated from such measurements; however the units are typically calibrated in solutions of known water potential.

The TCPs selected for the SDPT use the Peltier effect to apply water to the sensing thermocouple junction. The Peltier effect applies a current to the sensing junction thermocouple causing it to cool and condense water from the surrounding air. After the current is turned off, the water begins to evaporate and the difference in temperature between the wet and reference thermocouple junctions creates a microvolt output in the circuit.

The practical difficulties in applying this method are due to the extreme sensitivity to any thermal differences between the sensor and sample as well as pressure and temperature effects on the measurement. The evaporation of water from the sensing junction primarily depends upon the relative humidity but is also significantly impacted by the diffusivity of water in air. Diffusivity decreases as the pressure increases and care must be taken to account for these effects through careful calibration. The electronics used to accurately read TCP need be able to resolve voltage differences of <1uV and also capable of applying a precise current to the sensing junction.

This method requires attention to the operational details to ensure accuracy of the collected data. Thorough cleaning and drying of the sample chambers prior to calibration are essential. Corrosion can be a problem in acidic conditions as well as any salts or organic compounds that penetrate the stainless screen and deposit on the sensing thermocouple junction. Sensors should be cleaned both before and after calibration and stored in sealed containers until installation. Sodium chloride solutions, spanning the osmotic potential range from -0.2 to 8 MPa, will be used for calibration. Measurements will be repeated over a range of temperatures that are expected to be observed at the field site (i.e., 10 to 25°C). If properly calibrated and maintained, the TCP should have an accuracy of 30kPa over the range from -0.2 to -8 MPa.

5.3 Heat Dissipation Unit

An HDU sensor consists of a heating element and a thermocouple encased in a ceramic matrix. The ceramic relies on hydraulic continuity with the soil for water exchange. Movement of water between the ceramic and the surrounding soil will occur when a water potential gradient exists. A change in water potential will change the water content of the ceramic. At low water contents, the thermal conductivity is controlled by the water content of the ceramic. The HDU uses a constant current power source to heat the unit causing a temperature increase that can be measured and that depends on the thermal conductivity. Sensor variability can be corrected by normalizing the temperature response using data from when the sensor is completely dry and when saturated as shown below.

$$T_{norm} = \frac{\Delta T_{dry} - \Delta T}{\Delta T_{dry} - \Delta T_{wet}} \quad [2]$$

The rise in temperature during the heating time is affected by the initial temperature. The thermal conductivity of the HDU ceramic matrix is a composite of the individual water, vapor, and solid components. The thermal conductivity of the vapor is temperature dependant and will impart temperature sensitivity to the HDU measurement. The manufacturer recommended calibration function that relates the normalized dimensionless temperature increase to the matric potential (Bilskie et al., 2007) is:

$$\psi = \frac{(\Delta T_{corr})^{-1/\beta}}{\alpha} \quad [3]$$

Where:

ΔT_{corr} is determined using the method outlined by Flint et al. (2002).

HDU resolution is approximately 1kPa for matric potentials between -0.1 MPa and -5 MPa. The HDU requires a second reference temperature for the measurement. This is typically provided by a thermistor or thermocouple located on the data logger. Additional error can occur if there are significant temperature differences between the HDU and reference. Using a thermistor located at or near the HDU could remove or reduce this source of error.

5.4 Thermistor

A thermistor is a resistor whose resistance depends on temperature and is typically made from a ceramic or polymer. Thermistors generally operate over a smaller temperature range but achieve a higher precision temperature measurement. A first order approximation considers the change in resistance to be linearly dependant on the change in temperature. The slope then can be used to classify thermistors into two groups: positive temperature coefficient or negative temperature coefficient (NTC). For larger temperature ranges, a linear approximation leads to large errors in the measurement. In order to achieve more accurate temperature measurements over the range of interest, a more detailed description must be utilized. The Steinhart-Hart equation is a commonly used approximation that can provide temperature accuracies of approximately 0.02°C. Higher order polynomial approximations also can be used if properly applied. The temperature sensors used for the DVZTT are encapsulated NTC thermistors. A fifth-order polynomial will be used for determining temperature from the resistance measurement. This approach has been tested on several hundred thermistors of this type that were carefully calibrated in a precision water bath spanning the 0-40°C temperature range. By fitting a fifth-order polynomial to all the sensors, accuracies greater than 0.07°C for more than 99 percent of thermistors were obtained.

5.5 Humidity

Measuring soil relative humidity in the range of 0-95 percent is beyond the wilting point for most plants and so it not commonly performed for agricultural studies. Humidity sensors for use in air or concrete are common and can be used to monitor the very dry end that is expected during soil desiccation. The most common relative humidity sensors consist of a thin hydrophilic polymer or ceramic layer that is applied to conductive electrodes and act as a capacitor. As the humidity of the surrounding media increases, the water content of the polymer or ceramic layer also increases. This increase in water content is accompanied by an increase in capacitance due to the high apparent permittivity of water. The capacitance is measured by applying a high frequency electrical voltage to the device and measuring the current that passes. The capacitance change is quite small and prohibits the use of long cables, even a few meters, between the sensor and the point where the signal is measured. To monitor sensors located 20 or more meters below the ground requires that the electronics are located close to or even as part of the device. For the unit selected for the SDPT, the signal excitation and measurement can all be performed within the device, which is converted to a digital signal that can be monitored remotely. The sensing element is housed within a sintered high-density polyethylene filter to protect it from impact and environmental conditions. Accuracy of the device is 2 percent within the 10 percent to 90 percent relative humidity range and 4 percent from 0 percent to 100 percent Relative Humidity (RH). Temperature dependence is better than 2 percent from -20° to 60°C.

5.6 Dual Probe Heat Pulse

Dual probe heat pulse (DPHP) sensors are a promising method for measuring soil heat capacity, temperature, and water content. This method has been used for very near surface water content monitoring as an alternative to other methods that are influenced by the air interface or large temperature changes. The sensor consists of two parallel hypodermic tubes separated by a fixed distance. A heating element is placed in one tube and a thermistor or thermocouple is located in the other tube. A controlled heat pulse is generated by the heating element and the temperature rise is measured. The maximum change in temperature T_m (°C) depends on the soil volumetric heat capacity C ($J\ ^\circ C^{-1}\ m^{-3}$), probe spacing r (m), and the amount of heat delivered q ($J\ m^{-1}$) (Campbell et.al., 1991).

$$C = \frac{q}{e\pi r^2 T_m} \quad [4]$$

The heat capacity is a composite of the effects from both the liquid and solid components and can be described using the relationship:

$$C = C_w \theta + \rho_b c_s \quad [5]$$

where:

C_w = the volumetric heat capacity of water

ρ_b = the soil bulk density

c_s = the specific heat of the soil component.

The soil volumetric water content can then be estimated by combining equations 4 and 5.

$$\theta = \frac{\left(\frac{q}{e\pi^2 T_m} - \rho_b c_s \right)}{C_w} \quad [6]$$

Significant bias in calculated water contents using equation 6 were observed by Basinger et al. (2003). An empirical correction was proposed to remove the bias:

$$\theta' = 1.09(\theta) - 0.045 \quad [7]$$

Water content calculated from equation 6 is very sensitive to changes in r . Installation of the DPHP sensors down boreholes must be performed carefully so that the tube separation is not significantly altered. The accuracy of volumetric water content estimates from DPHP sensors has been reported between 0.01 and 0.05 m³ m⁻³ (1-5 volume percent) can be obtained.

5.7 Ground Penetrating Radar

Soil apparent permittivity is strongly dependent on water content owing to the large difference between water and bulk soil apparent permittivity. The apparent permittivity is determined from the observed velocity of an electromagnetic (EM) pulse propagating through the soil matrix. The apparent permittivity for soils can be dispersive and so care must be taken when comparing values obtained using different frequencies.

Studies have demonstrated that GPR methods effectively estimate subsurface water content using measured EM velocities (Du and Rummel, 1999; Van Overmeeren et al., 1997; Huisman et al., 2003). GPR has also been used at the Hanford Site for water content determination (Kowalsky et al., 2005; Irving et al., 2007; Strickland et al., 2009).

Several GPR surveys can be used for subsurface water content determination. A GPR measurement fundamentally consists of placing a transmitting antenna at one location, which emits an EM pulse. The radiated pulse propagates within the ground and is subsequently detecting by a receiving antenna at an adjacent location. Cross-borehole GPR surveys are those where EM energy is transmitted directly through the ground to study the subsurface transmission properties. The transmitting and receiving antennae are placed in opposite boreholes and can determine EM velocity, attenuation and in some cases dispersion. There are two common types of cross-borehole GPR surveys termed zero-offset profile (ZOP) and multiple-offset gather (MOG) which interrogate a plane passing through the boreholes. In a ZOP survey, both antennae are positioned at the same depth and moved at equal steps in their respective boreholes. In this way, an average EM velocity or attenuation of the volume between adjacent boreholes can be determined for each depth. This method is much faster to acquire and requires less data processing to interpret. A MOG survey allows one to produce a two-dimensional image of the EM properties between boreholes. Using measurements acquired from antennae located at many different positions, a tomographic image of velocity and therefore apparent permittivity can be produced. MOG surveys provide much more information, but require substantially more time to both perform and process. Another common borehole survey type places the receiving antenna in a single borehole and places the transmitting antenna at various locations at the surface. This last type of survey investigates a volume near the surface immediately surrounding the borehole and is termed a vertical radar profile. At the SDPT field site, water content changes are expected to occur at significant depths below the surface. Survey geometries where antennas are located at the ground surface are limited in their depth of investigation and so cross-borehole methods are preferred for this application.

All borehole GPR methods require very precise measurements of the EM travel time through the material being investigated. Prior to and after each survey, a travel time calibration will be performed. This calibration procedure consists of positioning the antennae at a fixed separation within a material that has known transmission properties, typically air. Using the measured time at which the transmitted pulse arrived at the receiving antenna and the EM velocity in air, the time at which the transmitted pulse was emitted can be determined and is termed the absolute time zero. All subsequent travel times are measured relative to absolute time zero to give the actual EM travel time. Knowing the separation between antennae, the EM velocity of the material being investigated can then be determined:

$$\kappa_a = \frac{1}{v^2 \mu_0 \epsilon_0} \quad [8]$$

where:

κ_a = the apparent permittivity

v = the EM velocity of the media

μ_0 = the magnetic permeability

ϵ_0 = the electrical permittivity of free space.

Electrical conductivity of the soil must also be considered when performing a GPR survey. If the electrical conductivity is too high the signal may be completely attenuated. At intermediate conductivities, diffusion effects become significant and can alter the propagating wave packet. It is common to use only travel times to determine the apparent permittivity. This is valid under low loss conditions, i.e., when $\sigma_e \ll \omega \epsilon_e$, where σ_e and ϵ_e are the effective electrical conductivity and dielectric constant respectively and ω is the angular frequency of the pulse. For media with high electric loss, the apparent permittivity must be evaluated using both the velocity and attenuation, α :

$$\kappa_a = \frac{\left[\frac{1}{v^2} - \left(\frac{\alpha}{\omega} \right) \right]}{\mu_0 \epsilon_0} \quad [9]$$

The apparent permittivity of the medium within the GPR sampling volume can then be converted to water content using an appropriate petro-physical relationship. While relationships applicable to general soils such as Topp's equation (Topp et al., 1980) have found widespread use, it is preferred to use a one developed for the specific soil being measured. One common method describes the water content as a linear function of the square-root of the apparent permittivity (Evetts et al., 2005):

$$\theta = a\sqrt{\kappa_a} + b \quad [10]$$

Realistic two-dimensional images of EM velocity and attenuation from MOG surveys can be obtained from inversion of measured travel times and amplitudes. Different inversion methods can be used depending on the application and conditions at the site. The straight-ray method can be used when velocity contrasts are low, typically less than 20 percent. When significant differences in velocity are present, the EM pulse will refract and follow the fastest path requiring the use of a curved-ray approach. Straight-ray inversion software is commercially available as well as a curved-ray open-source code. Any deviation in the position of the boreholes must be accounted for and can be assessed using a borehole

deviation logging tool after well completion. If care is taken in data acquisition and processing, errors less than 0.002 m/ns (0.0066 ft/ns) can be obtained.

5.8 Electrical Resistivity Imaging

Field, laboratory, and theoretical studies have reported relationships between the electrical resistivity and physical properties of variably saturated soils. Excellent correlations between soil electrical resistivity and water content have been demonstrated at laboratory scales; however, application of the method at field scales presents more challenges to successful implementation. Relationships between electrical resistivity and soil moisture depend on soil mineralogy, texture, hydraulic properties, and chemistry. Several petrophysical relationships have been developed, each with their own advantages and disadvantages. Archie's law (Archie, 1942) is one such relationship that has seen widespread use relating the bulk electrical conductivity C_b (the inverse of resistivity) in terms of the porosity ϕ , degree of saturation $S_w = \theta/\phi$, and electrical conductivity of the saturating fluid C_w :

$$C_b = C_w \phi^m S_w^n \quad [11]$$

The cementation exponent, m , typically takes on values in the range 1.3-2.0 and depends upon the pore network. The saturation exponent, n , is related to the wettability of the soil with values normally very close to two. It is assumed here that the mineral component does not significantly contribute to electrical conduction of the sample. The presence of clay minerals can invalidate this assumption, therefore requiring the use of alternative descriptions. Determining the parameters that correctly describe the site specific electrical resistivity response to moisture changes is a crucial component for monitoring water content changes.

5.9 Neutron Probe

Soil water content determination using neutron scattering probes has become a standard method over the past several decades. Neutrons interact with matter by elastic and inelastic scattering and by nuclear capture. Each interaction depends on the type of nuclei and the energy of the neutron. Hydrogen efficiently scatters and slows neutrons largely due to the fact that its nuclear mass and size is very close to that of a neutron. This process is called thermalization and reduces the neutron energy to approximately the molecular kinetic energy at room temperature (0.025 eV).

A neutron probe consists of a high energy (greater than 5 MeV) neutron source, a thermal neutron detector, and the electronics required for counting and storing the measured response. A fast neutron source placed within moist soil develops a dense cloud of thermal neutrons around it. A thermal neutron detector placed near the source samples the density of the generated cloud. The concentration of thermalized neutrons is affected by both soil density and elemental composition. The clay content of soils can affect neutron probe calibration due to the presence of significant quantities of irremovable hydrogen in addition to carbon which is also effective at neutron scattering. Elements that affect the thermalized neutron density through neutron capture and commonly occur in soils are boron, cadmium, chlorine, iron, fluorine, lithium, and potassium. Neutrons are absorbed by these elements followed by nuclear disintegration and the emission of energy and other nuclear particles, reducing the thermalized neutron density. Soils that have large differences in the amounts of clay, organic matter, or elements with high neutron scattering or capture cross sections will require soil specific calibrations.

A neutron probe repeatedly counts the number of neutrons that are measured by the detector over a discrete interval of time. The statistics of neutron detection can be described by the Poisson distribution

with a mean, \bar{X} and standard deviation, $s = m^{1/2}$. The variance due to random neutron emission can also be calculated and used to estimate the count time required for this component to be below a specified limit. The Chi ratio, defined as $s/m^{1/2}$, should give values close to one for a properly operating neutron probe. Values observed that are appreciably greater or lower than one can signal probe malfunction. Most commercially available probes include a routine for calculating this value and it is recommended that this be frequently performed as part of the monitoring procedure. It is also a necessary practice to perform regular counts in a standard medium such as the probe shield or surrounded by a large volume of water. The probe must be located at least one meter above the ground and three meters laterally from any neutron moderators, including the operator.

Calibration is best performed using the count ratio C_r defined as the count taken in the material being measured, X divided by the standard count X_s . This allows the calibration to remain valid even as the source naturally decays. For modern neutron probes, volumetric soil water content θ_v can be well described as a linear function of the count ratio:

$$\theta_v = A \cdot C_r + B \quad [12]$$

6 Sampling and Analysis

The SAP (DOE/RL-2010-83) describes the field sampling activities and quality assurance processes for obtaining data of sufficient quality and quantity during conduct of the SDPT. Sampling locations and frequency are identified, including data collection from in situ and above-ground sensors, geophysical data collection, and laboratory analysis of sediment and condensate samples.

7 Data Management

The following types of data were collected:

- Signals from in situ instrumentation emplaced to monitor the desiccation process
- Periodic neutron moisture logging
- Periodic gas sampling
- Periodic cross-hole radar logging
- Borehole anemometry characterization of the injection and extraction wells
- Above-ground gauges that measure injected and extracted gas properties and power consumption
- Chemical and physical properties of collected condensate
- Chemical and physical properties of sediment samples collected during ground truthing following the period of active desiccation

A project-specific database will be developed and maintained to collect, organize, store, verify, validate, and manage analytical laboratory data and/or field measurements for environmental samples. The data will be stored electronically in Microsoft Excel spreadsheets, and paper copies will be maintained in the project files. A project data custodian will be designated to control and maintain the data. Figure 7-1 provides a data management flow diagram for information derived from monitoring components and testing.

Monitoring Components

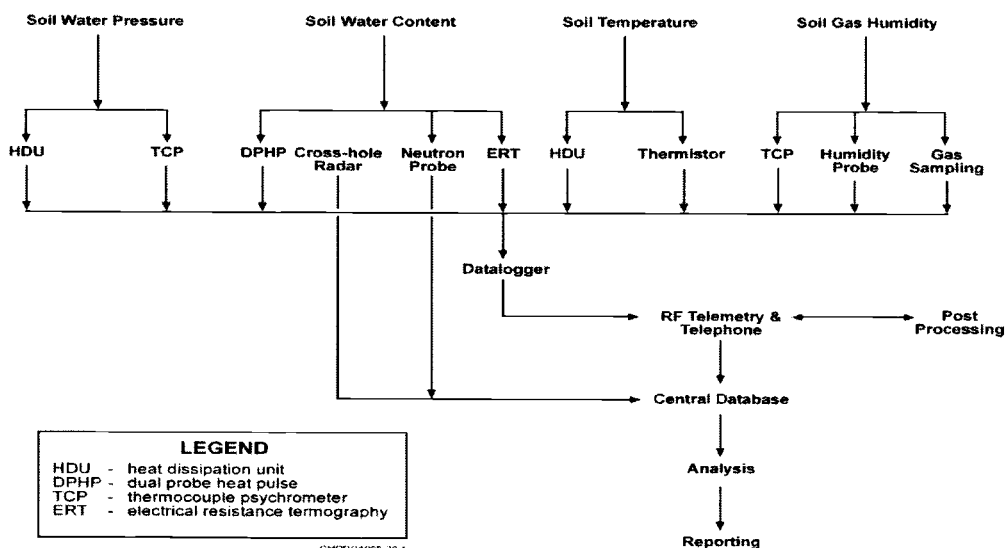


Figure 7-1. Vadose Zone Monitoring Components, Instrumentation, and Data-Collection Management Flow Diagram for the Soil Desiccation Pilot Test

The Sample Management and Reporting organization, in conjunction with the Project Manager, is responsible for ensuring that analytical data are appropriately reviewed, managed, and stored in accordance with applicable programmatic requirements governing data management procedures. Pertinent analytical data collected in the laboratory will also be recorded in the Hanford Environmental Information System.

Details of the data management plan are included in the SAP (DOE/RL-2010-83).

8 Data Analysis and Interpretation

Data analysis will be conducted in two phases. The first phase will involve assessment of the desiccation process in terms of operational success and compilation of parameters that can be used to support implementability, short-term effectiveness, and cost evaluation of the process. This information will be available based on initial field test data and can be analyzed to provide near-term information to describe desiccation as a potential technology in FSs (e.g., for the 200-BC-1 OU). Continued longer-term monitoring is needed to evaluate desiccation performance completely in terms of mitigating contaminant migration. The second phase of analysis will involve long-term monitoring, quantifying how the desiccation zone changes over time, and modeling. A report for each phase will be prepared to document the testing results.

8.1 Operational Desiccation Performance

Operational performance during desiccation will be assessed in terms of implementability, short-term effectiveness, and cost evaluation of the process. Data for the temporal variation of soil moisture and temperature at monitoring locations, and electrical resistance and cross-hole radar tomography will be used to evaluate the sweep volume, effective distribution of desiccation, and timeframe for desiccation. Soil moisture and post-desiccation borehole samples will also be used to assess the end-point soil moisture at the monitoring locations as a measure of the short-term desiccation effectiveness. Water removal during operations will also be quantified (e.g., via humidity and flow rate monitoring of extracted soil gas) as another measure of desiccation effectiveness. The ability to initiate and maintain operational conditions (e.g., nitrogen flow rate, temperature) and the necessary equipment and well spacing will be evaluated in terms of the implementability and cost for desiccation operations.

Examples of anticipated data from in situ probes (Figure 8-1), and periodic neutron logging (Figure 8-2) were developed as part of field test design and represent the type of information that will be available for interpretation of desiccation performance. Cross-hole tomography methods will also be employed, but example plots are complex and, therefore, not represented here.

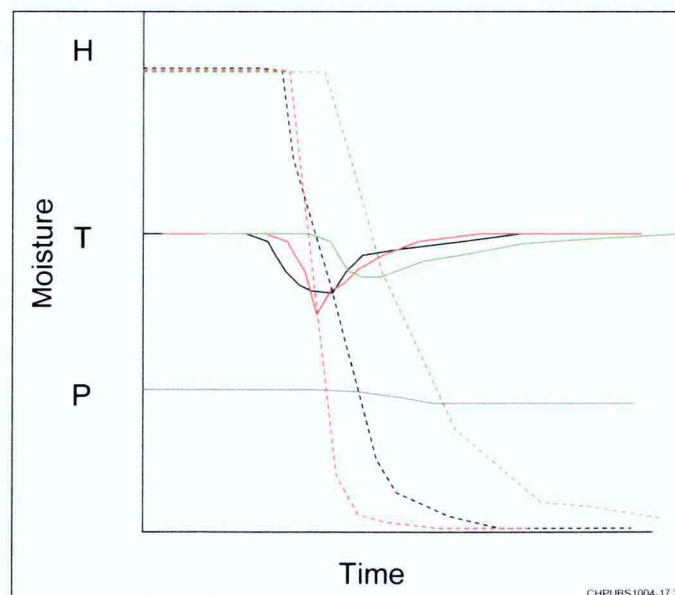


Figure 8-1. Conceptualization of Anticipated Data Response from In Situ Probes

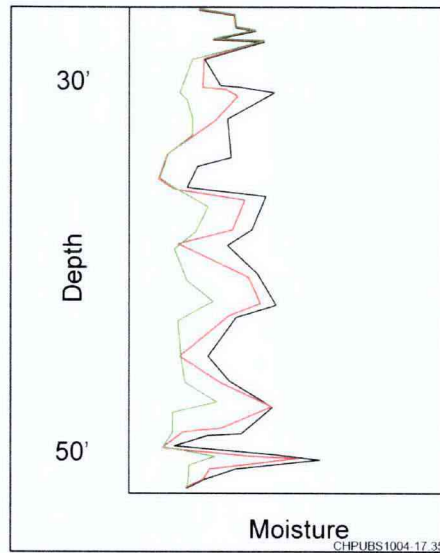


Figure 8-2. Conceptualization of Anticipated Data Response from Periodic Neutron Logging

The plots depict three vertically discrete sensors (black, red, and green) at a monitoring location. Conceptually, the desiccation front is expected to pass at somewhat different times for each vertical location and with a response dependent on the porous media at and above/below the sensor location. The conceptual pressure response (grey) from a single pressure port is depicted assuming a location near the injection well where the pressure decreases for the same flow rate due to a permeability increase as the subsurface is desiccated.

The plot depicts conceptual moisture data from neutron logging response at a monitoring location within the desiccated area for pre-desiccation (black), a time during desiccation operations (red), and after a relatively long period of desiccation (green) during active desiccation operations. From the initial conditions, interim desiccation results are expected to show decreases in moisture content first in the more permeable vertical intervals at a monitoring location. Over time, the moisture content will continue to decrease and become more uniform, although vertical variation in moisture content is still expected due to variation in sediment texture.

8.2 Long-Term Performance

Long-term performance assessment is focused on the effectiveness of the desiccation in terms of mitigating contaminant migration. Because contaminant migration is inherently slow in the vadose zone, long-term performance assessment will include measuring both contaminant migration and the maintenance of conditions that inhibit contaminant migration (e.g., low soil moisture within the targeted desiccation zone). Modeling predictions of how desiccation impacts contaminant and moisture migration will be used as a baseline for comparison with the measured trends during the long-term monitoring period. Modeling will be conducted using a similar format to the simulations summarized in Section 4.2.1.3 but will be updated to reflect data collected in the field test and laboratory information on rewetting processes (e.g., vapor and advective moisture movement) as discussed in the pending PNNL reference. These data will provide information that can be used to refine both the transport parameter values and, if necessary, the modeling approach for these long-term performance evaluation simulations. The modeling configuration will also include evaluation of lateral moisture flow in addition to the vertical moisture flow simulated as summarized in Section 4.2.1.3.

A key monitoring parameter will be the duration that soil moisture is retained below a target level, as determined based on modeling predictions of the soil moisture that mitigates contaminant migration. If soil moisture increases, contaminant concentrations will be evaluated against baseline concentrations to assess contaminant migration and how desiccation affects concentrations during any continued migration.

9 Health and Safety

The health and safety requirements for this treatability test are contained in the health and safety plan. Air monitoring will be conducted in accordance with the EPA-approved radiological air monitoring plan prepared for this study. Both of these plans will be issued separately before field work is initiated.

10 Waste Management

The waste management requirements for this treatability test are contained in the waste control plan (SGW-34277, Rev. 2, *Waste Control Plan for the BC Cribs and Trenches Area in the 200-BC-1 OU*). This revision addresses potential disposition of condensate contaminated with Tc-99.

11 Community Relations

A key goal of public involvement is to obtain stakeholder perspectives on issues affecting the TPA (Ecology, EPA, and DOE, 1989) and to facilitate broad based participation in the Hanford Site decision making process. The Tri-Parties, which include DOE, EPA, and Ecology, believe that public involvement is essential to the success of Hanford Site cleanup.

11.1 Purpose

The purpose of this chapter is to provide an overview of the public involvement opportunities for this treatability test. It identifies the opportunities to inform and involve stakeholders and the public.

11.1.1 Definition of Stakeholders and General Public

Stakeholders are described as individuals who see themselves affected by and/or have an interest in issues, and commit time and energy to participate in decisions. Hanford Site stakeholders include local governments, local and regional businesses, the Hanford Site workforce, local and regional environmental interests, and local and regional public health organizations.

The general public comprises those individuals who are aware of, but may choose not to be involved in, decisions. It is the responsibility of the agencies to provide the public with meaningful information on upcoming decisions so they can choose whether to become involved in Hanford Site decisions.

11.1.2 Availability of the Treatability Test Plan

The Tri-Parties are making this treatability test plan available to the public by including it in the Administrative Record. No public comment period is required for this test plan; therefore, no formal public review and comment period is scheduled. Tribal nations, stakeholders, and the general public are encouraged to use this document and other documents produced during this study as resources for considering the Tri-Parties' decisions concerning Hanford Site Central Plateau waste sites. Preferred alternatives for these waste sites will be selected only after the public comment period has ended for the applicable proposed plan, which is being supported by this treatability test, and the comments on the proposed plan have been received, reviewed, and considered.

11.2 Public Comments

All public comment periods on TPA documents are announced in regional newspapers. As described above, public comments on this treatability test plan will be received during the formal public review periods for proposed plans that invoke this treatability test.

12 Reports

An interim report will be issued following completion of the active portion of desiccation and collection of initial ground truthing data. That report will provide an assessment of operational success and compilation of parameters that can be used to support implementability, short-term effectiveness, and cost evaluation of the process. At the conclusion of long-term monitoring and evaluation of how the desiccation zone changes over time, a final report will be issued.

Reports to management on data quality issues will be made if and when these issues are identified. These issues will be reported to the project manager by laboratory or field sampling and analysis personnel. Subsequently, standard reporting protocols (e.g., project status reports) will be used to communicate these issues to management. Because no performance or system assessments are planned as part of this treatability test, the project manager will not be providing audit or assessment reports to management unless an unanticipated request is made to conduct such an assessment.

At the end of the project, a data quality assessment (DQA) report will be prepared to evaluate whether the type, quality, and quantity of data that were collected met the intent of the DQO prepared for this treatability test.

13 Schedule

A summary project schedule and the schedule drivers are listed in Table 13-1. A more detailed schedule is provided in Figure 13-1.

Table 13-1. Project Schedule

Activity	Due Date	Driver
Initiate field testing for the characterization phase of the SDPT	June 30, 2009	Tri-Party Agreement Milestone M-015-53 ^a
Issue SDPT characterization phase report	March 30, 2010	Project goal ^b
Initiate SDPT field operations	October 30, 2010	Project goal ^b
Complete active portion of SDPT	April 30, 2011	Project goal ^b
Submit Draft A test report to Regulator	June 30, 2012	Tentative Tri-Party Agreement Milestone M-015-110D ^c

a. Ecology, EPA, and DOE, 2007, *Approved Tri-Party Agreement Modifications for Central Plateau Waste Site and Groundwater Remediation*.

b. DE-AC06-96RL13200, *Contract Between the U.S. Department of Energy, Richland Operations Office, and Fluor Hanford, Inc.*

c. Ecology, EPA, and DOE, 2010, *Tentative Agreement on Hanford Federal Facility Agreement and Consent Order Change Forms Implementing the Central Plateau Cleanup Strategy*.

This treatability test does have an associated TPA milestone, M-015-110D, which has been tentatively accepted (Ecology et al., 2010) to emphasize increasing focus on deep vadose technology development and testing. An associated TPA milestone focuses on a uranium sequestration pilot test.

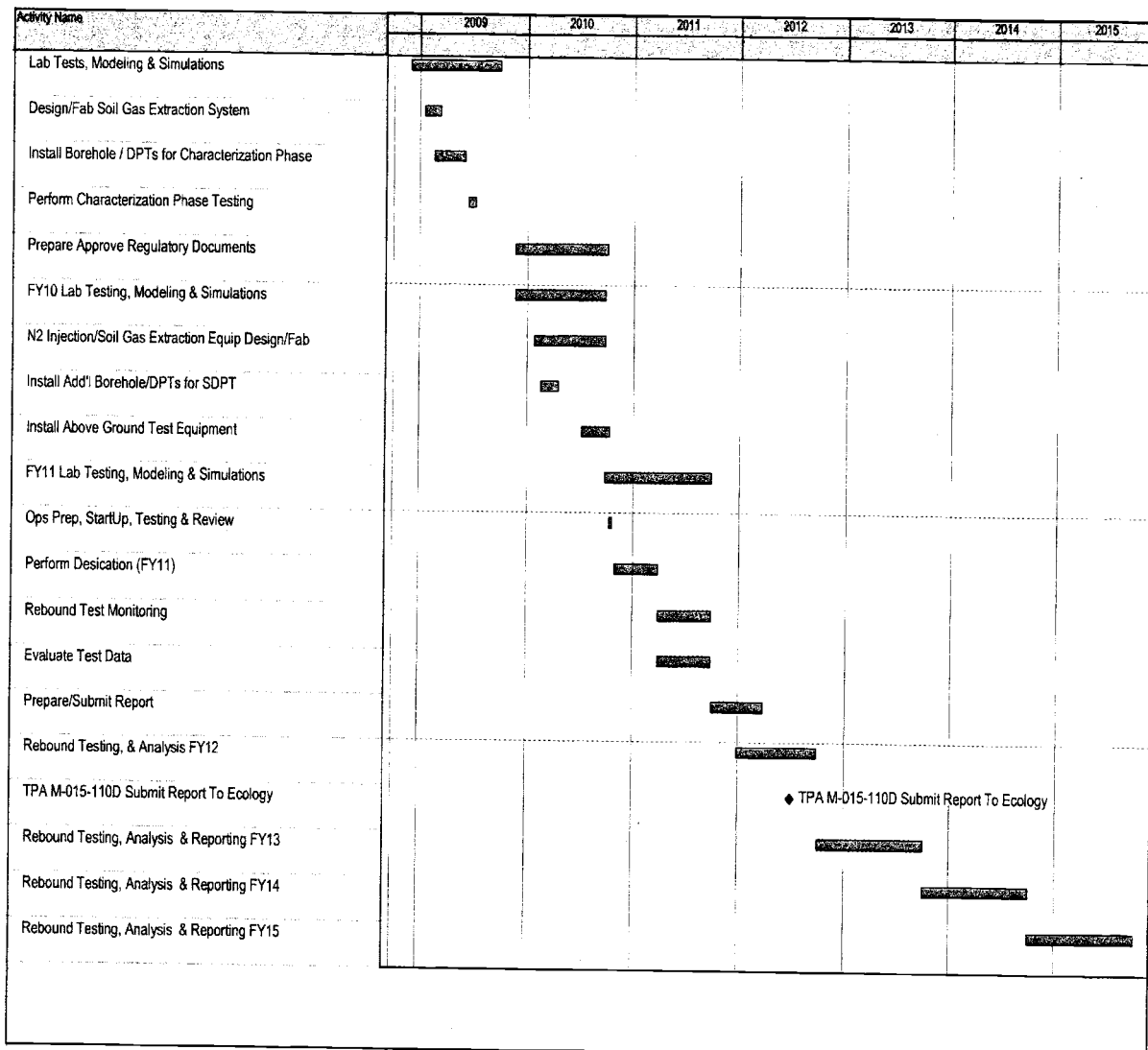


Figure 13-1. Soil Desiccation Pilot Test Schedule

14 Management and Staffing

This treatability test will be conducted by RL. The test will be managed by CH2M HILL Plateau Remediation Company (CHPRC) Soil and Groundwater Remediation Project personnel. Staffing will include personnel from CHPRC, other Hanford Site contractors, and subcontractors as specified by the CHPRC project manager. The CHPRC project manager will ensure that the personnel selected are qualified to perform all activities in accordance with the requirements specified in this test plan. Specific staffing plans are specified in work planning documents or subcontracts prepared on a task specific basis. Figure 14-1 provides a high-level organization for the project; the SAP (DOE/RL-2010-83) provides roles and responsibilities.

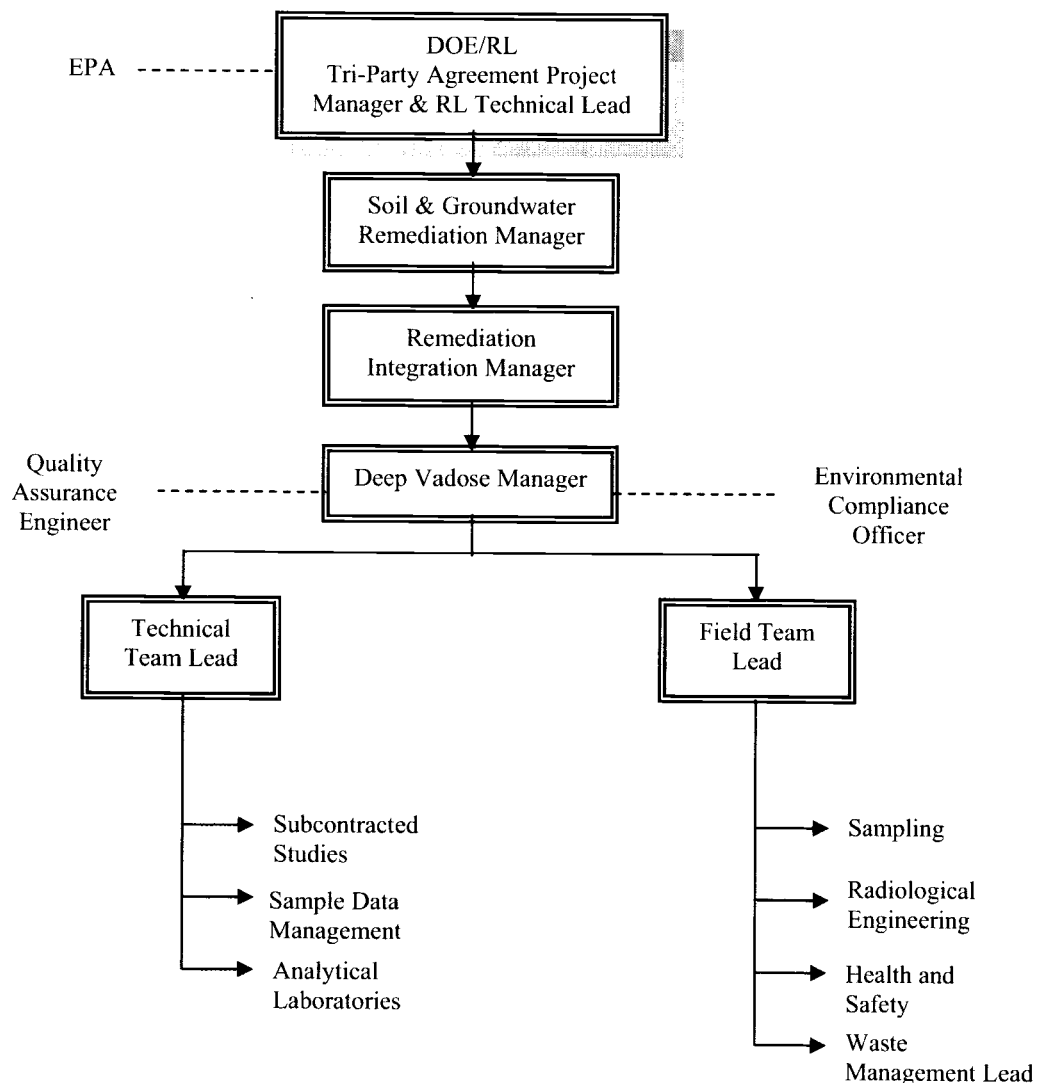


Figure 14-1. Project Organization Chart

15 Budget

This treatability test will be conducted by RL. Funding for all environmental restoration conducted at the Hanford Site is distributed to RL from the DOE Headquarters. Distribution of funds is based on the allocation provided to DOE in the President's Budget. Because of this, it is possible that not all funds requested for performance of activities are provided in a given FY.

CHPRC project management has prepared detailed cost estimates for the work required to complete this treatability test. Because not all activities will be completed in a single FY, all that is known about the budget for completion of this project is what is available in the current FY. As of publication of this test plan, the activities planned to be completed in FY2010 of the treatability test are funded and will be performed as described. Project cost-to-date through FY 2010 is estimated at approximately \$3.9M, including supporting laboratory experiments and numerical simulations. Final startup preparations will be completed in the first month of FY 2011, and then the active desiccation portion of the SDPT will commence. Anticipated additional cost to complete the test is approximately \$3.4M, which includes five years of monitoring and data collection.

16 References

- Archie, G.E., 1942, "The Electrical Resistivity Log as Aid in Determining Some Reservoir Characteristics," *Petroleum Transactions of AIME* 146:54-62.
- Basinger, J.M., G.J. Kluitenberg, J.M. Ham, J.M. Frank, P.L. Barnes, and M.B. Kirkham, 2003, "Laboratory Evaluation of the Dual-Probe Heat-Pulse Method for Measuring Soil Water Content," *Vadose Zone J.* 2:389-399.
- Bilskie, Jim., Bob Clawson, and Jason Ritter, 2007, *Calibration of Heat Pulse Sensors for Soil Water Matric Potential*, Cambell Scientific, Inc., Logan, Utah. Available at: <http://acs.confex.com/crops/2007am/techprogram/P32981.HTM>.
- Brooks, R.H., and A.T. Corey, 1964, "Hydraulic Properties of Porous Media," *Hydrology Paper No. 3*, Colorado State University, Fort Collins, Colorado.
- Campbell, G.S., C. Calissendorff, and J.H. Williams, 1991, "Probe for Measuring Soil Specific Heat Using a Heat-Pulse Method," *Soil Sci. Soc. Am. J.*, 55:291-293.
- Carlson, T.D., M.S. Costanza-Robinson, J. Keller, P.J. Wierenga, and M.L. Brusseau, 2003, "Intermediate-Scale Tests of the Gas-Phase Partitioning Tracer Method for Measuring Soil-Water Content," *Soil Sci. Soc. Am. J.* 67(2):483-486.
- Comprehensive Environmental Response, Compensation, and Liability Act of 1980*, 42 USC 9601, et seq. Available at: <http://uscode.house.gov/download/pls/42C103.txt>.
- DE-AC06-96RL13200, 1996, *Contract Between the U.S. Department of Energy, Richland Operations Office, and Fluor Hanford, Inc.*, U.S. Department of Energy, Richland Operations Office, Richland, Washington, as amended. Available at: <http://www.hanford.gov/phmc/contract/phmc-contract-new.htm>.
- DOE, 2008, *Technology Readiness Assessment (TRA)/Technology Maturation Plan (TMP) Process Guide*, U.S. Department of Energy, Washington, D.C. Available at: <http://www.em.doe.gov/Pages/TechReadinessAssessments.aspx>.
- DOE/RL-2004-66, 2005, *Focused Feasibility Study for the BC Cribs and Trenches Area Waste Sites*, Draft A, U.S. Department of Energy, Richland Operations Office, Richland, Washington. Available at: <http://www2.hanford.gov/arpir/?content=findpage&AKey=DA170624>, <http://www2.hanford.gov/arpir/?content=findpage&AKey=DA170919>, <http://www2.hanford.gov/arpir/?content=findpage&AKey=DA171165>, <http://www2.hanford.gov/arpir/?content=findpage&AKey=DA171467>.
- DOE/RL-2004-69, 2005, *Proposed Plan for the BC Cribs and Trenches Area Waste Sites*, Draft A, U.S. Department of Energy, Richland Operations Office, Richland, Washington. Available at: <http://www5.hanford.gov/arpir/?content=findpage&AKey=DA169911>.
- DOE/RL-2007-56, 2008, *Deep Vadose Zone Treatability Test Plan for the Hanford Central Plateau*, Rev. 0, U.S. Department of Energy, Richland Operations Office, Richland, Washington. Available at: <http://www5.hanford.gov/arpir/?content=findpage&AKey=0804160110>.
- DOE/RL-2009-36, 2009, *BC Cribs and Trenches Excavation-Based Treatability Test Report*, Draft A, U.S. Department of Energy, Richland Operations Office, Richland, Washington. Available at: <http://www5.hanford.gov/arpir/?content=findpage&AKey=0096025>.

- DOE/RL-2009-119, 2009, *Characterization of the Soil Desiccation Pilot Test Site*, Draft A, U.S. Department of Energy, Richland Operations Office, Richland, Washington. Available at: <http://www5.hanford.gov/arpir/?content=findpage&AKey=0084573>.
- DOE/RL-2010-83, pending, *Sampling and Analysis Plan for the Soil Desiccation Pilot Test Site*, U.S. Department of Energy, Richland Operations Office, Richland, Washington.
- Du, S., and P. Rummel, 1999, "Reconnaissance studies of moisture in the subsurface with GPR," *Fifth International Conference on Ground Penetrating Radar*, Waterloo Center for Groundwater Research, Waterloo, Ontario, Canada, pp.1241-1248.
- Ecology, EPA, and DOE, 1989, *Hanford Federal Facility Agreement and Consent Order*, 2 vols., as amended, Washington State Department of Ecology, U.S. Environmental Protection Agency, and U.S. Department of Energy, Olympia, Washington. Available at: <http://www.hanford.gov/?page=81>.
- Ecology, EPA, and DOE, 2007, *Approved Tri-Party Agreement Modifications for Central Plateau Waste Site and Groundwater Remediation*, Washington State Department of Ecology, U.S. Environmental Protection Agency, and U.S. Department of Energy, Richland Washington, February 27, REISSUED.
- EM 1110-1-4001, 2002, *Engineering and Design: Soil Vapor Extraction and Bioventing*, U.S. Army Corps of Engineers, Washington, D.C. Available at: <http://140.194.76.129/publications/engine-manuals/em1110-1-4001/entire.pdf>.
- Evett, Steven R., Judy A. Tolks, and Terry A. Howell, 2005, "Time Domain Reflectometry Laboratory Calibration in Travel Time, Bulk Electrical Conductivity, and Effective Frequency," *Vadose Zone J.* 4(4):1020-1029.
- Flint, A.L., G.S. Campbell, K.M. Ellett, and C. Calissendorff, 2002, "Calibration and Temperature Correction of Heat Dissipation Matric Potential Sensors," *Soil Sci. Soc. Am. J.* 66(5):1439-1445.
- Huisman, J.A., S.S. Hubbard, J.D. Redman, and A.P. Annan, 2003, "Measuring Soil Water Content with Ground Penetrating Radar: A Review," *Vadose Zone J.* 2:476-491.
- Irving, James D., Michael D. Knoll, and Rosemary J. Knight, 2007, "Improving Crosshole Radar Velocity Tomograms: A New Approach to Incorporating High-Angle Traveltime Data," *Geophysics* 72(4):J31-J41. Available at: http://cgiss.boisestate.edu/pubs/BHRS/Peer-reviewed/Irving_et_al_2007_Geophysics.pdf.
- Kowalsky, M.B., S. Finsterle, J. Peterson, S. Hubbard, Y. Rubin, E. Majer, A. Ward, and G. Gee, 2005, "Estimation of Field-Scale Soil Hydraulic and Dielectric Parameters Through Joint Inversion of GPR and Hydrological Data," *Water Resour. Res.* 41:19.
- Oostrom, M., T.W. Wietsma, G.D. Tartakovsky, and M.J. Truex, 2010, "Gas Tracer Tests to Detect and Quantify Water During Soil Desiccation," submitted to *Vadose Zone J.*
- Peng, Sheng and Mark L. Brusseau, 2005, "Gas-Phase Partitioning Tracer Test Method for Water Content Measurement: Evaluating Efficacy for a Range of Porous-Medium Textures," *Vadose Zone Journal*, 4(3):881-884.

- PNL-4015, 1981, *Hydraulic and Thermal Properties of Soil Samples from the Buried Waste Test Facility*, Pacific Northwest Laboratory, Richland, Washington. Available at:
<http://www.osti.gov/energycitations/purl.cover.jsp?purl=/6040632-nvNSsB/>.
- PNNL-14907, 2004, *Vadose Zone Contaminant Fate-and-Transport Analysis for the 216-B-26 Trench*, Pacific Northwest National Laboratory, Richland, Washington. Available at:
http://www.pnl.gov/main/publications/external/technical_reports/PNNL-14907.pdf.
- PNNL-15782, 2006, *STOMP Subsurface Transport Over Multiple Phases, Version 4.0, User's Guide*, Pacific Northwest National Laboratory, Richland, Washington.
- PNNL-17134, 2007, *Geotechnical, Hydrogeologic, and Vegetation Data Package for 200-UW-1 Waste Site Engineered Surface Barrier Design*, Pacific Northwest National Laboratory, Richland, Washington. Available at:
http://www.pnl.gov/main/publications/external/technical_reports/PNNL-17134.pdf.
- PNNL-17274, 2008, *Experimental and Numerical Investigations of Soil Desiccation for Vadose Zone Remediation: Report for Fiscal Year 2007*, Pacific Northwest National Laboratory, Richland, Washington. Available at:
http://www.pnl.gov/main/publications/external/technical_reports/PNNL-17274.pdf.
- PNNL-17821, 2008, *Electrical Resistivity Correlation to Vadose Zone Sediment and Pore-Water Composition for the BC Cribs and Trenches Area*, Pacific Northwest National Laboratory, Richland, Washington.
- PNNL-18800, 2009, *Characterization of Sediments from the Soil Desiccation Pilot Test (SDPT) Site in the BC Cribs and Trenches Area*, Pacific Northwest National Laboratory, Richland, Washington. Available at:
http://www.pnl.gov/main/publications/external/technical_reports/PNNL-18800.pdf.
- PNNL document pending, *Laboratory and Modeling Evaluations in Support of Field Testing for Desiccation at the Hanford Site*, Pacific Northwest National Laboratory, Richland, Washington.
- RHO-LD-45, 1978, *Granulometric Data 216-B Crib Facilities Monitoring Well Sediments*, Rockwell Hanford Operations, Richland, Washington.
- SGW-34277, 2010, *Waste Control Plan for the BC Cribs and Trenches Area in the 200-BC-1 OU*, Rev. 2, Fluor Hanford, Inc., Richland, Washington.
- SGW-41327, 2009, *Data Quality Objectives Summary Report for the Soil Desiccation Pilot Test*, Rev. 0, CH2M HILL Plateau Remediation Company, Richland, Washington.
- SGW-43938, 2009, *Independent Technical Review of the Deep Vadose Zone Treatability Test, Second Review*, Rev. 0, CH2M HILL Plateau Remediation Company, Richland, Washington.
- Strickland, Christopher E., Andy L. Ward, William P. Clement, and Kathryn E. Draper, 2010, "Engineered Surface Barrier Monitoring Using Ground-Penetrating Radar, Time Domain Reflectometry, and Neutron-Scattering Techniques," *Vadose Zone J.* 9(2):415-423.
- Topp, G.C., J.L. Davis, and A.P. Annan, 1980, "Electromagnetic Determination of Soil Water Content: Measurements in Coaxial Transmission Lines," *Water Resour. Res.* 16(3):574-582.

- Toride, N., F.J. Leij, and M. Th. van Genuchten, 1999, *The CXTFIT Code for Estimating Transport Parameters from Laboratory of Field Tracer Experiments*, Version 2.1, Research Report No. 137, U.S. Salinity Laboratory, Agricultural Research Service, and the U.S. Department of Agriculture, Riverside, California.
- Truex, M.J., 2004, *Feasibility Study Evaluation of In Situ Technologies for Immobilization of Technetium Beneath the BC Cribs*, Letter Report, Pacific Northwest National Laboratory, Richland, Washington.
- Van Overmeeren, R.A., S.V. Sariowan, J.C. Gehrels, 1997, "Ground Penetrating Radar for Determining Volumetric Soil Water Content; Results of Comparative Measurements at Two Sites," *Journal of Hydrology*, 197(1-4):316-338.
- WMP-27397, 2006, *Evaluation of Vadose Zone Treatment Technologies to Immobilize Technetium-99*, Rev. 1, Fluor Hanford, Inc., Richland, Washington. Available at:
http://www.osti.gov/bridge/product.biblio.jsp?query_id=2&page=0&osti_id=881671.

Distribution

	<u>MS</u>	<u>Quantity</u>
<u>U.S. Department of Energy, Richland Operations Office</u>		
J. G. Morse	A5-11	2
DOE Public Reading Room	H2-53	1
 <u>CH2M HILL Plateau Remediation Company</u>		
M. W. Benecke	R3-60	1
G. B. Chronister	R3-60	
M. H. Doornbos	H8-15	
S. W. Petersen	R3-50	
J. G. Riddelle	R3-50	
V. J. Rohay	H8-15	
Publications Technical Library	H3-21	1
 <u>Washington River Protection Solutions</u>		
D. A. Myers	E6-31	1
 <u>Pacific Northwest National Laboratory</u>		
M. J. Truex	K6-96	
V. J. Freedman	K9-36	
M. Ostrom	K9-33	
 <u>Administrative Record</u>	 H6-08	 1
 <u>Document Clearance</u>	 H6-08	 1

